Discovery of Novel Piperidinyl/piperazinyl-benzothiazole Derivatives as Potent and Selective PPARδ Agonists

2023

Terukazu Kato

Contents

Abbreviations

ADME	absorption, distribution, metabolism and excretion
ApoB100	apolipoprotein B100
ADDP	1,1'-(azodicarbonyl)dipiperidine
AUC	area under the curve
CETP	cholesteryl ester transfer protein
CHO	Chinese hamster ovary
CL_t	total body clearance
C_{max}	maximum concentration
CPK model	Corey-Pauling-Koltun model
CYP	cytochrome P450
DEAD	diethyl azodicarboxylate
DMAP	4-dimethylaminopyridine
EC_{50}	half maximum effective concentration
EDC	1-ethyl-3-(3-dimethylaminopropyl)carbodiimide
E_{max}	maximum efficacy
FXR	farnesoid X receptor
GCR	glucocorticoid receptor
HDL-C	high-density lipoprotein cholesterol
hERG	human ether-a-go-go-related gene
HRMS	high-resolution mass spectrometry
IL-1β	interleukin-1β

iv	intravenous
LDL-C	low-density lipoprotein cholesterol
LXRα	liver X receptor α
MCP-1	monocyte chemoattractant protein 1
MsCl	methanesulfonyl chloride
PAI-1	plasminogen activator inhibitor-1
PDB	Protein Data Bank
PK	pharmacokinetic
po	per oral
PPAR	peroxisome proliferator-activated receptor
RARα	retinoic acid receptor α
RXRα	retinoid X receptor α
TC	total cholesterol
TG	triglyceride
TMSOTf	trimethylsilyl trifluoromethansulfonate
TNF-α	tumor necrosis factor-α
TRβ	thyroid hormone receptor β
VDR	vitamin D receptor

Chapter 1

Introduction

Cardiovascular diseases have remained the leading causes of death and disability worldwide. Atherosclerosis, the most common form of arteriosclerosis, is the major factor of the cardiovascular diseases and its major clinical manifestations include ischemic heart disease, ischemic stroke, and peripheral arterial disease.[1] Atherosclerosis is a pattern of the disease resulting from the accumulation of atherosclerotic plaques on the inner walls of blood vessels and the subsequent inflammatory response. Based on abundant evidence from epidemic research and the benefits of statin therapy, it has been widely accepted that low-density lipoprotein cholesterol (LDL-C) and high-density lipoprotein cholesterol (HDL-C) levels have a great influence on the development of atherosclerosis. HDL particles, which are acceptors of cholesterol from arterial cholesterol-laden macrophage, are deeply involved in the maintenance of cholesterol balance in the arterial wall.[2] Now it is evident that atherosclerosis is a chronic inflammatory disease which is induced by various risk factors such as dyslipidemia and is closely related to the effects of proinflammatory and anti-inflammatory cytokines/chemokines.[3]

Peroxisome proliferator-activated receptors (PPARs) are ligand-activated transcription factors belonging to the nuclear receptor superfamily that regulate energy balance by influencing the metabolism of lipids and glucose. They exist in three different isoforms: PPARα, PPARγ and PPARδ (also called PPARβ or PPARβ/δ), and are activated by fatty acids and their derivates.[4] PPARα and PPARγ have been well studied and their synthetic agonists are widely used clinically. PPARα is expressed mainly in high energy-requiring tissues such as brown adipose tissue, liver, kidney, heart, and skeletal muscle, and involved in regulation of fatty-acid catabolism and ketogenesis. Fibrates as synthetic ligands for PPARα have been widely used for clinical treatment of dyslipidemia since

these drugs can effectively decrease triglyceride (TG) and LDL-C levels.[5] PPARγ is highly expressed in white and brown adipose tissues and to a lesser degree in liver, kidney, skeletal muscles, pancreas and small intestine. Since PPARγ controls adipogenesis, insulin sensitivity, cell cycle regulation and cell differentiation, thiazolidinediones such as pioglitazone and rosiglitazone, which are known as highly potent PPARγ agonists, have been used for the clinical treatment of type 2 diabetes.[6] Although treatments with PPARα and PPARγ activators have mostly favorable effects on the risk factors for cardiovascular disease, they also lead to adverse effects such as rhabdomyolysis of fibrates and edema of thiazolidinediones, respectively, and therefore their clinical uses are limited in patients with complication risk.[7] In contrast, there are no synthetic ligands of PPARδ currently in clinical use.

PPARδ is widely expressed throughout the body, especially in the organs closely associated with fatty acid metabolism. Previous reports have suggested that activation of PPARδ leads to improved lipid profiles and reduced adiposity due to its involvement in β-oxidation and triglyceride utilization in adipocytes and myocytes.[8] Although the physiological functions of PPARδ still remain uncertain, the roles of PPARδ have been gradually elucidated using several high-affinity synthetic PPARδ agonists such as GW501516 from GlaxoSmithKline, MBX-8025 (Seladelpar) from Johnson & Johnson and L-165041 from Merck (Figure 1_1).[9] GW501516 was reported to increase serum HDL-C level in obese rhesus monkeys and ameliorate diet-induced obesity and insulin resistance in mice fed high-fat diets.[10] In addition to its role in the control of lipid metabolism, numerous recent studies have found that PPARδ is also involved in inflammatory mediators in endothelial cells, monocytes and macrophages and that its

agonists contribute to the anti-inflammatory effects in vitro and in vivo.[11] These findings indicate that PPARδ agonists have the potential to suppress the inflammatory response that triggers atherosclerosis. Although, to date, there is no effective and safe PPARδ agonist available for clinical use, PPARδ remains a promising drug target to treat metabolic diseases including atherosclerosis.

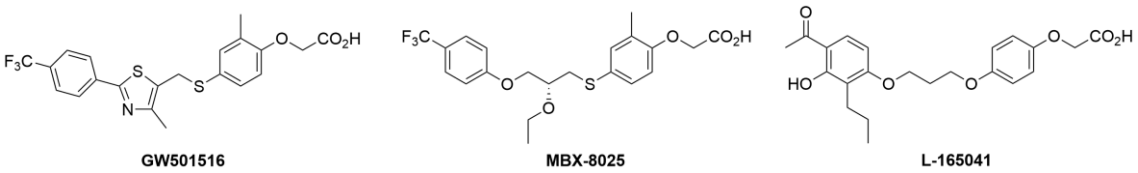

Figure 1_1. Structures of GW501516, MBX-8025 and L-165041.

Chapter 2

Structure-based design of novel piperidinylbenzothiazole derivatives as PPARδ agonists utilizing a virtual screening method

To explore for novel PPARδ agonists, the author started with identification of a potent hit compound by docking simulations and virtual screening. All docking simulations and virtual screening calculations in this study were performed by using ADAM and ADAM&EVE systems from IMMD.[12] These software have the advantages that the conformational flexibility of ligands and the local induced-fit motion of target proteins are effectively considered and correct docking modes can be predicted in the most cases, even for the ligands whose structures are very different from those of the previously cocrystallized ligands. Although a structure/shape/electrostatic similarity screening and a pharmacophore search were also carried out before to screen initial hits, the author consider that such screening steps based on the known ligand structures might filter out the promising hit compounds with entirely different scaffolds or interaction patterns from the known actives. Therefore, the author adopted the docking-based approach throughout the entire course of this study.

As a first step of this study, the author performed ADAM docking calculation of selective PPARδ agonist GW501516 to the crystal structure of PPARδ (PDB ID = 1GWX), which was the only experimental PPARδ structure reported at the beginning of this study.[13] The predicted docking mode indicated the importance of hydrogen bond networks with the activation function helix (AF-2 helix), which is involved in the binding of co-activators, and the neighboring helixes to show PPAR agonist activity, just like the other PPAR agonists (Figure 2_1).[14] Furthermore, the tight fitting of the methylthiazole moiety to the middle of hydrophobic site of PPARδ would contribute to the PPARδ selectivity of GW501516, since the corresponding sites in PPARα and PPARγ were appreciably narrow compared to PPARδ. Small molecule ligands with bulky structures at

the region corresponding to methylthiazole moiety of GW501516 would be hardly to bind to PPARα and PPARγ and express PPARδ agonist activity. It is noticed that the calculated binding mode of GW501516 was almost consistent with the X-ray crystallographic structure (PDB ID = 5U46) which was reported by C. C. Wu et al.[15] Then, the author tried to search for new seed structures of PPAR agonists by means of the ADAM&EVE virtual screening technique. Based on the docking simulation of GW501516, the hit criteria for virtual screening were set as follows: 1) More than two hydrogen bonds with the AF-2 helix and/or the neighboring helixes should be formed; 2) a planar ring structure such as aromatic ring should occupy the site where the trifluoromethylbenzene of GW501516 would bind; and 3) sterically bulky hydrophobic structure should occupy the site where the methylthiazole of GW501516 would bind.

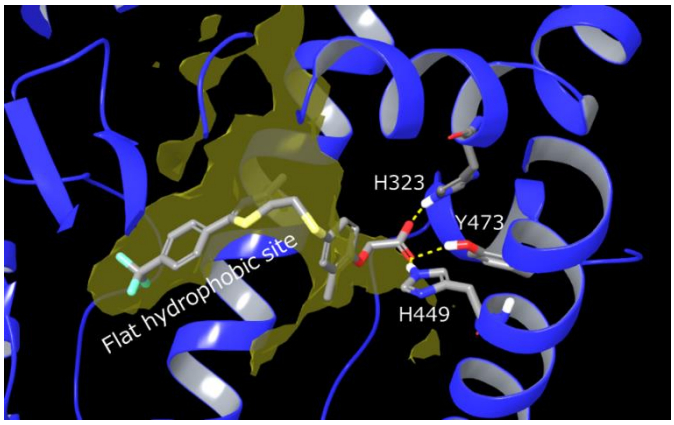

Figure 2_1. Docking model of GW501516 to PPARδ. Blue line and yellow region show backbone of PPARδ structure and hydrophobic surface, respectively. Yellow dotted lines delineate the relation of hydrogen bond dummy atoms and original protein atoms.

Prior to the virtual screening calculation, a 3D grid was generated inside the ligand-binding region of the 1GWX structure in the default condition, and several dummy atoms were set in order to whose match between the protein hydrogen bonding site and ligand hydrogen bonding heteroatoms or between the protein hydrophobic site and ligand hydrophobic groups. Three dummy atom positions were selected according to our hit criteria described above, i.e., at the hydrogen bonding site related to the side chains of both Y473 on the AF-2 helix and H449 on the helix 11, at the hydrogen bonding site from the side chain of H323 on the helix 6 and at the hydrophobic site where the trifluoromethylbenzene and methylthiazole of GW501516 would bind. Totally, about 100,000 3D ligand structural data were prepared from the in-house compound library and MAYBRIDGE catalog database by using the KEY3D program from IMMD,[16] and the virtual screening calculation was performed by using the ADAM-SEARCH program, a member of the ADAM&EVE system, in the default condition.

277 compounds were selected as hit compounds by this virtual screening, on the basis of the computational criteria (i.e., the hit criteria of hydrogen bonds and binding to the flat hydrophobic site, total energy score, molecular weight, etc.) and visual inspection (docking mode, chemical tractability, drug-likeness, intellectual property consideration, etc.). PPAR agonist activities of the selected compounds were assessed by GAL4 hybrid reporter gene assays and 37 active compounds with new scaffolds were identified. Among them, the author decided to focus on compound **2_1** even though its activity was weak (fold activation at 10 μM: PPARα 2.8, PPARγ 1.4, PPARδ 2.3) (Table 2_1). The docking model of compound **2_1** to PPARδ predicted by ADAM was further energetically minimized considering the protein atom motion around the ligand-binding site by means

of the BLUTO program from IMMD.[17] The optimized model suggests that compound **2_1** should satisfy all the criteria set for the virtual screening calculation; i.e., the terminal carboxylic acid group formed hydrogen bonds with the side chains of H323, H449 and Y473, and the benzothiazole and piperazinyl ring structure bound to the hydrophobic site. The piperazinyl ring structure occupied as the same binding site as the methylthiazole of GW501516 (Figure 2_2). Thus, compound **2_1** seemed very suitable for the structure modification to improve the PPARδ agonist activity with the selectivity over PPARα and PPARγ. Interestingly, its piperidine analogue **2_2** showed slightly higher potency for PPARδ than compound **2_1** (Table 2_1). Then, the author selected compound **2_2** as the starting structure for further optimization. Although some compounds containing benzothiazole and phenylpropionic acid were previously reported as selective PPARδ agonists by other groups, this starting structure has a piperidine ring as characteristic linker moiety to enhance the PPARδ agonist activity with the selectivity over PPARα and PPARγ between terminal benzothiazole and the carboxylic acid moiety.

Table 2_1. The PPAR agonist activities of hit compound **2_1** and its analogue **2_2**.

Cmpd	Structure	Fold activation at 10 μM / 1 μM		
		hPPARδ	hPPARα	hPPARγ
2_1	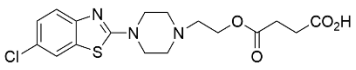	2.8 / 1.3	3.0 / 1.5	1.5 / 1.3
2_2	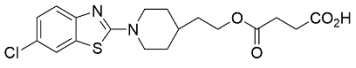	11.0 / 2.1	8.6 / 2.4	1.5 / 1.3

CHO cells were transiently co-transfected with GAL4-hPPAR/mPPAR hybrid expression vector and pG5-Luc reporter vector.[18] Cells were cultured with each compound or DMSO. After 24-28 hr, luciferase activities were measured. Fold activation is shown above relative to DMSO-treated cells.

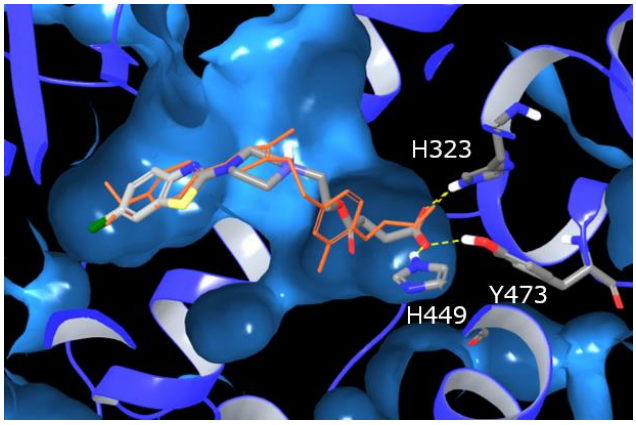

Figure 2_2. Docking models of compound **2_1** (stick) to PPARδ. Thin orange lines show GW501516 structure. Yellow dotted lines represent hydrogen bonds.

As the first strategy for the structure optimization, the author tried to introduce an aromatic ring to the chain part between the piperidine ring and the carboxylic acid. The purposes were; 1) to decrease the entropic loss on conformational flexibility of the long chain part in binding to the protein, 2) to improve the intermolecular van der Waals interaction by increasing volume of that part, 3) to remove the ester group which would be undesirable in terms of metabolic stability. *In vitro* activities of synthesized compounds were measured by reporter gene assay and their transactivation activities for all PPAR subtypes in human at concentrations of 1 μM were summarized in Table 2_2. The author assessed their activities for mouse PPARδ (mPPARδ) in addition to that for human PPARδ (hPPARδ) to evaluate the HDL-C elevation effects in a mice model. Compound **2_3** with the benzoic acid did not improve PPARδ agonist activity, whereas **2_4** and **2_5** with the phenylacetic acid showed greater enhancement of the fold activation for PPARδ (hPPARδ fold activation at 1 μM: 14.6 for **2_4**; 14.4 for **2_5**). Although the hPPARδ agonist potencies of the phenylacetic acid derivatives **2_4** and **2_5** showed the similar values, the fold activation value for mPPARδ of **2_5** having an ethylene-oxy linker was higher than

that of **2_4** having a methylene-oxy linker (mPPARδ fold activation at 1 μM: 7.0 for **2_4**; 11.0 for **2_5**). As a consequence, compound **2_5** containing a phenylacetic acid moiety and an ethylene-oxy linker had agonist potencies for both hPPARδ and mPPARδ and was selected as a lead scaffold. In contrast, compound **2_6** containing a phenylpropionic acid, which is one methylene longer than a phenylacetic acid, displayed only weak PPARδ agonist activity.

Table 2_2. Activity of compounds **2_2**−**6** in cell-based transactivation assay against PPARs.

Cmpd	Structure	Fold activation at 1 μM			
		hPPARδ	hPPARα	hPPARγ	mPPARδ
2_2	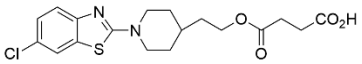	2.1	2.4	1.3	2.0
2_3	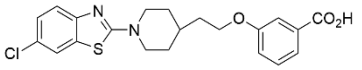	1.5	7.5	1.1	1.4
2_4	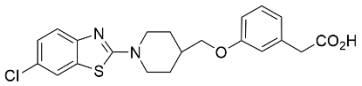	14.6	2.5	2.1	7.0
2_5	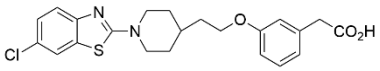	14.4	4.9	2.3	11.0
2_6	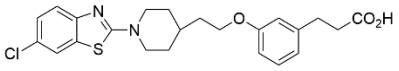	4.5	1.5	1.4	2.2
GW501516		22.7	3.1	1.1	30.4
Rosiglitazone		1.2	1.2	13.1	

CHO cells were transiently co-transfected with GAL4-hPPAR/mPPAR hybrid expression vector and pG5-Luc reporter vector.[18] Cells were cultured with each compound or DMSO. After 24-28 hr, luciferase activities were measured. Fold activation is shown above relative to DMSO-treated cells.

The docking model of **2_5** with PPARδ suggested the tight hydrogen boding networks with the important sites from the AF-2 and surrounded helixes, especially H323, H449 and Y473, as a result of the appropriate position of its carboxylic acid moiety due to the introduction of a benzene ring (Figure 2_3, right). Meanwhile for compounds **2_3**, the carboxylic acid was less likely to reach the hydrogen bonding sites around the AF-2 helix and didn't have enough hydrophobic interaction in the docking model (Figure 2_3, left), and actually it displayed only weak activity. The docking model suggested that a little difference in position of the benzene ring could have a profound effect on the hydrophobic interaction. Therefore, introduction of a substituent into the benzene ring was considered effective to optimize the hydrogen bond length and improve PPARδ agonist activity.

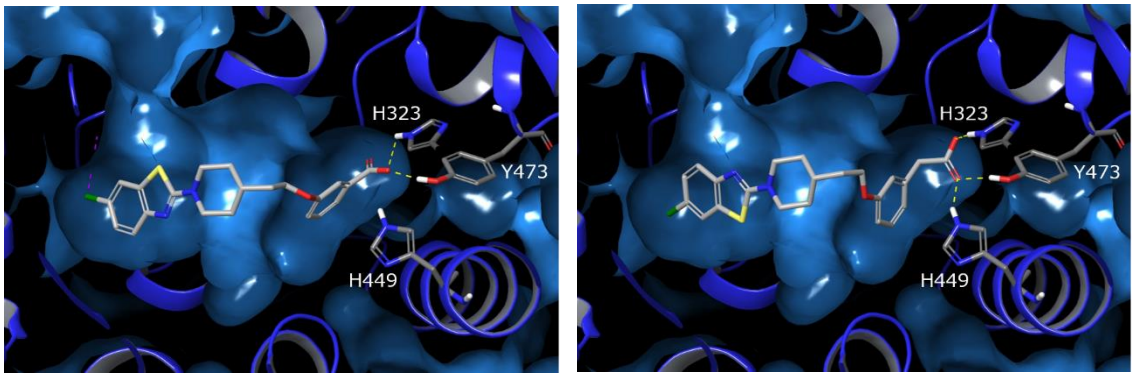

Figure 2_3. Docking models of compound **2_3** (left) and **2_5** (right) to PPARδ. Yellow dotted lines delineate hydrogen bonds.

First, methyl group was introduced to probe a best position to increase the activity. 2-Methylphenylacetic acid **2_7** lost all of agonist activities of PPARs. By contrast, other methyl-substituted phenylacetic acids **2_8**-**10**, especially 4-Methylphenylacetic acid **2_8**, showed higher PPARδ agonist potency than compound **2_5** (hPPARδ EC_{50}: 16.4 nM for

2_8; 92.9 nM for **2_9**; 110 nM for **2_10**). This suggested that a substitution in 4-position on the benzene ring was preferable to increase PPARδ binding activity. The following exploration of 4-position revealed that the substituent should be of modest size according to the PPARδ agonist activities of compound **2_11** (R = 4-chloro, EC_{50} = 19.1 nM) and **2_12** (R = 4-ethyl, EC_{50} = 120 nM). It is notable that the most potent PPARδ agonist **2_8** had selectivity against PPARα (38-fold) and PPARγ (33-fold).

Table 2_3. Activity of compounds **2_5** and **2_7−12** in cell-based transactivation assay against PPARs.

Cmpd	Structure	Transactivation EC_{50} (nM)			
		hPPARδ	hPPARα	hPPARγ	mPPARδ
2_5	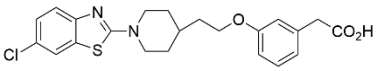	263	2220	2580	1060
2_7	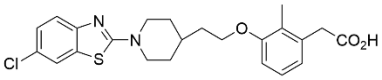	NC	NC	NC	NC
2_8	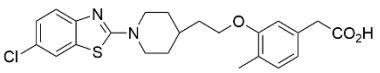	16.4	637	542	71.2
2_9	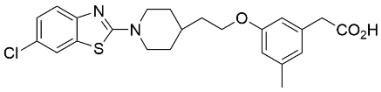	92.9	955	1070	151
2_10	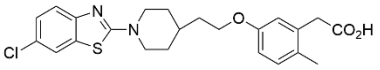	110	NC	980	830
2_11	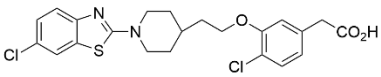	19.1	603	987	49.3
2_12	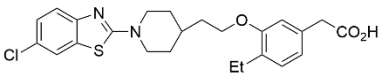	120	3600	680	330
GW501516		9.5	2200	4400	76

CHO cells were transiently co-transfected with GAL4-hPPAR/mPPAR hybrid expression vector and pG5-Luc reporter vector.[18] Cells were cultured with each compound or DMSO. After 24-28 hr, luciferase activities were measured. EC_{50} value was calculated as the concentration of the test compound to give half the maximal fold increase. When the maximal fold increase was below 2-fold, EC_{50} was not calculated ("NC" in the table).

The author also confirmed the docking mode of **2_8** with PPARδ and its image was shown in Figure 2_4. It suggested that the methyl group of its benzene ring occupied the vacant hydrophobic pocket of the receptor and its phenylacetic acid moiety formed the hydrogen bonds with H323, H449 and Y473.

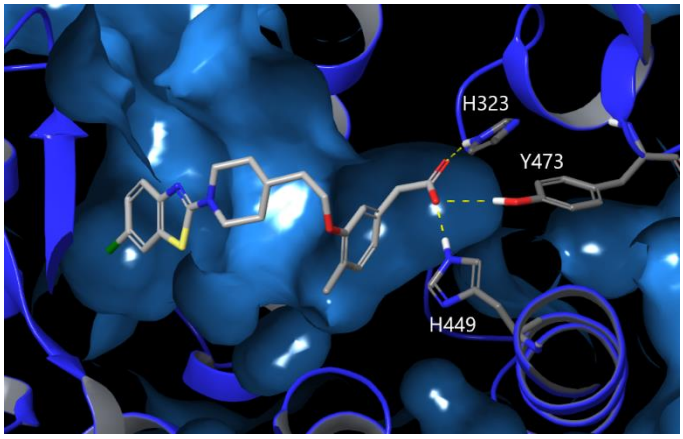

Figure 2_4. The docking model of compound **2_8** to PPARδ. Yellow dotted lines delineate hydrogen bonds.

Compound **2_8** was evaluated for metabolic stability, CYP inhibition, solubility and pharmacokinetic studies, and all of the values were acceptable as a lead compound. (Table 2_4). **2_8** was also applied to *in vivo* evaluation in mice. Male db/db mice were dosed orally once daily (q.d.) for 8 days with 30 mg/kg of **2_8** and GW501516, respectively. The results are summarized in Table 2_5. GW501516 is known to increase HDL-C levels and to lower serum TG levels moderately in the model through activating PPARδ. In this study, **2_8** showed a little increase of HDL-C level and more prominent effects on the reduction of plasma TG and blood glucose levels than GW501516. These results suggest that **2_8** has potential to deliver significant therapeutic benefits for the treatment of dyslipidemia and hypertriglyceridemia.

Table 2_4. ADME data of compound **2_8**.

Cmpd	Metabolic stability[a] (%)		Remaining activity of CYP[b] (%)				Solubility[c] (μM)	PK parameters[d]	
	Rat	Human	1A2	2C9	2D6	3A4		CL_t (mL/min/kg)	$T_{1/2}$ (hr)
2_8	101	96	92	58	94	>99	21.8	14.3	1.8

CL_t: total clearance

[a] Metabolic stability in liver microsome was determined as remaining percentage of compound after 0.5 hr.

[b] Remaining activity at 20 μM was determined by enzyme assay (% of control).

[c] Kinetic solubility at pH 6.8 was determined by HPLC.

[d] Compounds were administered as a mixture of four compounds. Rat, n = 2.

Table 2_5. Activity of compound **2_8** on HDL-C, TG and glucose in db/db mice model.

Cmpd	HDL-C (% Initial)		TG (mg/dL)		Glucose (mg/dL)	
Control	103.5 ± 3.2		162.8 ± 21.4		737 ± 52	
GW501516	132.9 ± 2.7	*	82.4 ± 7.4	**	493 ± 60	**
2_8	118.0 ± 3.5	**	63.9 ± 22.9	**	415 ± 48	*

Dose: 30 mg/kg q.d., 8 days, n = 6 mice per group. * $p < 0.05$, ** $p < 0.01$ compared to vehicle-treated group (Dunnett's multiple comparison test).

In summary, the author obtained a new series of small molecule PPARδ agonists containing piperidinylbenzothiazole structure through the virtual screening and the subsequent structure optimization, which showed high PPARδ agonist activity and selectivity over PPARα and PPARγ. Compound **2_8** had good ADME profiles and showed *in vivo* efficacy to increase HDL-C level in db/db mice model.

Chapter 3

Identification of a novel piperazinylbenzothiazole derivative as potent and selective PPARδ agonist with an HDL-C elevating effect

In chapter 2, the author described the discovery of 2-(1-piperidinyl)-1,3-benzothiazole derivatives as a new series of PPARδ agonists by using docking-based virtual screening techniques. A subtype-selective PPARδ agonist **2_8** was obtained as a result of the structure-activity relationship study, but the author believed that there still remained a margin for improvement in its potency and selectivity. Docking images of lead compound **2_8** and its piperazine analogue **3_1** to the ligand binding domain of hPPARδ indicated that one side of central piperidine/piperazine ring could fit into the bottom hydrophobic surface of the binding pocket and there was an unoccupied space on the opposite side (Figure 3_1, left). Thus, the author considered that introduction of a hydrophobic group into the central six-membered ring could enhance binding activity of PPARδ. In addition, the author obtained another scaffold **3_12** having a methylene linker, instead of an ethylene-oxy linker, between the piperidine ring and the phenylacetic acid moiety of **2_8** by the virtual screening. The docking simulation of compound **3_12** suggested that it would efficiently fit into the cavity of PPARδ as well as the ethylene-oxy linker derivatives (Figure 3_1, right). Therefore, the author introduced various substituents into the 2- or 3-position of the piperidine/piperazine ring in both of the scaffolds and evaluated their substituent effects on PPARδ activity and selectivity.

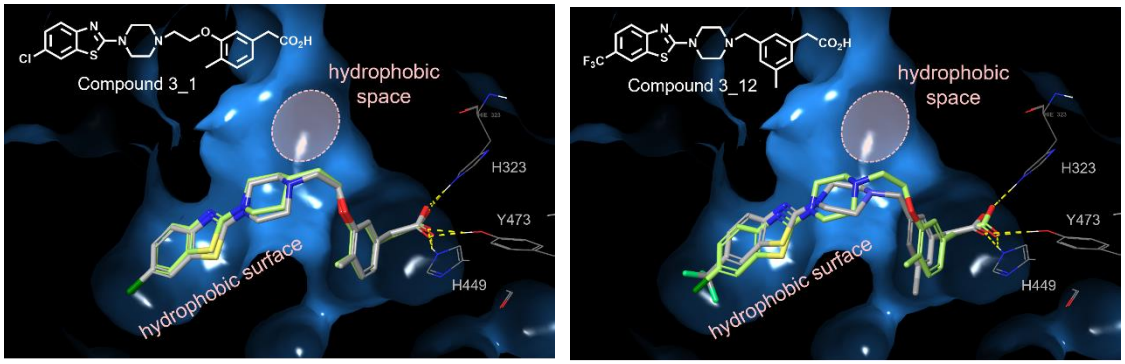

Figure 3_1. Docking models of compound **2_8** (green), compound **3_1** (left, gray) and compound **3_12** (right, gray) to hPPARδ (PDB ID = 1GWX).

Initially, the author confirmed that piperazine analog **3_1** exhibited agonist activity for PPARδ, although slightly inferior to that of lead compound **2_8**, and that the piperidine moiety could be replaced with a piperazine structure. In comparison with lead compound **2_8**, methylpiperazine derivative **3_2** showed improved PPARδ agonist activity and selectively. Interestingly, replacement of the methyl group by the chlorine group at the same position in the right benzene moiety of **3_2** also increased activity for mouse PPARδ and compound **3_3** exhibited excellent selectivity for PPARδ. On the other hand, compound **3_4**, which is a stereoisomer of **3_3**, showed lower PPARδ activity than **3_3**. The author made a piperidine derivative **3_5** to investigate influence on the alkyl side chain arrangement, and it revealed that the PPARδ agonist activity of **3_5** was similar to that of piperazine derivative **3_3** with considering that **3_5** was prepared as a mixture of stereoisomers. Thus, the subsequent structure-activity relationship study was performed by using the piperazine scaffold in terms of synthetic easiness. Next, the author investigated the effect of substituted position and stereoisomer of methyl group on the piperazine ring. Although PPARδ agonist activities of 3-methylpiperazine derivatives **3_6**

and **3_7** had almost the same as those of **3_3** and **3_4** respectively, **3_6** and **3_7** showed low selectivities against PPARγ. For this reason, it is suggested that (*S*)-2-alkylpiperazine derivative is appropriate in terms of PPARδ agonist activity and selectivity. Further investigation of alkyl side chains at this position demonstrated that (*S*)-2-ethylpiperazine analogue **3_8** has higher PPARδ activity than **3_3**. In contrast, (*S*)-2-isobutylpiperazine analogue **3_9** showed significant decreased PPARδ activity, therefore methyl and ethyl groups could fit the binding cavity well. A docking image of compound **3_8** to PPARδ supported this experimental fact. It suggested that the (*S*)-ethyl group tightly fitted to the hydrophobic cavity and more bulky alkyl chains caused large conformational changes in the central piperazine moiety in order to avoid intersect with the cavity surface (Figure 3_2, left). In addition, it seemed to be difficult to extend (*R*)-alkyl chains in the narrow space around the opposite hydrophobic surface (Figure 3_2, right). Meanwhile, 6-trifluoromethylbenzothiazole derivatives **3_10** and **3_11,** which were designed to enhance the hydrophobic interaction in the left benzothiazole moiety, showed better potency as PPARδ agonists and kept excellent selectivity against hPPARα and hPPARγ. Since (*S*)-2-ethylpiperazine derivatives like **3_11** showed higher E_{max} values of PPARδ activity than GW501516, they are considered as full PPARδ agonists. In contrast, there is a possibility that (*S*)-2-methylpiperazine derivatives like **3_10** are partial agonists for hPPARδ.

Table 3_1. Agonistic activities of compounds **2_8** and **3_1**–**11** in cell-based transactivation assay against PPARs.

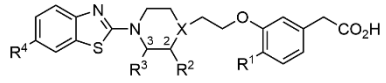

Cmpd	R^4	R^3	R^2	R^1	X	Transactivation EC_{50} (nM)					
						hPPARδ (E_{max})	hPPARα (E_{max}, hα/hδ)	hPPARγ (E_{max}, hγ/hδ)	mPPARδ (E_{max})	mPPARα (E_{max}, mα/mδ)	mPPARγ (E_{max}, mγ/mδ)
2_8	Cl	H	H	Me	CH	16 (16.2)	637 (8.0, 39)	542 (9.0, 33)	71 (20.0)	1126 (15.5, 16)	744 (10.2, 10)
3_1	Cl	H	H	Me	N	33 (14.4)	-	-	110 (25.3)	-	-
3_2	Cl	H	(*S*)-Me	Me	N	5.4 (15.8)	1400 (3.4, 259)	1100 (14.2, 204)	25 (21.7)	4900 (6.9, 196)	500 (8.2, 20)
3_3	Cl	H	(*S*)-Me	Cl	N	5.0 (15.5)	1000 (3.4, 200)	800 (8.2, 160)	12 (23.2)	7100 (8.3, 592)	900 (6.0, 75)
3_4	Cl	H	(*R*)-Me	Cl	N	16 (19.8)	900 (3.8, 56)	440 (12.6, 28)	47 (28.3)	3200 (21.0, 68)	200 (6.4, 4)
3_5	Cl	H	Me	Cl	CH	19 (19.9)	NC (3.0, NC)	1400 (14.5, 75)	47 (28.7)	3600 (14.2, 76)	1000 (11.4, 22)
3_6	Cl	(*R*)-Me	H	Cl	N	7.9 (21.9)	200 (5.1, 25)	16 (16.0, 2)	46 (27.6)	3900 (12.5, 85)	4.1 (5.7, <1)
3_7	Cl	(*S*)-Me	H	Cl	N	17 (23.9)	520 (5.6, 31)	480 (13.0, 28)	27 (27.9)	13000 (16.7, 481)	150 (5.2, 6)
3_8	Cl	H	(*S*)-Et	Cl	N	2.7 (24.6)	310 (5.4, 115)	710 (24.9, 263)	5.8 (31.3)	3400 (6.1, 586)	390 (17.5, 67)
3_9	Cl	H	(*S*)-*i*-Bu	Cl	N	17 (23.2)	NC (3.1, NC)	1100 (15.0, 65)	61 (28.3)	NC (4.6, NC)	660 (13.2, 11)
3_10	CF_3	H	(*S*)-Me	Cl	N	1.5 (15.1)	730 (4.7, 487)	890 (15.0, 593)	6.9 (34.0)	2700 (7.2, 391)	240 (10.1, 35)
3_11	CF_3	H	(*S*)-Et	Cl	N	3.6 (24.6)	400 (5.8, 111)	370 (16.3, 103)	6.1 (31.7)	2500 (8.0, 410)	240 (10.1, 39)
GW501516						9.5 (16.8)	2200 (4.0, 232)	4400 (2.3, 463)	76 (23.9)	6100 (10.4, 80)	3500 (2.8, 46)

CHO cells were transiently co-transfected with GAL4-hPPAR/mPPAR hybrid expression vector and pG5-Luc reporter vector.[18] Cells were cultured with each compound or DMSO. After 24-28 hr, luciferase activities were measured. EC_{50} value was calculated as the concentration of the test compound to give half the maximal fold increase. When the maximal fold increase was below 2-fold, EC_{50} was not calculated ("NC" in the table). E_{max} means maximal fold increase value relative to DMSO-treated cells. Compound **3_5** is a mixture of stereoisomers.

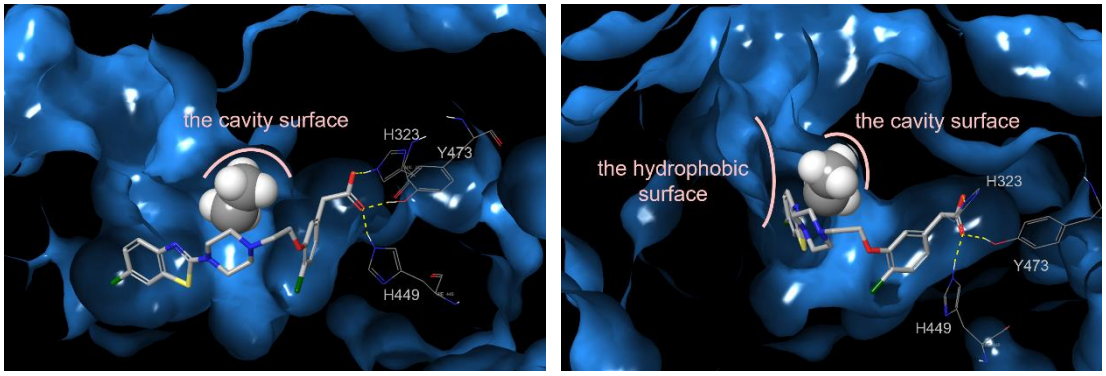

Figure 3_2. Docking images of compound **3_8** to PPARδ (PDB ID = 1GWX) from two directions. The (*S*)-ethyl group of its piperazine ring is displayed by the CPK model.

Next, the author replaced an ethylene-oxy linker between the piperazine ring and the phenylacetic acid moiety with a methylene linker. A series of compounds having methylene linkers were synthesized and their agonist activities for all PPAR subtypes were summarized in Table 3_2. Since compound **3_12** with the unsubstituted piperazine ring showed similar agonist activities as the lead compound **2_8**, the author next synthesized four isomers **3_13–16** with mono methylated piperazine rings and discovered that all of them had superior PPARδ agonist activities to the unsubstituted piperazine compound **3_12**. When compared their activities of PPARα and PPARγ between the two compounds having a methyl group on the same side of their piperazine ring, **3_15** and **3_16** showed a tendency to have larger half maximal effective concentration (EC_{50}) values and smaller maximal increase values (E_{max}) of PPARα and PPARγ than **3_13** and **3_14** respectively. Therefore, the author assumed that alkylation on 3-position of the piperazine moiety was preferable in this scaffold in terms of the selectivities against PPARα and PPARγ unlike the ethylene-oxy linker scaffold. Subsequently, the author examined the effects of sterically bulky substituents at 3-position of the piperazine ring to agonist potency and selectivity against PPARs by introducing ethyl, isopropyl or

isobutyl group instead of the methyl group on the piperazine ring (**3_17–22**). Consequently, all of the compounds except **3_21** showed higher PPARδ activity than the corresponding methylated isomer **3_15** and **3_16**. As to their selectivity against PPARγ, (*S*)-isopropylpiperazine derivative **3_19** and (*R*)-isobutylpiperazine derivative **3_22** exhibited significant lower efficacy for PPARγ activation than their respective stereoisomers. Because of this, the author selected **3_19** and **3_22** for further evaluation in addition to **3_10** and **3_11** with ethylene-oxy linkers. Docking simulation suggested that (*S*)-isopropyl group of **3_19** and (*R*)-isobutyl group of **3_22** fit to hydrophobic surface of PPARδ in the same region by varying the twist angle of the piperazine ring with inversion of the benzothiazole moiety (Figure 3_3). This result is in agreement with the concept of ligand design focused on introduction of a hydrophobic group into the unoccupied space. It is considered that the methylene linker scaffold can accept relatively large substituents unlike the ethylene-oxy linker scaffold as mentioned above and both of its *R*- and *S*-isomers have the potential to fit the hydrophobic surface.

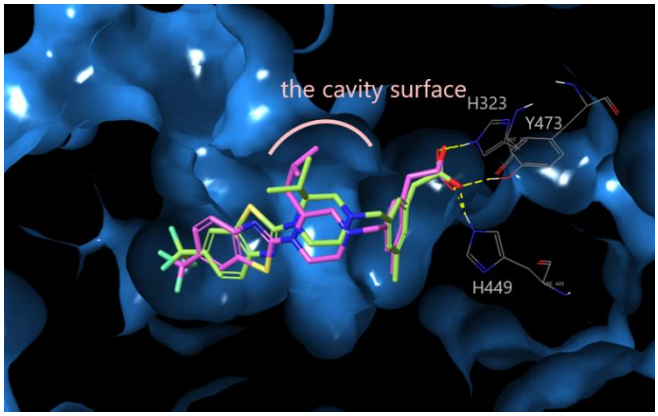

Figure 3_3. Docking models of compound **3_19** (green) and compound **3_22** (magenta) to PPARδ (PDB ID = 1GWX).

Table 3_2. Agonistic activities of compounds **3_12−22** in cell-based transactivation assays against PPARs.

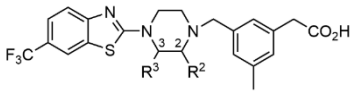

Cmpd	R^3	R^2	Transactivation EC_{50} (nM)					
			hPPARδ (E_{max})	hPPARα (E_{max}, hα/hδ)	hPPARγ (E_{max}, hγ/hδ)	mPPARδ (E_{max})	mPPARα (E_{max}, mα/mδ)	mPPARγ (E_{max}, mγ/mδ)
3_12	H	H	20.9 (13.4)	1100 (4.0, 53)	2100 (3.1, 100)	110 (19)	3000 (6.6, 27)	3300 (3.2, 30)
3_13	H	(*R*)-Me	9.9 (15.5)	1400 (6.6, 141)	1400 (10.6, 141)	34 (22.1)	8000 (19.0, 235)	1400 (7.8, 41)
3_14	H	(*S*)-Me	6.9 (19.5)	350 (7.8, 51)	1200 (6.5, 174)	28 (22.1)	NC (1.1, NC)	1600 (7.5, 57)
3_15	(*S*)-Me	H	10 (14.0)	1800 (6.3, 175)	3100 (3.5, 301)	39 (20.4)	3900 (9.0, 100)	2700 (3.1, 69)
3_16	(*R*)-Me	H	6.2 (13.5)	1600 (6.3, 258)	1200 (6.1, 194)	24 (20.8)	3700 (1.7, 152)	1800 (6.0, 74)
3_17	(*S*)-Et	H	6.2 (25.0)	1100 (4.2, 177)	1900 (11.0, 306)	26 (30.8)	3800 (9.1, 146)	670 (6.6, 26)
3_18	(*R*)-Et	H	3.1 (25.7)	530 (7.6, 171)	430 (21.7, 139)	6.2 (33.1)	8500 (2.8, 1371)	40 (6.8, 6)
3_19	(*S*)-*i*-Pr	H	4.1 (18.6)	NC (2.9, NC)	NC (3.0, NC)	12 (25.0)	2000 (10.3, 167)	NC (2.4, NC)
3_20	(*R*)-*i*-Pr	H	3.7 (13.1)	390 (3.6, 105)	270 (6.3, 73)	7.5 (14.6)	NC (1.3, NC)	230 (6.3, 31)
3_21	(*S*)-*i*-Bu	H	19 (13.6)	NC (1.4, NC)	1500 (6.8, 79)	79 (17.9)	5800 (4.5, 73)	NC (5.2, NC)
3_22	(*R*)-*i*-Bu	H	4.3 (17.5)	NC (1.6, NC)	NC (3.5, NC)	6.9 (24.8)	NC (1.4, NC)	NC (4.3, NC)

CHO cells were transiently co-transfected with GAL4-hPPAR/mPPAR hybrid expression vector and pG5-Luc reporter vector.[18] Cells were cultured with each compound or DMSO. After 24-28 hr, luciferase activities were measured. EC_{50} value was calculated as the concentration of the test compound to give half the maximal fold increase. When the maximal fold increase was below 2-fold, EC_{50} was not calculated ("NC" in the table). E_{max} means maximal fold increase value relative to DMSO-treated cells.

As previously stated, the suitable alkylated position of the piperazine ring was different between the two chemotypes in terms of subtype selectivity; 2-position of the ethylene-oxy linker compounds and 3-position of the methylene linker compounds. Their docking images suggest that the carboxyl group acts as a pivot point in ligand binding at the receptor pocket and locates an alkyl group of the piperazine ring near the distinctive cavity with the same distance from it (Figure 3_4). Since the cavities of PPARα and PPARγ are relatively narrow, it is considered that the synthetic compounds having suitable substituents showed not only high PPARδ agonist activity but also good selectivities against PPARα and PPARγ. This result is consistent with the description in the previous section that the tight H-bonding networks between the carboxylic acid group and the three side chains of H323, Y473 and H449 were important for PPARδ agonist activity.

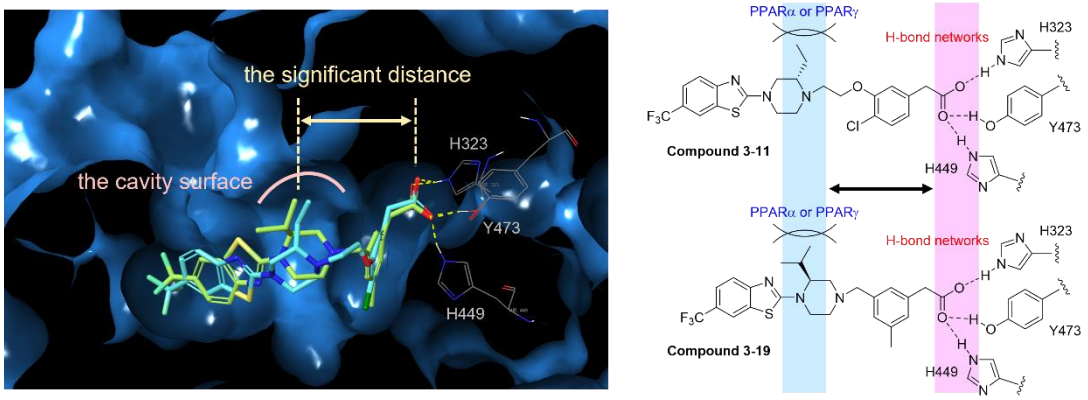

Figure 3_4. The positional relationships between the alkyl groups and the carboxyl moieties of **3_11** with an ethylene-oxy linker (cyan) and **3_19** with a methylene linker (green).

The pharmacokinetic (PK) properties of compound **3_10**, **3_11**, **3_19** and **3_22** were evaluated in rats (Table 3_3). The methylene linker compounds, **3_19** and **3_22**, demonstrated higher maximum concentration (C_{max}) values after oral administration and more favorable oral exposure at a dose of 1 mg/kg than the ethylene-oxy linker compounds.

Table 3_3. Pharmacokinetic profiles of **3_10**, **3_11**, **3_19** and **3_22**.

Cpmd	iv, 0.5 mg/kg, n = 2 [a]			po, 1 mg/kg, n = 2 [b]		
	AUC (μg*h/mL)	CL_t (mL/min/kg)	$T_{1/2}$ (h)	AUC (μg*h/mL)	C_{max} (μg/mL)	F [c] (%)
3_10	0.190	45.6	1.4	0.101	0.011	26.4
3_11	0.399	21.5	2.7	0.151	0.010	18.9
3_19	26.74	0.31	9.5	45.90	2.051	85.8
3_22	5.677	1.47	6.7	7.145	0.895	62.9

[a] Dosed as a solution of test compounds in *N*,*N*-dimethylacetamide/propylene glycol = 1/2.

[b] Dosed as a suspension of test compounds in 0.5% methylcellulose (MC, 400 cP).

[c] Oral bioavailability.

Human apolipoprotein B100 and cholesteryl ester transfer protein double transgenic (hApoB100/hCETP-dTg) mice were used to investigate the *in vivo* efficacy of **3_10**, **3_11**, **3_19** and **3_22** on serum HDL-C level. This model exhibits hypercholesterolemia with human-like serum HDL-C/non-HDL-C distribution and is known to reflect human pathology well. The four compounds or GW501516 at the dose of 3 mg/kg or vehicle (0.5% methylcellulose) was orally administered to the mice once-daily for 8 days, and then the serum levels of HDL-C, total cholesterol (TC) and non-HDL-C were assessed (Table 3_4). The non-HDL-C level was calculated by subtracting HDL-C from TC. As reported previously, GW501516 increased HDL-C level in this study ($p < 0.05$). The four compounds also elicited HDL-C elevation compared to the vehicle

control group, and especially **3_11** and **3_19** exhibited higher HDL-C level than that of GW501516 ($p < 0.01$). Since the TC level in mice treated with these compounds was lower than that in vehicle control mice, it was suggested that these PPARδ agonists specifically increased HDL-C and improved hypercholesterolemia in the mouse model.

Table 3_4. *In vivo* efficacy of **3_10**, **3_11**, **3_19**, **3_22** and GW501516.

Cmpd	Serum lipid levels (% control)					
	HDL-C		TC		non-HDL-C	
3_10	113 ± 7.3		76 ± 5.3		80 ± 15.1	
3_11	156 ± 8.4	**	94 ± 5.7		82 ± 13.5	
3_19	188 ± 9.0	**	72 ± 4.7	**	56 ± 7.6	**
3_22	145 ± 12.7	*	83 ± 5.5	*	75 ± 8.7	*
GW501516	141 ± 10.6	*	83 ± 3.7	*	67 ± 11.1	**

Mice (n = 6/group) were orally dosed with the compounds (3 mg/kg) once daily for 8 days. Data are presented as mean ± SE. The values were calculated as percentage compared to the control group (0.5% methylcellulose (400 cP), 10 mL/kg). Significance was calculated by one-way analysis of variance (ANOVA) followed by Dunnett's test (** $p < 0.01$, * $p < 0.05$ vs control).

In summary, based on the insight that compound **2_8** would not utilize hydrophobic interaction effectively with the binding site surrounding its piperidine moiety, the author designed piperazinylbenzothiazole derivatives which had various alkyl side chains on 2- or 3-position of their center piperazine rings. As a result, the author confirmed that the additional alkyl groups intensified their interactions with the hydrophobic surface of PPARδ and found that the distance between the alkyl group and the carboxyl moiety was important for subtype selectivity. Among them, methylene linker compound **3_19** displayed a significant upregulation of HDL-C level in rodent model and therefore has potential to be an efficient treatment agent for hypercholesterolemia.

Chapter 4

Identification of a novel piperidinylbenzothiazole derivative as potent and selective PPARδ agonist with an anti-inflammatory effect

In chapter 2 and 3, the author described the discovery of piperidinyl/piperazinyl benzothiazole derivatives as a new series of PPARδ agonists. Compound **3_19** which has isopropyl group on the 3-position of its center piperazine ring showed high agonist activity for PPARδ and subtype selectivity and also led to significant elevation of the HDL-C level in a mouse model. Although the effect of side chain introduction on 2- or 3-position of the center piperazine ring was clarified, the author thought that further exploration of other modification points was necessary to identify the best PPARδ agonist.

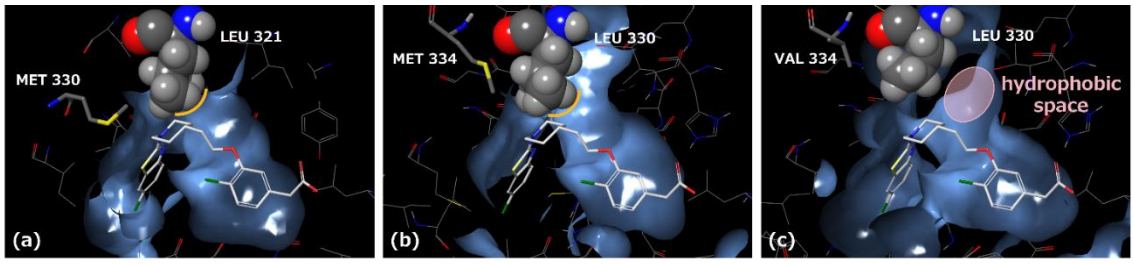

Figure 4_1. Docking images of compound **2_11** to hPPARα (PDB ID = 1I7G, a), hPPARγ (PDB ID = 1FM6, b) and hPPARδ (PDB ID = 1GWX, c). The Leu residues forming the hydrophobic surface are represented by the CPK model.

Docking images of lead compound **2_11** to hPPARs are shown in Figure 4_1. All hPPARs contains a Leu residue as a component of the upper hydrophobic pocket of **2_11**, but the amino acid residues on their back are Met for hPPARα/γ and Val for hPPARδ. Therefore, hPPARδ was expected to have a larger hydrophobic pocket than those of hPPARα/γ due to the extrusion of Leu by their Met side chains. Focusing on this point, the author considered that introduction of a bulky hydrophobic group into 4-position of the central piperidine ring of **2_11** could enhance the binding activity of PPARδ and at the same time its selectivity in comparison with PPARα and PPARγ.

As listed in Table 4_1, various alkyl groups were initially introduced to the 4-position of piperidine based on the docking mode of **2_11**. The efficiency and selectivity of the synthesized compounds were evaluated by reporter gene assays to measure their transactivation activities for all subtypes of human and mouse PPARs. First, the author evaluated an ethyl derivative **4_1** and found it to have lower E_{max} values of hPPARα/γ and higher selectivity than **2_11**. This result added support to the assumption that the hydrophobic pocket around its piperidine moiety is important for PPAR subtype selectivity. Unfortunately, no significant improvement was noted in hPPARδ activity (**4_1**: EC_{50} = 13 nM). To increase the agonist activity for hPPARδ of this chemotype, the ethyl group of compound **4_1** was replaced with longer linear alkyl groups. The author found that *n*-propyl (**4_2**) and *n*-butyl (**4_3**) analogs had higher binding affinity toward hPPARδ (**4_2**: EC_{50} = 9.2 nM, **4_3**: EC_{50} = 8.4 nM) than **4_1** and confirmed that a hydrophobic chain in 4-position of the piperidine ring was also favorable for increasing hPPARδ activity. Next, the effect of branched chains on the activity and selectivity was investigated. Isopropyl (**4_4**), isobutyl (**4_5**), *sec*-butyl (**4_6**) analogs showed lower EC_{50} values for hPPARδ (**4_4**: EC_{50} = 7.5 nM, **4_5**: EC_{50} = 5.9 nM, **4_6**: EC_{50} = 4.5 nM) than corresponding compounds having linear alkyl groups and had good subtype selectivity from the viewpoint of E_{max} values in comparison with PPARα/γ. In particular, **4_6** with a *sec*-butyl group demonstrated the lowest EC_{50} value of PPARδ among the compounds described above. The branched structure near the substitution point was considered to contribute the subtype selectivity, because in comparison with the other linear structures, it had a tendency to exist in the equatorial conformation due to steric hindrance and positioned the side chain toward the hydrophobic cavity.

Table 4_1. Agonistic activities of compounds **2_11** and **4_1**–**10** in cell-based transactivation assay against PPARs.

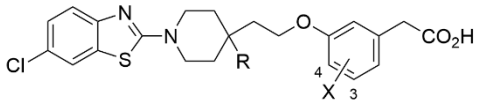

Cmpd	R	X	Transactivation EC_{50} (nM)					
			hPPARδ (E_{max})	hPPARα (E_{max}, hα/hδ)	hPPARγ (E_{max}, hγ/hδ)	mPPARδ (E_{max})	mPPARα (E_{max}, mα/mδ)	mPPARγ (E_{max}, mγ/mδ)
2_11	H	4-Cl	19 (15.0)	603 (12.0, 32)	987 (18.0, 52)	49 (20.0)	1720 (12.0, 35)	744 (17.0, 15)
4_1	Et	4-Cl	13 (13.5)	900 (2.1, 68)	770 (4.9, 58)	160 (22.9)	1900 (9.1, 12)	1200 (4.2, 7.9)
4_2	*n*-Pr	4-Cl	9.2 (22.3)	NC (2.6, NC)	880 (4.5, 96)	33 (31.1)	1800 (21.4, 55)	230 (4.7, 6.8)
4_3	*n*-Bu	4-Cl	8.4 (18.2)	770 (3.0, 92)	660 (6.8, 79)	20 (26.7)	1300 (22.0, 66)	450 (5.2, 22)
4_4	*i*-Pr	4-Cl	7.5 (16.8)	270 (1.4, 36)	690 (3.2, 92)	170 (26.2)	5300 (4.4, 31)	910 (2.9, 5.2)
4_5	*i*-Bu	3-Cl	5.9 (21.6)	NC (2.0, NC)	460 (4.5, 78)	14 (26.9)	2600 (7.7, 190)	400 (4.3, 29)
4_6	*sec*-Bu	3-Cl	4.5 (14.6)	NC (1.9, NC)	230 (2.2, 51)	26 (22.7)	3200 (2.8, 120)	420 (2.2, 16)
4_7		3-Cl	7.1 (13.7)	NC (1.3, NC)	220 (2.6, 31)	16 (28.8)	2900 (7.9, 190)	1100 (3.1, 69)
4_8		3-Cl	11 (22.8)	NC (1.6, NC)	NC (2.5, NC)	29 (29.2)	NC (1.9, NC)	NC (2.2, NC)
4_9		4-Cl	20 (17.4)	NC (1.4, NC)	NC (1.4, NC)	67 (21.5)	6000 (9.7. 90)	NC (1.3, NC)

CHO cells were transiently co-transfected with GAL4-hPPAR/mPPAR hybrid expression vector and pG5-Luc reporter vector.[18] Cells were cultured with each compound or DMSO. After 24-28 hr, luciferase activities were measured. EC_{50} value was calculated as the concentration of the test compound to give half the maximal fold increase. When the maximal fold increase was below 2-fold, EC_{50} was not calculated ("NC" in the table). E_{max} means maximal fold increase value relative to DMSO-treated cells.

Subsequently, the author evaluated agonist activities of compounds having a cyclic aliphatic group at the 4-position of their piperidine ring. Cyclopentyl analog **4_7** unfortunately demonstrated slightly lower hPPARδ activity and lower selectivity against mPPARα/γ than the *sec*-butyl analog **4_6**. On the other hand, cyclohexyl analog **4_8** almost entirely suppressed binding activities to PPARα/γ in both species. The author described in chapter 2 that a chlorine or methyl group at the 3- or 4-position was acceptable for the benzene ring substituent in the right part of the molecules to fit the narrow hydrophobic pocket. For this reason, the 4-Cl analog of **4_8** was also synthesized and evaluated, showing that the 3-position substitution was indeed appropriate for the binding affinity as **4_9** showed lower PPARδ activity than **4_8**.

Cyclohexyl analog **4_8** had both high agonist activity for PPARδ and enough selectivity against PPARα/γ, whereas it showed high inhibition of cytochrome P450 (CYP) 2C9 activity and low metabolic stability in human liver microsomes (Table 4_2). Because these issues were caused by its high hydrophobicity (CLogP = 8.8), the author accordingly designed a series of compounds containing a polar functional group as the side chain in order to reduce the hydrophobicity and to help resolve those issues. Since it was predicted that the tip of the side chain had a hydrophobic interaction with the receptor, the carbon atom near the piperidine ring was selected as the position of aza-replacement as listed in Table 4_2. The author initially replaced the cyclohexane of **4_8** with a piperidine and found that 4-piperidinyl derivative **4_10** (CLogP = 4.4) improved CYP2C9 inhibition and metabolic stability. It is worthy of note that the agonist activity for PPARδ and subtype selectivity of **4_10** did not decrease much compared to **4_8**. With this finding, the author synthesized its analogs having seven- or five-membered heterocyclic amine

and investigated their physicochemical and metabolic properties. Homopiperidinyl analog **4_11** showed higher CYP2C9 inhibition and lower metabolic stability in human liver microsomes than **4_10**. On the other hand, pyrrolidinyl analog **4_12** exhibited the best properties among the above compounds including hPPARδ activity. 2-Methylpyrrolidinyl analog **4_13**, which has a slightly higher hydrophobicity than **4_12**, showed high agonist activity for PPARδ and selectivity to PPARα/γ, but had low metabolic stability similar to **4_10**. In the case of a cleaved structure in the pyrrolidine ring of **4_12**, dimethylamine derivative **4_14** was inferior to **4_12** in hPPARδ activity, CYP2C9 inhibition and metabolic stability. Therefore, it was considered that the pyrrolidine ring fitted suitably in the hydrophobic pocket of PPARδ and contributed to the hydrophobic balance of the entire molecule.

Table 4_2. Agonistic activities and metabolic properties of compounds **4_8** and **4_10**–**14**.

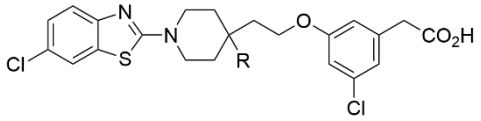

Cmpd	R	Transactivation EC_{50} (nM)						CLogP[a]	CYP inhibition[b] (μM)				Metabolic stability[c] (%)	
		hPPARδ (E_{max})	hPPARα (E_{max}, hα/hδ)	hPPARγ (E_{max}, hγ/hδ)	mPPARδ (E_{max})	mPPARα (E_{max}, mα/mδ)	mPPARγ (E_{max}, mγ/mδ)		1A2	2C9	2D6	3A4	Human	Rat
4_8		11 (22.8)	NC (1.6, NC)	NC (2.5, NC)	29 (29.2)	NC (1.9, NC)	NC (2.2, NC)	8.8	>20	10	>20	>20	31	79
4_10		15 (17.5)	NC (1.4, NC)	1000 (2.9, 71)	41 (27.6)	NC (1.4, NC)	96 (2.8, 2.4)	4.4	>20	>20	>20	>20	48	83
4_11		22 (16.1)	NC (1.2, NC)	NC (1.7, NC)	86 (23.8)	NC (1.3, NC)	NC (1.8, NC)	4.9	>20	18	>20	>20	38	85
4_12		10 (22.6)	NC (2.0, NC)	1200 (4.9, 120)	33 (36.6)	4600 (4.7, 140)	2400 (5.4, 74)	3.8	>20	>20	>20	>20	78	89
4_13		9.7 (17.5)	NC (1.7, NC)	NC (2.7, NC)	22 (25.1)	7000 (7.3, 320)	NC (2.5, NC)	4.2	>20	>20	>20	>20	49	73
4_14		30 (13.8)	NC (1.4, NC)	NC (3.5, NC)	45 (18.2)	NC (1.3, NC)	NC (3.5, NC)	4.3	>20	14	>20	>20	52	86

[a] CLogP value was calculated using ChemDraw version 21.0 (PerkinElmer, Waltham, MA, USA).

[b] CYP inhibition was determined by the decrease in metabolites of probe substrates (% of control).

[c] Metabolic stability in liver microsome was determined as the remaining percentage of compound after 0.5 h.

Next, the Cl group of the benzothiazole moiety of **4_12** was replaced with a CF_3 group according to the Topliss scheme, which led to **4_15** with slightly improved the PPARδ agonist activity and metabolic stability of **4_12** (Table 4_3).[19] Compound **4_15** had sufficient PPARδ agonist activity and subtype selectivity with good CYP inhibition and metabolic stability. However, it revealed that **4_15** strongly inhibited human ether-a-go-go-related gene (hERG) channel currents (78% at 1 μM). It is well-known that highly hydrophobic compounds having a basic group increase the likelihood of hERG channel inhibitor to cause arrhythmias via QT prolongation.[20] Therefore, the author first modified the pyrrolidine moiety of **4_15** by introducing an oxygen atom to decrease its basicity. Morpholine derivative **4_16** could significantly reduce the hERG inhibitory activity (15% at 1 μM), but its CYP2C9 inhibition reappeared. Alternatively, pyrrolidone analog **4_17** also showed low hERG inhibition (11% at 1 μM), but it unfortunately reduced PPARδ activity. Since it was difficult to achieve both reduction of hERG inhibition and other properties by reducing the basicity of the pyrrolidine ring, the author next modified its other hydrophobic moiety. With the substitution in the right part of the molecule, 3-Me and 4-Me derivatives, **4_18** and **4_19**, did not show significant improvement in the hERG inhibition even though their CLogP values were lower than that of **4_15**. On the other hand, introducing a nitrogen atom into the benzothiazole ring in the left part of the molecule contributed to reducing the hydrophobicity of the entire molecule (CLogP = 3.0) without loss of PPARδ agonist activity. 4-Aza-benzothiazole derivative **4_20** exhibited a lower hERG inhibition value (42% at 1 μM) than **4_15**, which met the criteria. This is considered to be due to the polarity of the aromatic ring being restricted by an electron-withdrawing substituent like the CF_3 group, and the hydrophobicity required for

interaction with the receptor being maintained. It was also confirmed that **4_20** did not induce QT prolongation in an anaesthetized guinea pig model. Lastly, the influence of the substitution position in the right benzene moiety was examined once again, revealing that 4-Cl analog **4_21** had lower PPARδ agonist activity and subtype selectivity than the 3-Cl analog **4_20** though it also reduced hERG inhibition. It is considered that **4_20** is comparable to GW501516, which is a strong and subtype-selective PPARδ agonist and was used as a positive control in our study, in point of PPARδ agonist activity and selectivity. As a result, compound **4_20,** which showed high PPARδ activity and subtype selectivity and also had excellent properties for the other evaluation tests, was selected as a candidate compound for our preclinical study.

Since many receptors belonging to the nuclear receptor superfamily recognize the same response elements, it was important to check that compound **4_20** did not show any binding affinity to them before *in vivo* evaluation. The author also investigated the agonist activities of **4_20** over seven other nuclear receptors (LXRα, RXRα, TRβ, RARα, FXR, VDR and GCR) and confirmed its receptor specificity (Table 4_4)**.**

Table 4_3. Agonistic activities, metabolic properties and hERG inhibition of compounds **4_15**–**21** and GW501516.

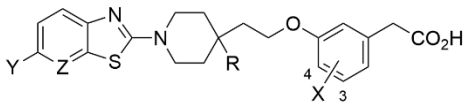

Cmpd	Y	Z	R	X	Transactivation EC_{50} (nM)						CLogP	CYP inhibition (μM)				Metabolic stability (%)		hERG inhibition (%)
					hPPARδ (E_{max})	hPPARα (E_{max}, hα/hδ)	hPPARγ (E_{max}, hγ/hδ)	mPPARδ (E_{max})	mPPARα (E_{max}, mα/mδ)	mPPARγ (E_{max}, mγ/mδ)		1A2	2C9	2D6	3A4	Human	Rat	
4_15	CF_3	CH		3-Cl	9.3 (24.0)	550 (2.9, 59)	1700 (4.5, 180)	14 (33.6)	4900 (6.3, 360)	1200 (4.3, 88)	4.0	>20	>20	>20	>20	88	104	78
4_16	CF_3	CH		3-Cl	22 (28.4)	NC (2.8, NC)	NC (4.7, NC)	120 (42.9)	NC (1.8, NC)	NC (4.2, NC)	3.4	>20	11	>20	>20	95	97	15
4_17	CF_3	CH		3-Cl	150 (11.4)	NC (1.6, NC)	NC (1.3, NC)	410 (22.3)	NC (1.7, NC)	NC (1.5, NC)	5.2	-	-	-	-	98	98	11
4_18	Cl	CH		3-Me	9.1 (29.4)	NC (3.3, NC)	1500 (6.3, 165)	34 (36.7)	NC (3.9, NC)	1800 (6.3, 53)	3.4	>20	>20	>20	>20	86	84	67
4_19	Cl	CH		4-Me	6.2 (26.4)	NC (3.5, NC)	1600 (6.6, 258)	28 (33.4)	3600 (7.9, 129)	NC (4.8, NC)	3.4	>20	>20	>20	8	75	81	78
4_20	CF_3	N		3-Cl	3.6 (18.9)	4300 (1.3, 1200)	4900 (2.9, 1360)	18 (28.7)	3100 (1.5, 172)	3900 (3.1, 217)	3.0	>20	>20	>20	>20	88	91	42
4_21	CF_3	N		4-Cl	22 (12.3)	6400 (5.8, 290)	3500 (6.7, 160)	70 (19.8)	17000 (9.6, 243)	3100 (6.8, 44)	2.8	-	-	-	-	-	-	44
GW501516					9.5 (16.8)	2200 (4.0, 232)	4400 (2.3, 463)	76 (23.9)	6100 (10.4, 80)	3500 (2.8, 46)	5.8	>20	>20	>20	>20	94	83	-

CLogP value was calculated using ChemDraw version 21.0 (PerkinElmer, Waltham, MA, USA). CYP inhibition was determined by the decrease in metabolites of probe substrates (% of control). Metabolic stability in liver microsome was determined as the remaining percentage of compound after 0.5 h. hERG inhibition was measured at 1 μM in HEK293 cells expressing hERG channels using an automated patch clamp system.

Table 4_4. Activation of nuclear receptors by **4_20** in transactivation assays using plasmid-introduced CHO-K1 cells.

Receptor	Concentration of **4_20** (μM)				
	0.1	0.3	1	3	10
LXRα	0.9 ± 0.2	1.0 ± 0.2	1.0 ± 0.1	1.1 ± 0.2	1.4 ± 0.3
RXRα	2.0 ± 0.1	2.1 ± 0.1	2.3 ± 0.2	2.5 ± 0.1	3.3 ± 0.3
TRβ	0.5 ± 0.1	0.6 ± 0.1	0.7 ± 0.1	0.8 ± 0.1	1.2 ± 0.2
RARα	1.0 ± 0.4	1.2 ± 0.3	1.0 ± 0.3	1.3 ± 0.2	1.5 ± 0.5
FXR	1.5 ± 0.4	1.4 ± 0.4	1.5 ± 0.3	1.7 ± 0.3	2.4 ± 0.6
VDR	0.4 ± 0.0	0.5 ± 0.0	0.5 ± 0.1	0.7 ± 0.1	0.9 ± 0.0
GCR	2.3 ± 0.1	2.4 ± 0.0	2.4 ± 0.0	2.7 ± 0.2	3.4 ± 0.4

Values are fold activation (% of positive control) expressed as the mean ± S.E. (n = 3). Fold activation values by positive control substances (1 μM) were 200.1 ± 53.7 for LXRα, 64.0 ± 1.7 for RXRα, 361.2 ± 90.7 for TRβ, 133.3 ± 31.0 for RARα, 110.1 ± 42.6 for FXR, 269.0 ± 60.2 for VDR, and 57.4 ± 9.0 for GCR, respectively. Positive control substances were T0901317 for LXRα, 9-*cis*-retinoic acid for RXRα and RARα, 3,3',5-triiodo-L-thyronine sodium salt for TRβ, chenodeoxycholic acid for FXR, 1α,25-dihydroxyvitamin D_3 for VDR, and dexamethasone for GCR, respectively.

The docking image of compound **4_20** to hPPARδ revealed that its pyrrolidinyl group fitted into the hydrophobic pocket while avoiding the Leu side chain (Figure 4_3). The docking score, calculated using Glide, was smaller than that of lead compound **2_11** (**4_20**: ΔG = -13 kcal/mol, **2_11**: ΔG = -11 kcal/mol). This added support to the agonist design which was mentioned above that introduction of the pyrrolidinyl group into the central piperidine ring of **2_11** would enhance the binding activity of PPARδ.

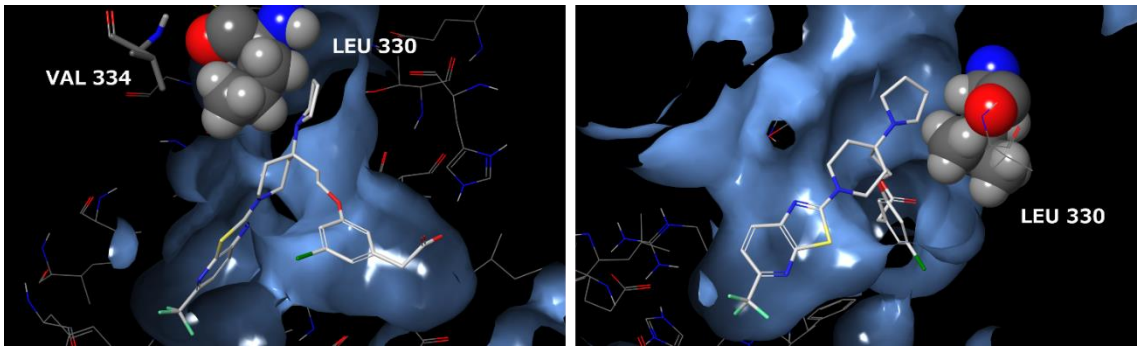

Figure 4_3. Docking images of compound **4_20** to hPPARδ (PDB ID = 1GWX) from two directions. Leu 330 of hPPARδ is represented by the CPK model.

The pharmacokinetic (PK) properties of compound **4_20** was evaluated in mouse, rat and dog (Table 4_5). The clearance (CL_t) values in rodents were lower than that of dog (mouse 3.16 mL/min/kg; rat 7.99 mL/min/kg; dog 15.4 mL/min/kg) and therefore the corresponding half-life ($T_{1/2}$) was longer in rodents than dog (mouse 8.37 h; rat 3.43 h; dog 0.6 h). Although the oral bioavailability (F) varied among animal species (mouse: 96.7%, rat: 38.0%, dog: 26.9%), the author decided these values were acceptable for *in vivo* efficacy study.

Table 4_5. Pharmacokinetic profiles of **4_20**.

Species	iv[a] (0.1 mg/kg, n = 3)			po[b] (1 mg/kg (mouse, rat), 0.3 mg/kg (dog), n = 3)			
	AUC (μg*h/mL)	CL_t (mL/min/kg)	$T_{1/2}$ (h)	AUC (μg*h/mL)	C_{max} (μg/mL)	T_{max} (h)	F (%)
mouse[c]	0.528	3.16	8.37	5.105	0.310	3.0	96.7
rat[d]	0.21 ± 0.023	7.99 ± 0.88	3.43 ± 1.35	1.050 ± 0.580	0.082 ± 0.034	4.67 ± 3.06	38.0 ± 21.0
dog[d]	0.11 ± 0.019	15.4 ± 2.50	0.6 ± 0.3	0.0852 ± 0.0212	0.0167 ± 0.0048	0.7 ± 0.3	26.9 ± 2.4

[a] Dosed as a solution of test compounds in *N*,*N*-dimethylacetamide/propylene glycol = 1/2.

[b] Dosed as a suspension of test compounds in 0.5% methylcellulose (MC, 400 cP).

[c] The PK parameters were calculated using the mean plasma concentrations of 3 mice at each time-point.

[d] Data are presented as mean ± SD.

The author evaluated serum parameters including monocyte chemoattractant protein 1 (MCP-1), which is considered to play an important role in recruitment of monocytes into atherosclerotic lesions,[21] in LDLr-KO mice fed with western diet. This model has been used extensively as an animal model of atherosclerosis induced by dyslipidemia and chronic inflammation.[22] It has been reported that PPARδ may modulate the progression of atherosclerosis via its anti-inflammatory effect, as well as its modulating effect on lipid metabolism.[23] Groups treated with **4_20** showed relatively low levels of serum MCP-1 compared with the vehicle-treated group (Table 4_6).

Table 4_6. Effect of **4_20** on serum MCP-1 in LDLr-KO mice.

Treatment		n	3w (pg/mL)		6w (pg/mL)	12w (pg/mL)		18w (pg/mL)	
Control (Vehicle)		15	154.0 ± 10.4		164.6 ± 14.1	365.2 ± 26.1		191.9 ± 19.3	
4_20	0.03 mg/kg	15	121.3 ± 9.7		134.0 ± 14.9	261.9 ± 27.0	**	143.9 ± 9.7	*
4_20	0.1 mg/kg	15	110.3 ± 13.5	**	129.6 ± 10.2	269.1 ± 24.5	*	127.3 ± 9.4	**
4_20	0.3 mg/kg	14	99.9 ± 4.3	***	129.5 ± 10.0	268.1 ± 20.8	*	162.6 ± 13.3	

Mice were orally dosed with the compounds or vehicle (0.5% methylcellulose 400 cP) once daily. Values are the mean ± S.E. of 14-15 mice. *p<0.05, **p<0.01, ***p<0.001 compared to vehicle-treated group (Dunnett's multiple comparison test).

Compound **4_20** was also examined to confirm the long-term effects on atherosclerotic lesion progression in the aorta. Aortic lesion areas (lesion% to total aortic surface) in **4_20**-treated groups were significantly smaller by 56.4% and 56.7% compared with the vehicle-treated group at the doses of 0.1 and 0.3 mg/kg, respectively (Figure 4_4). It was previously reported that, using LDLr-KO mice whose atherosclerosis was accelerated by angiotensin II, GW0742, a PPARδ agonist, suppressed atherosclerosis accompanied by the reduction of inflammatory markers such as MCP-1 and PAI-1 in blood, and MCP-1, TNF-α and IL-1β expression in atherosclerotic lesions with no significant effect on serum cholesterol profiles.[24] This present findings are consistent with these previous reports. Thus, it is considered that **4_20**, a selective PPARδ agonist, also inhibited the progression of atherosclerosis through a similar anti-inflammatory mechanism.

Figure 4_4. Effect of **4_20** on aortic lesion area in LDLr-KO mice.

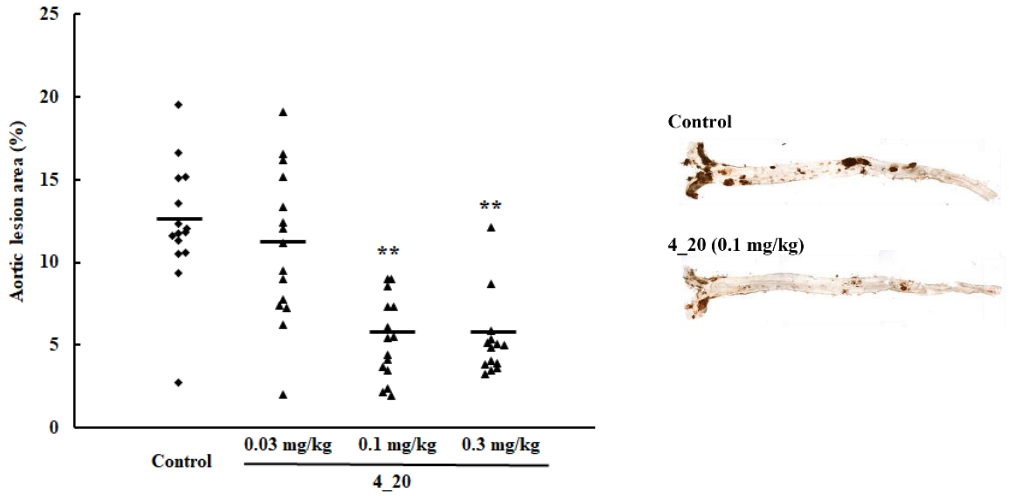

Vehicle (0.5% methylcellulose solution) or **4_20** (0.03, 0.1 or 0.3 mg/kg/day) was orally administered to 14–15 mice per treatment group once daily for 18 weeks. Values are the mean ± S.E. of 14-15 mice. **p<0.001 compared to vehicle-treated control group (Dunnett's multiple comparison test).

As previously reported, **4_20** induced reduction of the serum MCP-1 level and suppression of the atherosclerotic lesion progression with elevation of the serum HDL-C level in the hApoB100/hCETP-dTg mouse model with human-like dyslipidemia.[25] In this model, **4_20**-treated groups exhibited significant increase of the serum HDL-C level without influencing the non-HDL-C level at the doses of 0.1 and 0.3 mg/kg compared to the vehicle-treated group (133–134% vs control). On the other hand, treatment with **4_20** had limited effects on the serum HDL-C and non-HDL-C levels in the LDLr-KO mouse model, and there was no significant difference between control and **4_20**-treated groups after 18 weeks of treatment (Table 4_7 and Table 4_8). These results led to the conclusion that **4_20** also showed an inhibitory effect on the progression of atherosclerotic lesion area without influencing the serum HDL-C and non-HDL-C levels in the LDLr-KO mouse model. Thus, **4_20** has an anti-inflammatory potency independent of the effect on

lipids and has a beneficial effect against the lesion progression even at remarkably low doses, suggesting it may become a useful treatment option for preventing cardiovascular events.

Table 4_7. Serum HDL-C level of **4_20** in LDLr-KO mice and hApoB100/hCETP-dTg mice.

Treatment		LDLr-KO mice				hApoB100/hCETP-dTg mice		
		n	3w (mg/dL)		18w (mg/dL)	n	3w (mg/dL)	
Control (Vehicle)		15	105.7 ± 2.0		98.2 ± 2.8	12	47.1 ± 1.3	
4_20	0.1 mg/kg	15	114.8 ± 1.9	*	99.0 ± 3.3	12	62.8 ± 1.3	***
4_20	0.3 mg/kg	14	116.6 ± 1.8	**	90.5 ± 3.6	12	63.0 ± 1.0	***

Mice were orally dosed with the compounds or vehicle (0.5% methylcellulose 400 cP) once daily. Values are presented as mean ± SE of 14–15 or 12 mice. *p<0.05, **p<0.01, ***p<0.001 compared to vehicle-treated group (Dunnett's multiple comparison test).

Table 4_8. Serum non-HDL-C level of **4_20** in LDLr-KO mice and hApoB100/hCETP-dTg mice.

Treatment		LDLr-KO mice			hApoB100/hCETP-dTg mice	
		n	3w (mg/dL)	18w (mg/dL)	n	3w (mg/dL)
Control (Vehicle)		15	1531.9 ± 65.3	1871.6 ± 64.2	12	328.0 ± 15.9
4_20	0.1 mg/kg	15	1353.3 ± 52.4	1610.8 ± 120.1	12	311.2 ± 11.0
4_20	0.3 mg/kg	14	1437.9 ± 54.3	1828.3 ± 97.8	12	302.3 ± 9.7

Mice were orally dosed with the compounds or vehicle (0.5% methylcellulose 400 cP) once daily. Values are presented as mean ± SE of 14–15 or 12 mice.

In summary, based on information of the docking poses of PPAR isoforms and the lead compound **2_11**, cyclic aliphatic groups were introduced into the central piperidine ring to raise the hPPARδ activity and subtype selectivity. Insertion of a nitrogen atom into the cyclic side-chain led to clear improvement in CYP inhibition and metabolic stability by a decrease in hydrophobicity. Furthermore, the aza-replacement in the left benzothiazole moiety was effective for reducing hERG channel inhibition that causes arrhythmias. Consequently, 4-(1-pyrrolidinyl)piperidine derivative **4_20** was identified

as a potent and selective PPARδ agonist with excellent ADME properties. **4_20** strongly suppressed the atherosclerosis progression by 50–60% and lowered the serum level of MCP-1 in LDLr-KO mice. These findings indicate that **4_20** has anti-inflammatory potency and should be a valuable agent to help create novel therapeutics to prevent cardiovascular events.

Chapter 5

Summary

In this research, the author discovered novel PPARδ agonists having piperidinyl- or piperazinyl-benzothiazole structures and proved their serum HDL-C elevating and arterial anti-inflammatory effects *in vivo*. To explore for novel PPARδ agonists, the author initially identified the potent hit compound **2_1** from about 100,000 3D ligand structural data using docking simulations and virtual screening. Based on information of the docking poses of PPAR isoforms and the identified compounds, the author designed two chemotypes aiming at utilization of the relatively large hydrophobic pocket of PPARδ: alkyl substitution on the side of the piperazine ring and introduction of a cyclic amine at 4-position of the piperidine ring.

Among piperazinyl-benzothiazole derivatives having various alkyl chains on the 2- or 3-position of their central 6-membered rings, compound **3_11** with a 2-(*S*)-ethyl group and compound **3_19** with a 3-(*S*)-isopropyl group were identified as highly potent and selective PPARδ agonists. From the SAR study of this scaffold, it was found that the carboxyl group acted as a pivot point in ligand binding at the receptor pocket and located an alkyl group of the piperazine ring near the distinctive cavity. Compound **3_19** also exhibited a significant upregulation of serum HDL-C level in a rodent model of hypercholesterolemia.

4,4-Disubstituted piperidinyl-benzothiazole derivatives were also designed to enhance the subtype selectivity utilizing the difference in size of the binding cavities of PPARα, PPARγ and PPARδ. Compound **4_8** which have a cyclohexyl group at 4-position of the piperidine ring showed both high agonist activity for PPARδ and enough selectivity against PPARα/γ, whereas it had problems due to its high hydrophobicity. Insertion of a nitrogen atom into the cyclic side-chain led to clear improvement in CYP inhibition and

metabolic stability by the decrease in hydrophobicity. Furthermore, the aza-replacement in the left benzothiazole moiety was effective for reducing hERG channel inhibition that causes arrhythmias. Consequently, 4-(1-pyrrolidinyl)piperidine derivative **4_20** was identified as a potent and selective PPARδ agonist with excellent ADME properties. Compound **4_20** strongly suppressed the atherosclerosis progression by 50–60% and lowered the serum level of MCP-1 in LDLr-KO mice. This knowledge should be a valuable tool for drug discovery research.

Chapter 6

Synthetic routes to piperidinyl/piperazinyl-benzothiazole derivatives and experimentals

The synthesis of derivative **2_2** is shown in Scheme 6_1. Intermediate **6_2a** was prepared from commercially available 4-piperidineethanol (**6_1a**) and 2,6-dichlorobenzothiazole. **6_2a** was esterified with mono-*tert*-butyl succinate to afford *tert*-butyl ester 6_3, which was subsequently hydrolyzed to give derivative **2_2**. The virtual screening-hit compound **2_1** was commercially available.

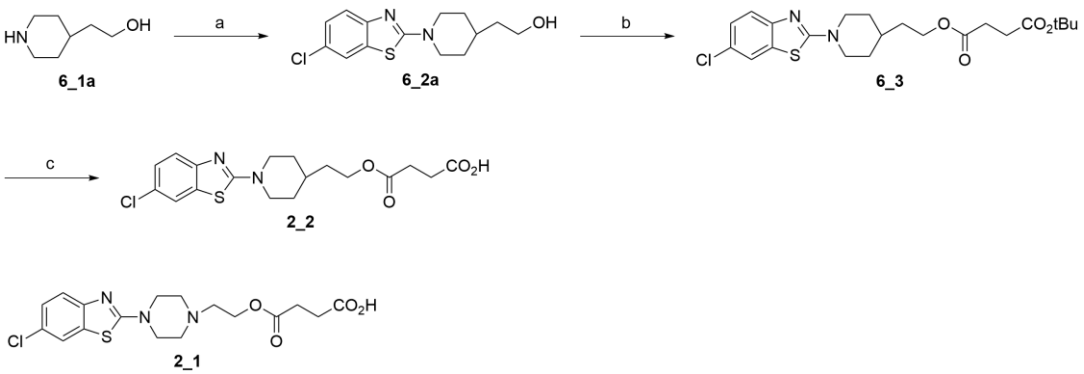

Scheme 6_1. Synthetic route to derivative **2_2**. Reagents and conditions: (a) 2,6-dichlorobenzothiazole, K_2CO_3, DMF, 60 °C; (b) mono-*tert*-butyl succinate, EDC·HCl, DMAP, DMF, rt; (c) 4 M HCl in 1,4-dioxane, rt.

Synthetic routes to derivatives **2_3–6** are shown in Scheme 6_2. Similar to the method above, intermediate **6_2b** was prepared from commercially available 4-piperidinemethanol (**6_1b**). The hydroxyl group of **6_2a–b** were replaced by chloride to give alkyl chloride **6_4a–b**, and then they were coupled with various phenols to afford ethyl esters **6_5a–d**. The intermediate esters were hydrolyzed to corresponding carboxylic acids **2_3–6**.

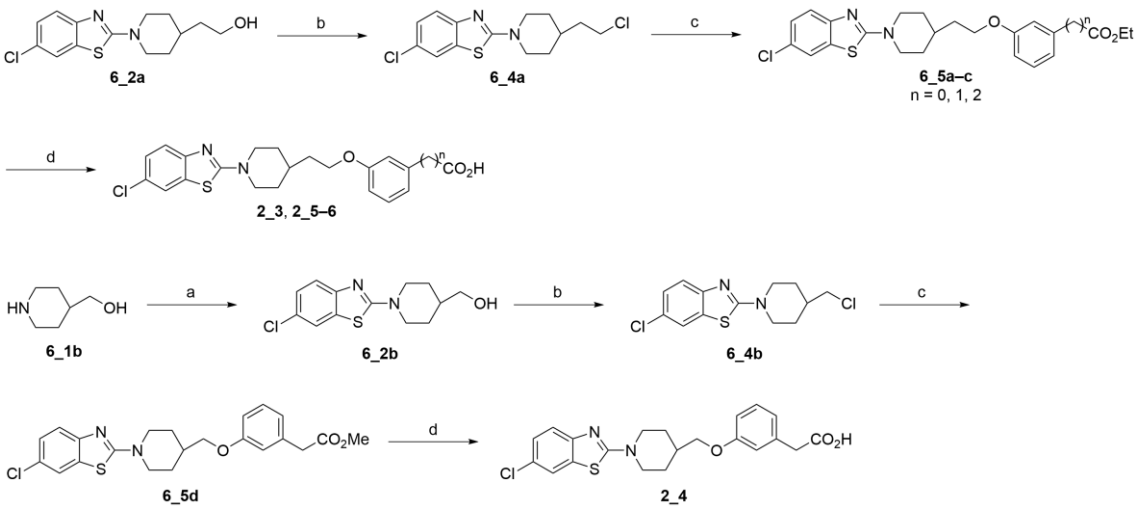

Scheme 6_2. Synthetic routes to derivatives **2_3–6**. Reagents and conditions: (a) 2,6-dichlorobenzothiazole, K_2CO_3, DMF, 60 °C; (b) $SOCl_2$, 60 °C; (c) phenols, Cs_2CO_3, DMF, 60 °C; (d) 2 M aq NaOH, MeOH, 60 °C.

Preparation of derivatives **2_7–12** are depicted in Scheme 6_3. Mitsunobu reaction between piperidineethanol **6_2a** and several substituted phenols gave ethers **6_6a–f**. Hydrolysis of ethyl esters **6_6a** and **6_6c–e** with 2 M aqueous NaOH afforded corresponding carboxylic acids **2_7** and **2_9–11**. On the other hand, nitriles **6_6b** and **6_6f** were converted into carboxylic acids **2_8** and **2_12** by base or acid treatment.

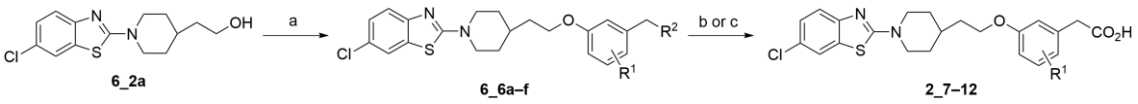

Scheme 6_3. Synthetic routes to derivatives **2_7–12**. Reagents and conditions: (a) phenols, ADDP, P(*n*-Bu)$_3$, THF, rt; (b) 2 M aq NaOH, MeOH, 60 °C; (c) NaOH, H_2O, EtOH, 80 °C / conc. H_2SO_4, H_2O, 80 °C.

As shown in Scheme 6_4, derivative **3_1** was synthesized similar to the method described above. Intermediate **6_8** was prepared from commercially available 1-piperazineethanol (**6_7**) and 2,6-dichlorobenzothiazole. The hydroxyl group of **6_7** was replaced by chloride to give alkyl chloride **6_9**, and then it was coupled with methyl 2-(3-hydroxy-4-methylphenyl)acetate to afford methyl ester **6_10**. The intermediate ester was hydrolyzed to carboxylic acid **3_1**.

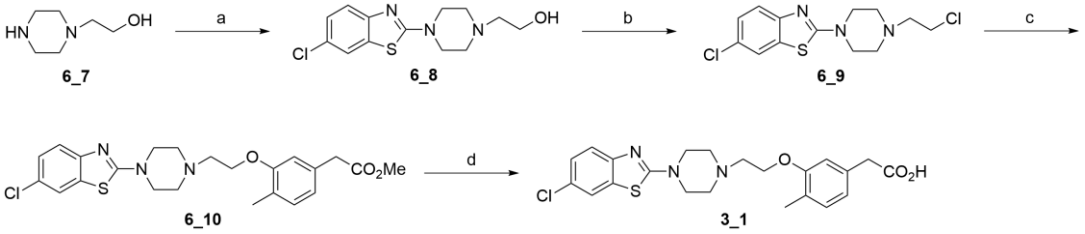

Scheme 6_4. Synthetic route to derivative **3_1**. Reagents and conditions: (a) 2,6-dichlorobenzothiazole, K_2CO_3, DMF, 60 °C; (b) $SOCl_2$, 60 °C; (c) methyl 2-(3-hydroxy-4-methylphenyl)acetate, Cs_2CO_3, DMF, 60 °C; (d) 2 M aq NaOH, MeOH, rt.

Synthetic routes to derivatives **3_2–4** and **3_8–11** are shown in Scheme 6_5. Commercially available 2,6-dichlorobenzothiazole (**6_11a**) or 2-chloro-6-trifluoromethylbenzothiazole (**6_11b**) was coupled with various unprotected piperazines, which were commercially available, to give intermediates **6_12a–f**. Each secondary amine of piperazine **6_12a–f** was made to react with methyl 2-bromoacetate, and then their ester groups were reduced by lithium aluminium hydride ($LiAlH_4$) under ice cooling to afford alcohols **6_14a–f** respectively. Reactions of methyl 2-(3-hydroxy-4-methylphenyl)acetate or methyl 2-(4-chloro-3-hydroxyphenyl)acetate were followed by conversion to mesylates using methanesulfonyl chloride (MsCl) to provide corresponding

methyl esters **6_15a–g**. Finally, their ester groups were hydrolyzed under basic condition to obtain carboxylic acids **3_2–4** and **3_8–11**.

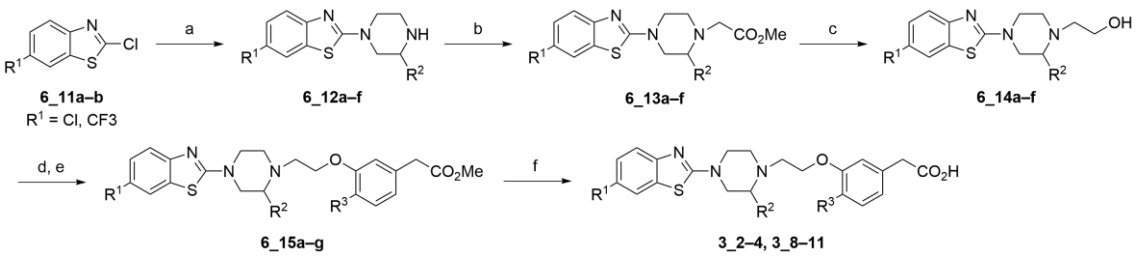

Scheme 6_5. Synthetic routes to derivatives **3_2–4** and **3_8–11**. Reagents and conditions: (a) piperazines, K_2CO_3, DMF, rt-50 °C; (b) methyl 2-bromoacetate, K_2CO_3, DMF, 60 °C; (c) $LiAlH_4$, THF, 0 °C; (d) MsCl, TEA, CH_2Cl_2, 0 °C-rt; (e) corresponding 3-hydroxyphenylacetic acid methyl esters, Cs_2CO_3, DMF, 60 °C; (f) 2 M aq NaOH, THF, MeOH, rt.

Synthesis of piperidine derivative **3_5** was commenced from 1-Boc-3-methyl-4-piperidone (**6_16**) as shown in Scheme 6_6. The Horner–Wadsworth–Emmons reaction of commercially available **6_16** with trimethyl phosphonoacetate gave α,β-unsaturated ester **6_17** as a mixture of stereoisomers (*E*:*Z* = ca. 4:3). This was followed by hydrogenation of the olefin and reduction with $LiAlH_4$ to provide alcohol **6_19**. Deprotection of Boc group of **6_19** followed by the reaction with 2,6-dichlorobenzothiazole gave **6_20**. After mesylation of the hydroxyl group using MsCl, it was coupled with methyl 2-(4-chloro-3-hydroxyphenyl)acetate, which was followed by hydrolysis of the methyl ester resulting in carboxylic acid **3_5** as a mixture of stereoisomers.

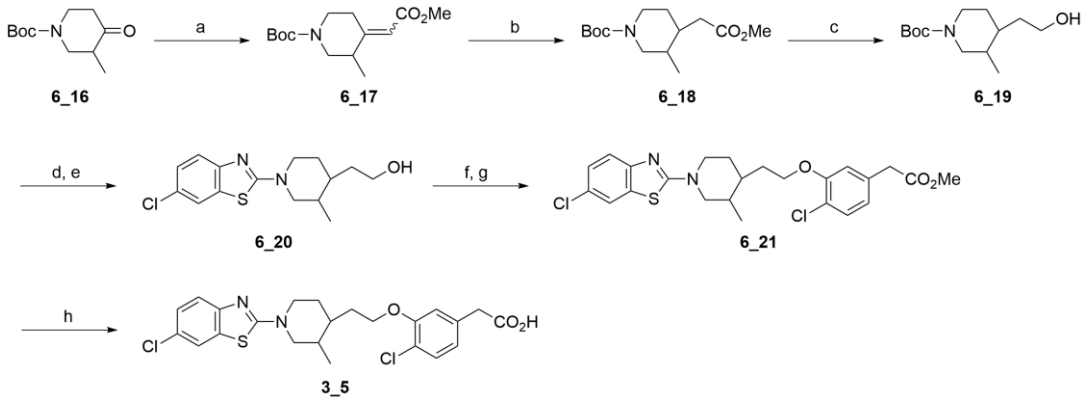

Scheme 6_6. Synthetic route to derivative **3_5**. Reagents and conditions: (a) trimethyl phosphonoacetate, NaOMe, THF, rt; (b) Pd/C, H_2, MeOH, rt; (c) $LiAlH_4$, THF, 0 °C; (d) 4 M HCl in 1,4-dioxane, rt; (e) 2,6-dichlorobenzothiazole, K_2CO_3, DMF, 60 °C; (f) MsCl, TEA, CH_2Cl_2, 0 °C; (g) methyl 2-(4-chloro-3-hydroxyphenyl)acetate, Cs_2CO_3, DMF, 60 °C; (h) 2 M aq NaOH, THF, MeOH, rt.

In the case of derivatives **3_6–7** with substituents at 3-position of piperazine ring, the initial coupling reactions were performed with Boc-protected piperazines to afford **6_22a–b**, and following deprotection reactions of the Boc groups by HCl solution gave intermediates **6_23a–b**. The secondary amines of piperazines **6_23a–b** were coupled with methyl 2-bromoacetate, and then their ester groups were reduced by $LiAlH_4$, mesylated using MsCl and coupled with methyl 2-(4-chloro-3-hydroxyphenyl)acetate to afford methyl esters **6_15h–i**. Their ester groups were hydrolyzed under basic condition to give carboxylic acids **3_6–7**.

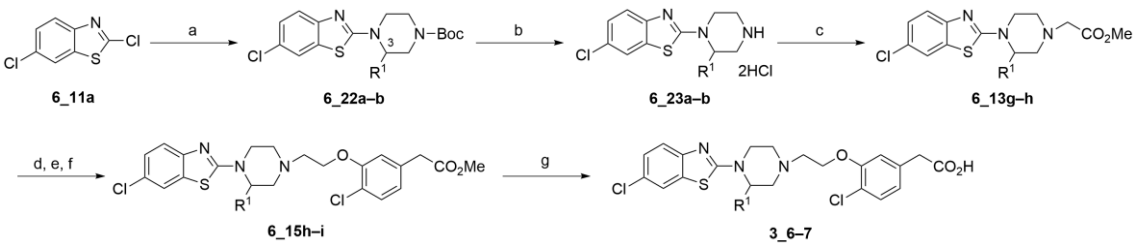

Scheme 6_7. Synthetic routes to derivatives **3_6–7**. Reagents and conditions: (a) *N*-Boc-piperazines, K_2CO_3, DMF, rt-50 °C; (b) 4 M HCl in 1,4-dioxane, rt; (c) methyl 2-bromoacetate, K_2CO_3, DMF, 60 °C; (d) $LiAlH_4$, THF, 0 °C; (e) MsCl, TEA, CH_2Cl_2, 0 °C-rt; (f) methyl 2-(4-chloro-3-hydroxyphenyl)acetate, Cs_2CO_3, DMF, 60 °C; (g) 2 M aq NaOH, THF, MeOH, rt.

Synthetic routes to derivatives **3_12–22** are shown in Scheme 6_8. Intermediates **6_25a**−**k** were prepared from **6_11b** and appropriate Boc-protected piperazines followed by deprotection. *N*-Boc deprotection reactions of some substrates carried out under heating conditions due to the steric hindrances around their nitrogen atoms. Alkylation of the piperazine secondary amines in **6_25a**−**k** with ethyl 2-(3-(bromomethyl)-5-methylphenyl)acetate and subsequent hydrolysis of the ethyl esters **26a**−**k** gave carboxylic acids **3_12–22** respectively.

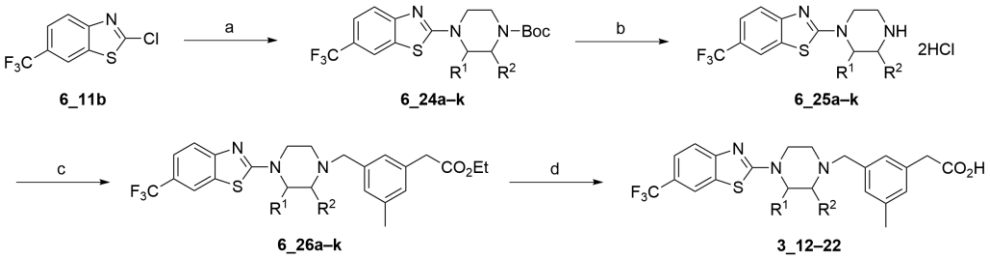

Scheme 6_8. Synthetic routes to derivatives **3_12–22**. Reagents and conditions: (a) *N*-Boc-piperazines, K_2CO_3, DMF, rt-50 °C; (b) 4 M HCl in 1,4-dioxane, 60 °C; (c) ethyl 2-(3-(bromomethyl)-5-methylphenyl)acetate, K_2CO_3, DMF, 60 °C; (d) 2 M aq NaOH, MeOH, 60 °C.

Synthetic routes to derivatives of **4_1–9** were prepared as outlined in Scheme 6_9. The synthesis began with the Horner-Wadsworth-Emmons reaction of commercially available 1-Boc-4-piperidone (**6_27**) and trimethyl phosphonoacetate to afford α,β-unsaturated methyl ester **6_28**. After deprotection of the Boc group of **6_28** using HCl solution, it was coupled with methyl 2,6-dichlorobenzothiazole to give intermediate **6_29**, which was followed by functionalization with alkyl groups using Grignard reagents in the presence of copper iodide to afford the corresponding 4,4-disubstituted piperidines **6_30a**–**h**. Their ester groups were reduced with $LiAlH_4$ to give alcohols **31a**–**h**. In the case of the ethyl or *iso*-propyl derivatives, nucleophilic substitution reaction with methyl 2-(4-chloro-3-hydroxyphenyl)acetate was followed by conversion to chloride using $SOCl_2$ to afford **32a** and **32d**. For the other derivatives, the coupling reaction was followed by conversion to mesylates using MsCl to afford the corresponding **32b**–**c** and **32e**–**i**. Finally, their ester groups were hydrolyzed under basic condition to obtain carboxylic acid **4_1–9**.

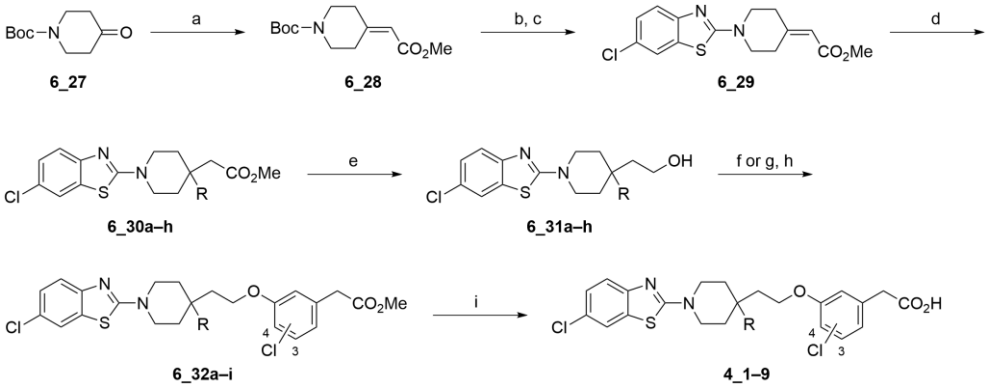

Scheme 6_9. Synthetic routes to derivatives **4_1–9**. Reagents and conditions: (a) NaH, trimethyl phosphonoacetate, DMF, 50 °C; (b) 4 M HCl in 1,4-dioxane, rt; (c) 2,6-dichlorobenzothiazole, K_2CO_3, DMF, 60 °C; (d) CuI, Grignard reagent, TMSOTf, −78 °C; (e) $LiAlH_4$, THF, 0 °C; (f) $SOCl_2$, 60 °C; (g) MsCl, TEA, CH_2Cl_2, rt; (h) corresponding phenylacetic acid methyl esters, Cs_2CO_3, DMF, 60 °C; (i) 2 M aq NaOH, THF, MeOH, rt.

As depicted in Scheme 6_10, the synthetic routes to derivatives of **4_10–16** and **4_18–19** are as follows. Commercially available 1-benzyl-4-piperidone (**6_33**) was first converted to the corresponding enamine intermediates with secondary amines under reflux condition. After iminium salt formation with AcOH, the Reformatsky reaction was performed successfully by addition of methyl bromoacetate in the presence of zinc to afford 4,4-disubstituted piperidine intermediates **34a**–**f**. After reduction with $LiAlH_4$, the removal of their benzyl group via Pd/C-catalyzed hydrogenolysis and subsequent coupling of the resulting amines with 2,6-dichlorobenzothiazole or 2-chloro-6-(trifluoromethyl)benzothiazole gave alcohols **35a**–**g**. Next, following the Mitsunobu reaction with methyl 2-(3-chloro-5-hydroxyphenyl)acetate, methyl 2-(3-hydroxy-5-methylphenyl)acetate or methyl 2-(3-hydroxy-4-methylphenyl)acetate, the resulting esters **36a**–**i** were hydrolyzed with NaOH to furnish carboxylic acids **4_10–16** and **4_18–19**.

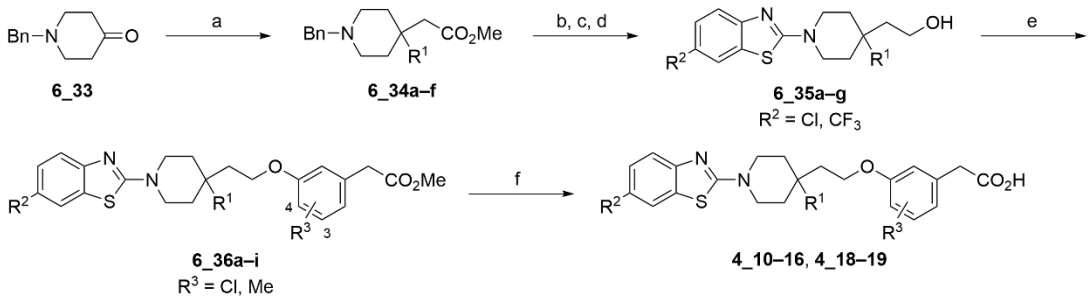

Scheme 6_10. Synthetic routes to derivatives **4_10–16** and **4_18–19**. Reagents and conditions: (a) corresponding amines, toluene, reflux, then AcOH, Zn, methyl bromoacetate, THF, rt; (b) $LiAlH_4$, THF, 0 °C; (c) Pd/C, H_2, MeOH, rt; (d) Ar-Cl, K_2CO_3, DMF, 60 °C; (e) corresponding phenylacetic acid methyl esters, ADDP, tri-*n*-butylphosphine, THF, rt; (f) 2 M aq NaOH, THF, MeOH, rt.

Scheme 6_11 shows the synthetic route of derivative **4_17**. First, *exo*-olefin **6_38** was prepared by the Wittig reaction of commercially available benzyl 4-oxopiperidine-1-carboxylate (**6_37**) with the phosphorous ylide which was generated from the reaction of methyltriphenylphosphonium bromide and *n*-BuLi. Cycloaddition of chlorosulfonyl isocyanate to alkene **6_38** provided β-lactam **6_39**, followed by hydrolysis and esterification of the resulting carboxylic acid using concentrated HCl in MeOH to afford methyl ester **6_40**. After amidation with 4-bromobutyryl chloride, pyrrolidone intermediate **6_42** was obtained via intramolecular cyclization. Subsequently, reduction of **6_42** by lithium borohydride provided alcohol **6_43**, which was deprotected via Pd/C-catalyzed hydrogenolysis, coupling with 2-chloro-6-(trifluoromethyl)benzothiazole, the Mitsunobu reaction with methyl 2-(3-chloro-5-hydroxyphenyl)acetate, and hydrolysis of the methyl ester to give carboxylic acid **4_17**.

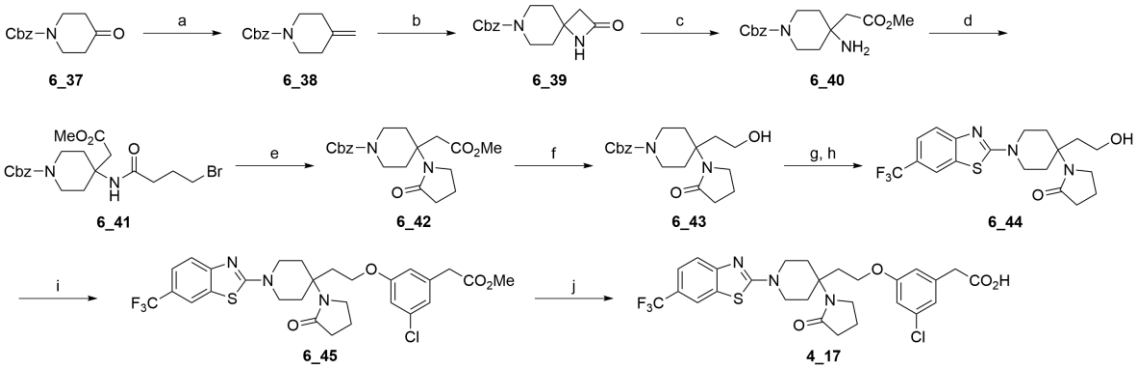

Scheme 6_11. Synthetic routes to derivatives **4_17**. Reagents and conditions: (a) *n*-BuLi, methyltriphenylphosphonium bromide, THF, 0 °C; (b) chlorosulfonyl isocyanate, Et_2O, 0 °C; (c) conc. HCl, MeOH, 95 °C; (d) 4-bromobutyryl chloride, pyridine, rt; (e) NaH, DMF, rt; (f) $LiBH_4$, Et_2O, MeOH, reflux; (g) Pd/C, H_2, THF, rt; (h) 2-chloro-6-(trifluoromethyl)benzothiazole K_2CO_3, DMF, 70 °C; (i) methyl 2-(3-chloro-5-hydroxyphenyl)acetate, DEAD, triphenylphosphine, THF, rt; (j) 2 M aq NaOH, THF, MeOH, rt.

The synthetic routes of 4-aza-benzothiazole derivatives **4_20** and **4_21** are shown in Scheme 6_12. Initially, commercially available 2-chloro-6-(trifluoromethyl)pyridin-3-amine (**6_46**) was treated with potassium ethylxanthate, followed by conversion of the thiol group to chloride via treatment with $SOCl_2$ to provide **6_48**. Coupling of chloride **6_48** with 2-(4-(pyrrolidin-1-yl)piperidin-4-yl)ethan-1-ol, prepared above, provided intermediate **6_49**, which was then subjected to the Mitsunobu reaction with methyl 2-(3-chloro-5-hydroxyphenyl)acetate or methyl 2-(4-chloro-3-hydroxyphenyl)acetate, and hydrolysis of the methyl esters to afford carboxylic acids **4_20** and **4_21**.

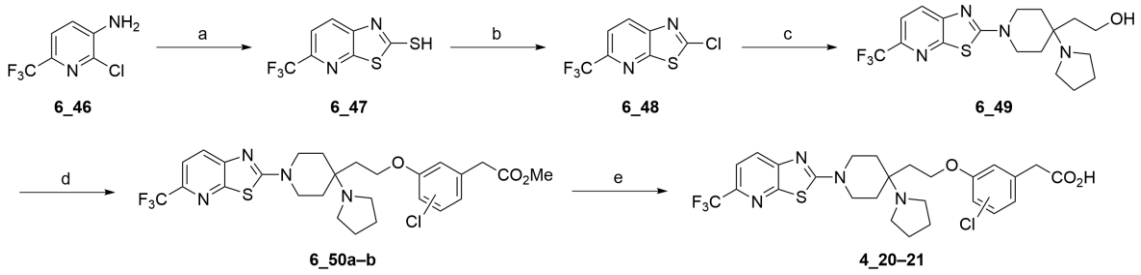

Scheme 6_12. Synthetic routes to derivatives **4_20** and **4_21**. Reagents and conditions: (a) potassium ethylxanthate, DMF, 120 °C; (b) $SOCl_2$, CH_2Cl_2, rt; (c) 2-(4-(pyrrolidin-1-yl)piperidin-4-yl)ethan-1-ol, K_2CO_3, DMF, 60 °C; (d) methyl 2-(3-chloro-5-hydroxyphenyl)acetate or methyl 2-(4-chloro-3-hydroxyphenyl)acetate, ADDP, tri-*n*-butylphosphine, THF, rt; (e) 2 M aq NaOH, THF, MeOH, rt.

Experimentals

General

All commercially available chemicals and reagents were used without any further purification unless otherwise indicated. Column chromatography was done on a purification system using prepacked silica gel columns. ^{1}H NMR spectra were measured on a Varian MERCURY system (300 MHz) or a Bruker AVANCE system (400 MHz). Chemical shifts (δ) are reported as parts per million (ppm), and tetramethylsilane was used as an internal reference. For peak multiplicities, the following abbreviations are used: singlet (s), doublet (d), double doublets (dd), double doublet (ddd), double triplet (dt), triplet (t), quartet (q), multiplet (m), and broad peak (br). Coupling constants (J) are given in Hertz (Hz). High-resolution mass spectral (HRMS) data were acquired with a Waters Xevo G2 Tof (ESI) and low-resolution mass spectral data were collected with a Waters SQD mass detector (ESI). The purity of the compounds was confirmed by LCMS. A Waters Acquity UPLC system comprising Binary Solvent manager, Sample Manager, PDA Detector, SQD mass spectrometer, and Acquity evaporative light scattering detector were employed. Column: Waters ACQUITY UPLC BEH C18 (1.7 μm, i.d. 2.1 × 50 mm). Flow rate: 0.8 mL/min. UV detection wavelength: 254 nm. Mobile phase: [A] is 0.1% formic acid-containing aqueous solution, and [B] is 0.1% formic acid-containing acetonitrile solution. Gradient: linear gradient of 5–100% solvent [B] for 3.5 min was performed, and 100% solvent [B] was maintained for 0.5 min. All compounds used in the bioassays are >95% pure based on HPLC-MS data. The animal study protocols were designed and refined by taking reduction of animal use into consideration and approved by the Institutional Animal Care and Use Committee of Shionogi Research Laboratories.

Typical procedure for synthesis of compounds **6_2a–b**

A mixture of 4-piperidine alcohol **6_1** (16.2 mmol), 2,6-dichlorobenzothiazole (3.00 g, 14.7 mmol), potassium carbonate (2.33 g, 16.2 mmol) and anhydrous DMF (15 mL) was stirred at room temperature for 16 hours. Water and EtOAc were added to the reaction solution. The organic layer was separated, washed with brine, dried over anhydrous Na_2SO_4, and evaporated under reduced pressure. The precipitate was washed with IPE to give the target compound.

Compound **6_2a**

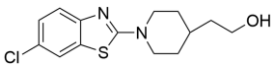

Yellow solid, 67% yield. ^{1}H NMR (400 MHz, $CDCl_3$) : δ 1.29-1.39 (m, 2H), 1.56 (q, J = 6.6 Hz, 2H), 1.72-1.80 (m, 1H), 1.81-1.87 (m, 2H), 3.13 (td, J = 12.8, 2.7 Hz, 2H), 3.73 (t, J = 6.6 Hz, 2H), 4.08-4.13 (m, 2H), 7.23 (dd, J = 8.6, 2.1 Hz, 1H), 7.43 (d, J = 8.6 Hz, 1H), 7.54 (d, J = 2.1 Hz, 1H). ^{13}C NMR (100 MHz, $CDCl_3$) : δ 31.56, 32.31, 38.94, 49.07, 60.01, 119.33, 120.31, 126.28, 126.42, 131.59, 151.09, 168.70. HRMS (ESI) : m/z [M + H]$^+$ calcd. for $C_{14}H_{18}ClN_2OS^+$, 297.0823; found, 279.0845.

Compound **6_2b**

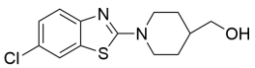

Yellow solid, 100% yield. ^{1}H NMR (400 MHz, $CDCl_3$) : δ 1.32-1.42 (m, 2H), 1.74-1.82 (m, 1H), 1.85-1.90 (m, 2H), 3.13 (td, J = 12.8, 2.8 Hz, 2H), 3.54 (d, J = 6.3 Hz, 2H), 4.12-4.16 (m, 2H), 7.23 (dd, J = 8.6, 2.1 Hz, 1H), 7.42 (d, J = 8.6 Hz, 1H), 7.54 (d, J = 2.1 Hz, 1H). ^{13}C NMR (100 MHz, $CDCl_3$) : δ 28.11, 38.50, 48.67, 67.18, 119.42, 120.30, 126.21,

126.37, 131.85, 151.45, 168.79. HRMS (ESI) : m/z $[M + H]^+$ calcd. for $C_{13}H_{16}ClN_2OS^+$, 283.0666; found, 283.0691.

Synthesis of compound **6_3**

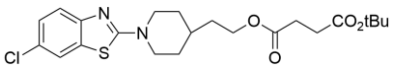

A mixture of **6_2a** (50.0 mg, 0.168 mmol), mono-*tert*-butyl succinate (35.2 mg, 0.202 mmol), EDC·HCl (38.8 mg, 0.202 mmol), (2.06 mg, 0.017 mmol) and DMF (1.0 mL) was stirred at room temperature for 3 hours. To the reaction mixture was added aqueous $NaHCO_3$ solution and extracted with EtOAc. The organic layer was washed with water and brine, and dried over Na_2SO_4. The solvent was evaporated under reduced pressure and the residue was purified by silica gel column chromatography to give compound **6_3** as a yellow solid (75.4 mg, 99%). ^{1}H NMR (400 MHz, DMSO-d_6) : δ 1.23 (ddd, J = 24.2, 12.4, 4.0 Hz, 2H), 1.38 (s, 9H), 1.55 (q, J = 6.6 Hz, 2H), 1.63-1.71 (m, 1H), 1.76-1.80 (m, 2H), 2.44-2.50 (m, 4H), 3.14 (td, J = 12.4, 2.3 Hz, 2H), 3.98-4.01 (m, 2H), 4.09 (t, J = 6.5 Hz, 2H), 7.27 (dd, J = 8.7, 2.3 Hz, 1H), 7.39 (d, J = 8.7 Hz, 1H), 7.88 (d, J = 2.3 Hz, 1H).

Synthesis of compound **2_2**

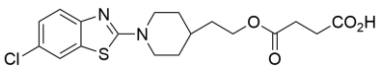

To 4 M solution of hydrochloric acid-dioxane (754 μL, 3.02 mmol) was added **6_3** (68.3 mg, 0.151 mmol). After stirring at room temperature for 2 hours, the reaction mixture was concentrated under reduced pressure and became pH 4 with aqueous $NaHCO_3$ solution. The precipitate was washed with water and IPE to give compound **2_2** as a white solid

(38.4 mg, 64%). ^{1}H NMR (400 MHz, DMSO-d_6) : δ 1.17-1.28 (m, 2H), 1.55 (q, J = 6.6 Hz, 2H), 1.63-1.71 (m, 1H), 1.75-1.81 (m, 2H), 3.10-3.19 (m, 2H), 3.98-4.01 (m, 2H), 4.09 (t, J = 6.5 Hz, 2H), 7.27 (dd, J = 8.6, 2.2 Hz, 1H), 7.40 (d, J = 8.7 Hz, 1H), 7.88 (d, J = 2.3 Hz, 1H), 12.23 (br s, 1H). ^{13}C NMR (100 MHz, DMSO-d_6) : δ 28.60, 28.68, 30.71, 31.81, 34.25, 48.27, 61.52, 119.09, 120.69, 124.55, 125.99, 131.80, 151.37, 168.23, 171.99, 173.30. HRMS (ESI) : m/z $[M + H]^+$ calcd. for $C_{18}H_{22}ClN_2O_4S^+$, 397.0983; found, 397.0983.

Typical procedure for synthesis of compounds **6_4a–b**

A mixture of **6_2a–b** (4.03 mmol) and $SOCl_2$ (10 mL) were stirred at 60 °C for 1 hour. The reaction mixture was poured into ice water and added with 5 M aqueous NaOH solution to neutralize. The precipitate was collected and washed with IPE to give the target compound.

Compound **6_4a**

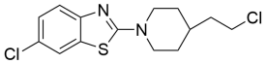

White solid, 77% yield. ^{1}H NMR (300 MHz, $CDCl_3$) : δ 1.25-1.44 (m, 2H), 1.70-1.94 (m, 5H), 3.08-3.22 (m, 2H), 3.62 (t, J = 6.5 Hz, 2H), 4.07-4.20 (m, 2H), 7.23 (dd, J = 8.5, 2.0 Hz, 1H), 7.43 (d, J = 8.5 Hz, 1H), 7.55 (d, J = 2.0, 1H).

Compound **6_4b**

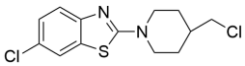

White solid, 89% yield. ^{1}H NMR (300 MHz, DMSO-d_6) : δ 1.20-1.42 (m, 2H), 1.80-2.00

(m, 3H), 3.10-3.25 (m, 2H), 3.60 (d, *J* = 6.5 Hz, 2H), 4.00-4.10 (m, 2H), 7.28 (dd, *J* = 8.5, 2.0 Hz, 1H), 7.41 (d, *J* = 8.5 Hz, 1H), 7.90 (d, *J* = 2.0 Hz, 1H).

Typical procedure for synthesis of compounds **6_5a–d**

A mixture of **6_4** (1.59 mmol), the corresponding phenol (2.39 mmol), Cs_2CO_3 (779 mg, 2.39 mmol) and DMF (5 mL) was stirred at 60 °C for 9 hours. Water was added, and the mixture was extracted with EtOAc. The extract was washed with brine, dried over Na_2SO_4, and concentrated under reduced pressure. The residue was purified by silica gel column chromatography to give the target compound.

Compound **6_5a**

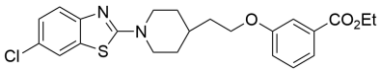

White solid, 62% yield. ^{1}H NMR (300 MHz, $CDCl_3$) : δ 1.30-1.51 (m, 5H), 1.74-1.97 (m, 5H), 3.09-3.22 (m, 2H), 4.04-4.18 (m, 4H), 4.38 (q, *J* = 7.0 Hz, 2H), 7.09 (dd, *J* = 8.0, 1.5 Hz, 1H), 7.23 (dd, *J* = 8.5, 2.0 Hz, 1H), 7.35 (t, *J* = 8.0 Hz, 1H), 7.42 (d, *J* = 8.5 Hz, 1H), 7.52-7.58 (m, 2H), 7.65 (dd, *J* = 8.0, 1.5 Hz, 1H).

Compound **6_5b**

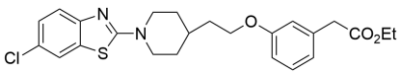

Colorless oil, 46% yield. ^{1}H NMR (300 MHz, $CDCl_3$) : δ 1.24 (t, *J* = 7.0 Hz, 3H), 1.23-1.44 (m, 2H), 1.67-1.92 (m, 5H), 3.02-3.16 (m, 2H), 3.57 (s, 2H), 3.98 (t, *J* = 6.0 Hz, 2H), 4.02-4.15 (m, 2H), 4.14 (q, *J* = 7.0 Hz, 2H), 6.75-6.90 (m, 3H), 7.16-7.26 (m, 2H), 7.41 (d, *J* = 8.5 Hz, 1H), 7.51 (d, *J* = 2.0 Hz, 1H).

Compound **6_5c**

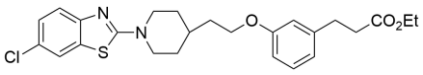

White solid, 71% yield. ^{1}H NMR (300 MHz, $CDCl_3$) : δ 1.24 (t, J = 7.0 Hz, 3H), 1.31-1.49 (m, 2H), 1.73-1.95 (m, 5H), 2.62 (t, J = 8.0 Hz, 2H), 2.93 (t, J = 8.0 Hz, 2H), 3.08-3.21 (m, 2H), 4.02 (t, J = 6.0 Hz, 2H), 4.07-4.20 (m, 2H), 4.13 (q, J = 7.0 Hz, 2H), 6.71-6.84 (m, 3H), 7.16-7.25 (m, 2H), 7.42 (d, J = 8.5 Hz, 1H), 7.54 (d, J = 2.0 Hz, 1H).

Compound **6_5d**

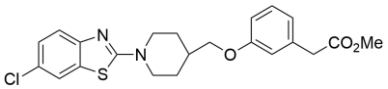

Colorless oil, 23% yield. ^{1}H NMR (400 MHz, $CDCl_3$) : δ 1.51 (ddd, J = 25.1, 12.6, 4.4 Hz, 2H), 1.97-2.01 (m, 2H), 2.07-2.13 (m, 1H), 3.18 (dt, J = 12.9, 2.7 Hz, 2H), 3.60 (s, 2H), 3.70 (s, 3H), 3.85 (d, J = 6.3 Hz, 2H), 4.17-4.20 (m, 2H), 6.79-6.87 (m, 3H), 7.21-7.25 (m, 2H), 7.43 (d, J = 8.7 Hz, 1H), 7.56 (d, J = 2.1 Hz, 1H).

Typical procedure for synthesis of compounds **2_3–6**

To a solution of **6_5** (0.300 mmol) in THF (1 mL) and MeOH (1 mL) was added 2 M aqueous NaOH solution (0.45 mL, 0.900 mmol), and the mixture was stirred at 60 °C for 1 hour. To the reaction mixture was added 2 M aqueous HCl solution to be pH 4. The precipitate was collected and washed with water and IPE to give the target compound.

Compound **2_3**

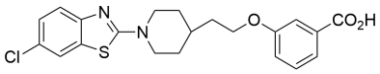

White solid, 93% yield. ^{1}H NMR (400 MHz, DMSO-d_6) : δ 1.25-1.34 (m, 2H), 1.70-1.75 (m, 2H), 1.81-1.88 (m, 3H), 3.17 (t, J = 12.2 Hz, 2H), 4.01 (d, J = 11.9 Hz, 2H), 4.09 (t, J = 6.2 Hz, 2H), 7.20 (d, J = 7.9 Hz, 1H), 7.27 (d, J = 8.7 Hz, 1H), 7.38-7.43 (m, 2H), 7.45 (s, 1H), 7.53 (d, J = 7.5 Hz, 1H), 7.87 (s, 1H), 12.93 (br s, 1H). ^{13}C NMR (100 MHz, DMSO-d_6) : δ 30.88, 32.05, 34.76, 48.32, 65.33, 114.47, 119.13, 119.25, 120.65, 121.41, 124.54, 125.97, 129.61, 131.89, 132.10, 151.53, 158.49, 167.03, 168.25. HRMS (ESI) : m/z $[M + H]^+$ calcd. for $C_{21}H_{22}ClN_2O_3S^+$, 417.1034; found, 417.1037.

Compound **2_4**

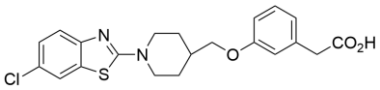

White solid, 87% yield. ^{1}H NMR (400 MHz, DMSO-d_6) : δ 1.34-1.44 (m, 2H), 1.88-1.93 (m, 2H), 2.03-2.12 (m, 1H), 3.17-3.25 (m, 2H), 3.50 (s, 2H), 3.86 (d, J = 6.4 Hz, 2H), 4.07 (d, J = 13.2 Hz, 2H), 6.80-6.83 (m, 3H), 7.20 (t, J = 7.8 Hz, 1H), 7.28 (dd, J = 8.5, 2.3 Hz, 1H), 7.41 (d, J = 8.5 Hz, 1H), 7.89 (d, J = 2.1 Hz, 1H), 12.38 (br s, 1H). ^{13}C NMR (100 MHz, DMSO-d_6) : δ 27.68, 35.04, 40.82, 47.95, 71.27, 112.39, 115.54, 119.16, 120.67, 121.53, 124.56, 125.98, 129.08, 131.88, 136.59, 151.50, 158.42, 168.29, 172.45. HRMS (ESI) : m/z $[M + H]^+$ calcd. for $C_{21}H_{22}ClN_2O_3S^+$, 417.1034; found, 417.1028.

Compound **2_5**

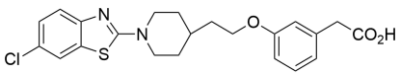

White solid, 78% yield. ^{1}H NMR (400 MHz, DMSO-d_6) : δ 1.24-1.34 (m, 2H), 1.67-1.73 (m, 2H), 1.79-1.86 (m, 3H), 3.17 (t, J = 12.2 Hz, 2H), 3.52 (s, 2H), 3.99-4.04 (m, 4H),

6.82 (d, J = 7.5 Hz, 2H), 6.84 (s, 1H), 7.21 (t, J = 7.7 Hz, 1H), 7.27 (d, J = 8.5 Hz, 1H), 7.40 (d, J = 8.5 Hz, 1H), 7.87 (s, 1H), 12.25 (br s, 1H). ^{13}C NMR (100 MHz, DMSO-d_6) : δ 30.89, 32.05, 34.87, 40.59, 48.32, 64.92, 112.42, 115.60, 119.13, 120.64, 121.45, 124.53, 125.96, 129.12, 131.89, 136.32, 151.53, 158.42, 168.25, 172.41. HRMS (ESI) : m/z $[M + H]^+$ calcd. for $C_{22}H_{24}ClN_2O_3S^+$, 431.1191; found, 431.1205.

Compound **2_6**

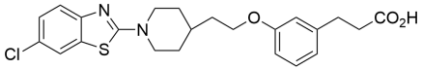

White solid, 35% yield. ^{1}H NMR (400 MHz, DMSO-d_6) : δ 1.25-1.34 (m, 2H), 1.67-1.72 (m, 2H), 1.80-1.86 (m, 3H), 2.51-2.54 (m, 2H), 2.79 (t, J = 7.6 Hz, 2H), 3.17 (t, J = 12.2 Hz, 2H), 3.99-4.03 (m, 4H), 6.77 (t, J = 8.5 Hz, 2H), 6.81 (s, 1H), 7.17 (t, J = 7.8 Hz, 1H), 7.27 (d, J = 8.5 Hz, 1H), 7.40 (d, J = 8.5 Hz, 1H), 7.87 (s, 1H), 12.07 (s, 1H).. ^{13}C NMR (100 MHz, DMSO-d_6) : δ 30.29, 30.89, 32.06, 34.90, 35.04, 48.33, 64.86, 111.87, 114.38, 119.14, 120.31, 120.65, 124.54, 125.97, 129.18, 131.91, 142.38, 151.55, 158.55, 168.26, 173.63. HRMS (ESI) : m/z $[M + H]^+$ calcd. for $C_{23}H_{26}ClN_2O_3S^+$, 445.1347; found, 445.1346.

Typical procedure for synthesis of compounds **6_6a–f**

To a mixture of **6_2a** (10.2 mmol), the corresponding phenol (the corresponding phenols 10.2 mmol), 1,1-azodicarbonyldipiperidine (3.86 g, 15.3 mmol) and anhydrous THF (100 mL) was added dropwise tributyl phosphine (3.81 mL, 15.3 mmol) under ice-cooling. After stirring the reaction solution at the same temperature for 3 hours, water and EtOAc were added thereto. The organic layer was separated, washed with brine, dried over

anhydrous sodium sulphate, and evaporated under reduced pressure. The residue was purified by silica gel column chromatography to give the target compound.

Compound **6_6a**

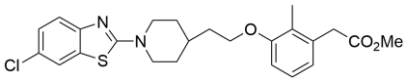

Colorless oil, 65% yield. 1H NMR (400 MHz, CDCl3) : δ 1.36-1.46 (m, 2H), 1.79-1.83 (m, 2H), 1.88-1.93 (m, 3H), 2.18 (s, 3H), 3.11-3.18 (m, 2H), 3.66 (s, 2H), 3.69 (s, 3H), 4.03 (t, *J* = 6.0 Hz, 2H), 4.11-4.15 (m, 2H), 6.76-6.84 (m, 2H), 7.12 (t, *J* = 7.9 Hz, 1H), 7.23 (dd, *J* = 8.5, 2.1 Hz, 1H), 7.43 (d, *J* = 8.5 Hz, 1H), 7.55 (d, *J* = 2.1 Hz, 1H).

Compound **6_6b**

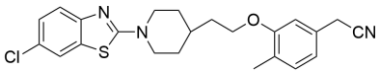

Yellow oil, 71% yield. ^{1}H NMR (300 MHz, $CDCl_3$) : *δ* 1.38-1.48 (m, 2H), 1.81-1.93 (m, 5H), 2.21 (s, 3H), 3.10-3.18 (m, 2H), 3.71 (s, 2H), 4.05 (t, *J* = 5.7 Hz, 2H), 4.11-4.15 (m, 2H), 6.76-6.80 (m, 2H), 7.12 (d, *J* = 7.5 Hz, 1H), 7.22 (dd, *J* = 8.6, 2.0 Hz, 1H), 7.42 (d, *J* = 8.6 Hz, 1H), 7.54 (d, *J* = 2.0 Hz, 1H).

Compound **6_6c**

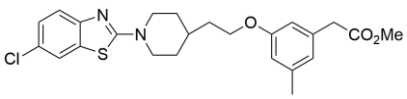

Yellow oil, 33% yield. ^{1}H NMR (400 MHz, $CDCl_3$) : *δ* 1.35-1.44 (m, 2H), 1.74-1.79 (m, 2H), 1.85-1.91 (m, 3H), 2.31 (s, 3H), 3.11-3.17 (m, 2H), 3.56 (s, 2H), 3.70 (s, 3H), 4.01

(t, *J* = 6.1 Hz, 2H), 4.09-4.15 (m, 2H), 6.64 (s, 2H), 6.69 (s, 1H), 7.23 (dd, *J* = 8.6, 2.2 Hz, 1H), 7.42 (d, *J* = 8.5 Hz, 1H), 7.54 (d, *J* = 2.1 Hz, 1H).

Compound **6_6d**

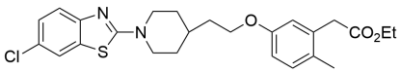

Colorless oil, 79% yield. ^{1}H NMR (300 MHz, $CDCl_3$) : δ 1.28 (t, *J* = 7.2 Hz, 3H), 1.36-1.48 (m, 2H), 1.80 (t, *J* = 6.0 Hz, 2H), 1.88-1.94 (m, 3H), 2.27 (s, 3H), 3.13-3.21 (m, 2H), 3.61 (s, 2H), 4.03 (t, *J* = 6.0 Hz, 2H), 4.11-4.15 (m, 2H), 4.18 (q, *J* = 7.1 Hz, 2H), 6.74 (d, *J* = 2.6 Hz, 1H), 6.80 (d, *J* = 2.6 Hz, 1H), 7.10 (d, *J* = 8.2 Hz, 1H), 7.25 (dd, *J* = 8.6, 2.1 Hz, 1H), 7.45 (d, *J* = 8.6 Hz, 1H), 7.57 (d, *J* = 2.1 Hz, 1H).

Compound **6_6e**

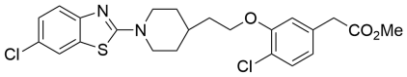

Yellow oil, 82% yield. ^{1}H NMR (400 MHz, $CDCl_3$) : δ 1.36-1.48 (m, 2H), 1.81-1.87 (m, 2H), 1.90-1.95 (m, 3H), 3.12-3.20 (m, 2H), 3.59 (s, 2H), 3.70 (s, 3H), 4.09-4.15 (m, 4H), 6.81 (dd, *J* = 8.0, 1.9 Hz, 1H), 6.86 (d, *J* = 1.8 Hz, 1H), 7.23 (dd, *J* = 8.5, 2.1 Hz, 1H), 7.30 (d, *J* = 8.0 Hz, 1H), 7.42 (d, *J* = 8.5 Hz, 1H), 7.54 (d, *J* = 2.1 Hz, 1H).

Compound **6_6f**

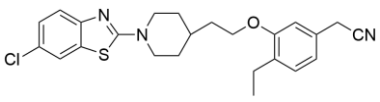

White solid, 78% yield. ^{1}H NMR (300 MHz, $CDCl_3$) : δ 1.18 (t, *J* = 7.6 Hz, 3H), 1.37-1.49 (m, 2H), 1.80-1.94 (m, 5H), 2.63 (q, *J* = 7.5 Hz, 2H), 3.11-3.19 (m, 2H), 3.71 (s,

2H), 4.05 (t, *J* = 6.0 Hz, 2H), 4.12-4.16 (m, 2H), 6.77-6.79 (m, 1H), 6.82 (dd, *J* = 7.7, 1.2 Hz, 1H), 7.14 (d, *J* = 7.7 Hz, 1H), 7.23 (dd, *J* = 8.6, 2.1 Hz, 1H), 7.44 (d, *J* = 8.6 Hz, 1H), 7.54 (d, *J* = 2.1 Hz, 1H).

Typical procedure for synthesis of compounds **2_7** and **2_9–11**

To a solution of **6_6** (0.214 mmol) in THF (0.6 mL) and MeOH (0.6 mL) was added 2 M aqueous NaOH solution (0.322 mL, 0.642 mmol), and the mixture was stirred at room temperature for 2 hours. To the reaction mixture was added 2 M aqueous HCl solution to be pH 4. The precipitate was collected and washed with water and IPE to give the title compound.

Compound **2_7**

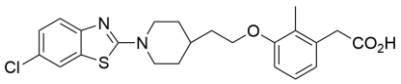

White solid, 82% yield. ^{1}H NMR (400 MHz, DMSO-d_6) : δ 1.25-1.35 (m, 2H), 1.71-1.76 (m, 2H), 1.83-1.87 (m, 3H), 2.08 (s, 3H), 3.14-3.21 (m, 2H), 3.57 (s, 2H), 3.99-4.03 (m, 4H), 6.78 (d, *J* = 7.5 Hz, 1H), 6.86 (d, *J* = 8.0 Hz, 1H), 7.07 (t, *J* = 7.8 Hz, 1H), 7.27 (dd, *J* = 8.6, 2.2 Hz, 1H), 7.40 (d, *J* = 8.7 Hz, 1H), 7.87 (d, *J* = 2.3 Hz, 1H), 12.27 (br s, 1H). ^{13}C NMR (100 MHz, DMSO-d_6) : δ 11.40, 30.91, 32.26, 35.02, 38.94, 48.34, 65.32, 109.95, 119.12, 120.65, 122.48, 124.52, 124.79, 125.91, 125.96, 131.89, 134.81, 151.54, 156.47, 168.25, 172.37. HRMS (ESI) : m/z $[M + H]^+$ calcd. for $C_{23}H_{26}ClN_2O_3S^+$, 445.1347; found, 445.1342.

Compound **2_9**

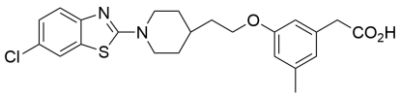

White solid, 99% yield. ^{1}H NMR (400 MHz, DMSO-d_6) : δ 1.24-1.33 (m, 2H), 1.67-1.71 (m, 2H), 1.79-1.85 (m, 3H), 2.25 (s, 3H), 3.14-3.21 (m, 2H), 3.47 (s, 2H), 3.98-4.04 (m, 4H), 6.62-6.66 (m, 3H), 7.27 (dd, *J* = 8.5, 1.6 Hz, 1H), 7.40 (d, *J* = 8.5 Hz, 1H), 7.87 (d, *J* = 1.5 Hz, 1H), 12.17 (br s, 1H). ^{13}C NMR (100 MHz, DMSO-d_6) : δ 20.96, 30.88, 32.05, 34.89, 40.61, 48.34, 64.84, 112.66, 113.14, 119.09, 120.66, 122.21, 124.56, 125.99, 131.83, 135.97, 138.57, 151.41, 158.45, 168.24, 172.45. HRMS (ESI) : m/z $[M + H]^+$ calcd. for $C_{23}H_{26}ClN_2O_3S^+$, 445.1347; found, 445.1345.

Compound **2_10**

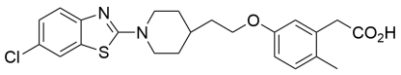

White solid, 39% yield. ^{1}H NMR (400 MHz, DMSO-d_6) : δ 1.24-1.33 (m, 2H), 1.68 (q, *J* = 6.2 Hz, 2H), 1.76-1.85 (m, 3H), 2.14 (s, 3H), 3.13-3.21 (m, 2H), 3.52 (s, 2H), 3.96-4.02 (m, 4H), 6.73 (dd, *J* = 8.3, 2.6 Hz, 1H), 6.78 (d, *J* = 2.6 Hz, 1H), 7.05 (d, *J* = 8.4 Hz, 1H), 7.27 (dd, *J* = 8.5, 2.3 Hz, 1H), 7.40 (d, *J* = 8.7 Hz, 1H), 7.88 (d, *J* = 2.1 Hz, 1H), 12.31 (br s, 1H). ^{13}C NMR (100 MHz, DMSO-d_6) : δ 18.17, 30.99, 32.13, 35.03, 38.98, 48.43, 64.97, 112.43, 116.70, 119.24, 120.78, 124.63, 126.08, 128.39, 130.62, 132.00, 134.91, 151.63, 156.63, 168.36, 172.45. HRMS (ESI) : m/z $[M + H]^+$ calcd. for $C_{23}H_{26}ClN_2O_3S^+$, 445.1347; found, 445.1347.

Compound **2_11**

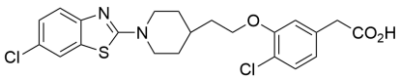

White solid, 90% yield. ^{1}H NMR (400 MHz, DMSO-d_6) : δ 1.27-1.36 (m, 2H), 1.72-1.77 (m, 2H), 1.83-1.89 (m, 3H), 3.17 (t, J = 12.1 Hz, 2H), 3.57 (s, 2H), 4.01 (d, J = 12.9 Hz, 2H), 4.11 (t, J = 6.3 Hz, 2H), 6.84 (d, J = 8.2 Hz, 1H), 7.08 (s, 1H), 7.27 (d, J = 8.7 Hz, 1H), 7.33 (d, J = 8.2 Hz, 1H), 7.40 (d, J = 8.5 Hz, 1H), 7.87 (s, 1H), 12.27 (br s, 1H). ^{13}C NMR (100 MHz, DMSO-d_6) : δ 30.84, 32.15, 34.63, 40.15, 48.35, 66.35, 115.10, 119.07, 119.56, 120.68, 122.35, 124.59, 125.99, 129.33, 131.79, 135.44, 151.33, 153.48, 168.22, 172.18. HRMS (ESI) : m/z $[M + H]^+$ calcd. for $C_{22}H_{23}Cl_2N_2O_3S^+$, 465.0801; found, 465.0798.

Synthesis of compound **2_8**

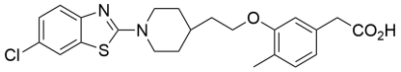

A mixture of compound **6_6b** (1.14 g, 2.68 mmol), NaOH (0.54 g, 13.5 mmol), water (1.6 mL) and EtOH (21 mL) was stirred at 80 °C for 6 hours. The reaction solution was concentrated under reduced pressure and became pH 7 with 2 M aqueous HCl solution. The precipitate was collected and washed with water and IPE to give compound **2_8** as a white solid (0.63 g, 53%). ^{1}H NMR (400 MHz, DMSO-d_6) : δ 1.25-1.36 (m, 2H), 1.73 (q, J = 6.1 Hz, 2H), 1.81-1.88 (m, 3H), 2.12 (s, 3H), 3.17 (t, J = 11.9 Hz, 2H), 3.50 (s, 2H), 3.99-4.04 (m, 4H), 6.72 (d, J = 7.5 Hz, 1H), 6.84 (s, 1H), 7.05 (d, J = 7.5 Hz, 1H), 7.25-7.29 (m, 1H), 7.40 (d, J = 8.5 Hz, 1H), 7.86-7.88 (m, 1H), 12.23 (br s, 1H). ^{13}C NMR (100 MHz, DMSO-d_6) : δ 15.58, 30.92, 32.28, 34.92, 40.61, 48.34, 65.12, 112.34, 119.12,

120.64, 120.90, 123.80, 124.53, 125.96, 129.95, 131.89, 133.67, 151.54, 156.35, 168.25, 172.61. HRMS (ESI) : m/z $[M + H]^+$ calcd. for $C_{23}H_{26}ClN_2O_3S^+$, 445.1347; found, 445.1354.

Synthesis of compound **2_12**

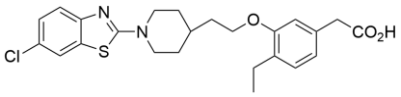

A mixture of compound **6_6f** (214 mg, 0.486 mmol), concentrated sulfuric acid (10 ml) and water (10 ml) was stirred at 80 °C for 20 hours. After air cooling, 5 N aqueous NaOH solution was added to be pH 4. The mixture was extracted with EtOAc. The extract was washed with brine, dried over Na_2SO_4, and concentrated under reduced pressure. The residue was collected and washed with water to give compound **2_12** as a white solid (89.1 mg; 61%). ^{1}H NMR (400 MHz, DMSO-d_6) : δ 1.12 (t, J = 7.5 Hz, 3H), 1.25-1.36 (m, 2H), 1.71-1.76 (m, 2H), 1.83-1.86 (m, 3H), 2.51-2.57 (m, 2H), 3.16 (t, J = 11.7 Hz, 2H), 3.49 (s, 2H), 3.97-4.03 (m, 4H), 6.74 (d, J = 7.5 Hz, 1H), 6.85 (s, 1H), 7.05 (d, J = 7.5 Hz, 1H), 7.27 (dd, J = 8.6, 2.1 Hz, 1H), 7.40 (d, J = 8.5 Hz, 1H), 7.88 (d, J = 2.0 Hz, 1H), 12.32 (br s, 1H). ^{13}C NMR (100 MHz, DMSO-d_6) : δ 14.25, 22.45, 30.89, 32.26, 34.93, 41.15, 48.35, 65.01, 112.45, 119.13,120.65, 121.06, 124.53, 125.96, 128.33, 129.64, 131.89, 134.19, 151.53, 155.92, 168.25, 172.82. HRMS (ESI) : m/z $[M + H]^+$ calcd. for $C_{24}H_{28}ClN_2O_3S^+$, 459.1504; found, 459.1510.

Synthesis of compound **6_8**

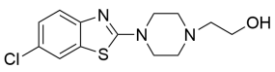

A mixture of 2,6-dichlorobenzothiazole (1.01 g, 4.95 mmol), 1-piperazineethanol (637 μL, 5.19 mmol), potassium carbonate (2.05 g, 14.9 mmol) and anhydrous DMF (10 mL) was stirred at 60 °C for 4 hours. Water and EtOAc were added to the reaction solution. The organic layer was separated, washed with brine, dried over anhydrous Na_2SO_4, and evaporated under reduced pressure. The residue was purified by silica gel column chromatography to give compound **6_8** (1.25 g, 85%). ^{1}H NMR (300 MHz, $CDCl_3$) : δ 2.60-2.67 (m, 6H), 3.63-3.69 (m, 6H), 7.23 (d, J = 8.5, 2.0 Hz, 1H), 7.44 (d, J = 8.5 Hz, 1H), 7.57 (d, J = 2.0 Hz, 1H).

Synthesis of compound **6_9**

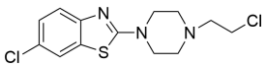

A mixture of **6_8** (1.24 g, 4.16 mmol) and $SOCl_2$ (12 mL) were stirred at 60 °C for 1 hour. To the reaction mixture was added aqueous $NaHCO_3$ solution to neutralize, and extracted with EtOAc. The extract was washed with water, dried over Na_2SO_4, and concentrated under reduced pressure. The residue was purified by silica gel column chromatography to give compound **6_9** (1.02 g, 77%). ^{1}H NMR (300 MHz, $CDCl_3$) : δ 2.63-2.72 (m, 4H), 2.80 (t, J = 7.0 Hz, 2H), 3.58-3.73 (m, 6H), 7.23 (dd, J = 8.5, 2.0 Hz, 1H), 7.44 (d, J = 8.5 Hz, 1H), 7.56 (d, J = 2.0 Hz, 1H).

Synthesis of compound **6_10**

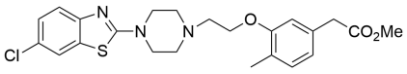

A mixture of **6_9** (153 mg, 0.484 mmol), methyl 2-(3-hydroxy-4-methylphenyl)acetate (95.9 mg, 0.532 mmol), Cs_2CO_3 (473 mg, 1.45 mmol) and DMF (6 mL) was stirred at

60 °C for 4 hours. Water was added, and the mixture was extracted with EtOAc. The extract was washed with brine, dried over Na_2SO_4, and concentrated under reduced pressure. The residue was purified by silica gel column chromatography to give compound **6_10** (128 mg, 57%). ^{1}H NMR (300 MHz, $CDCl_3$) : δ 2.19 (s, 3H), 2.73-2.79 (m, 4H), 2.91 (t, J = 5.2 Hz, 2H), 3.58 (s, 2H), 3.63-3.67 (m, 4H), 3.68 (s, 3H), 4.15 (t, J = 5.2 Hz, 2H), 6.75-6.79 (m, 2H), 7.08 (d, J = 7.5 Hz, 1H), 7.24 (dd, J = 8.5, 2.1 Hz, 2H), 7.43 (d, J = 8.5 Hz, 1H), 7.55 (d, J = 2.1 Hz, 1H).

Synthesis of compound **3_1**

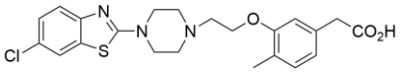

To a solution of **6_10** (128 mg, 0.278 mmol) in THF (2.0 mL) and MeOH (2.0 mL) was added 2 M aqueous NaOH solution (1.0 mL), and the mixture was stirred at room temperature for 2 hours. To the reaction mixture was added 2 M aqueous HCl solution to be neutral, and extracted with EtOAc. The extract was washed with brine, dried over Na_2SO_4, and concentrated under reduced pressure. The obtained solid was washed with IPE to give compound **3_1** (74.4 mg, 60%) as a white solid. ^{1}H NMR (400 MHz, DMSO-d_6) : δ 2.14 (s, 3H), 2.60-3.00 (m, 6H), 3.51 (s, 2H), 3.61 (br s, 4H), 4.15 (br s, 2H), 6.74 (d, J = 7.4 Hz, 1H), 6.87 (s, 1H), 7.07 (d, J = 7.4 Hz, 1H), 7.30 (dd, J = 8.6, 2.1 Hz, 1H), 7.44 (d, J = 8.6 Hz, 1H), 7.92 (s, 1H), 12.27 (br s, 1H). ^{13}C NMR (100 MHz, DMSO-d_6) : δ 15.75, 40.65, 47.95, 52.18, 56.36, 65.87, 112.62, 119.49, 120.90, 121.23, 123.99, 124.93, 126.17, 130.10, 132.00, 133.78, 151.36, 156.27, 168.57, 172.74. HRMS (ESI) : m/z $[M + H]^+$ calcd. for $C_{22}H_{25}ClN_3O_3S^+$, 446.1300; found, 446.1310.

Typical procedure for synthesis of compounds **6_12a–f**

A mixture of **6_11** (2.45 mmol), the corresponding piperazine (2.94 mmol), K_2CO_3 (406 mg, 2.94 mmol) and anhydrous DMF (5 mL) was stirred at room temperature for 12 hours. Water was added, and the mixture was extracted with EtOAc. The extract was washed with brine, dried over Na_2SO_4, and concentrated under reduced pressure. The residue was purified by silica gel column chromatography to give the target compound.

Compound **6_12a**

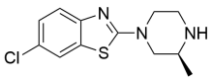

Yellow solid, 87% yield. ^{1}H NMR (300 MHz, $CDCl_3$) : δ 1.15 (d, J = 6.4 Hz, 3H), 2.80 (dd, J = 12.0, 10.4 Hz, 1H), 2.90-3.02 (m, 2H), 3.10-3.26 (m, 2H), 3.90-4.00 (m, 2H), 7.24 (dd, J = 8.4, 2.0 Hz, 1H), 7.43 (d, J = 8.4 Hz, 1H), 7.56 (d, J = 2.0 Hz, 1H).

Compound **6_12b**

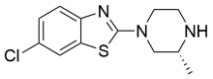

Yellow solid, 77% yield. ^{1}H NMR (300 MHz, $CDCl_3$) : δ 1.17 (d, J = 6.3 Hz, 3H), 2.83 (dd, J = 12.3, 10.5 Hz, 1H), 2.94-3.03 (m, 2H), 3.10-3.26 (m, 2H), 3.90-4.01 (m, 2H), 7.24 (dd, J = 8.5, 2.1 Hz, 1H), 7.44 (d, J = 8.5 Hz, 1H), 7.56 (d, J = 2.1 Hz, 1H).

Compound **6_12c**

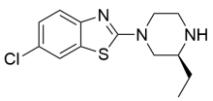

White solid, 99% yield. ^{1}H NMR (400 MHz, $CDCl_3$) : δ 1.01 (t, J = 7.5 Hz, 3H), 1.41-

1.56 (m, 2H), 2.68-2.75 (m, 1H), 2.83 (dd, *J* = 12.2, 10.4 Hz, 1H), 2.96 (td, *J* = 11.8, 3.3 Hz, 1H), 3.10-3.15 (m, 1H), 3.21 (td, *J* = 12.2, 3.3 Hz, 1H), 3.92-4.02 (m, 2H), 7.24 (dd, *J* = 8.6, 2.1 Hz, 1H), 7.44 (d, *J* = 8.6 Hz, 1H), 7.56 (d, *J* = 2.1 Hz, 1H).

Compound **6_12d**

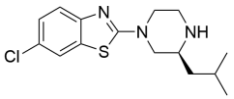

Yellow solid, quantitative yield. ^{1}H NMR (300 MHz, $CDCl_3$) : δ 0.94 (d, *J* = 6.4 Hz, 3H), 0.97 (d, *J* = 6.4 Hz, 3H), 1.25-1.38 (m, 2H), 1.69-1.80 (m, 1H), 2.78-2.90 (m, 2H), 2.92-3.00 (m, 1H), 3.09-3.23 (m, 2H), 3.92-3.99 (m, 2H), 7.24 (dd, *J* = 8.4, 2.4 Hz, 1H), 7.43 (d, *J* = 8.4 Hz, 1H), 7.55 (d, *J* = 2.4 Hz, 1H).

Compound **6_12e**

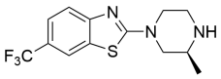

White solid, 71% yield. ^{1}H NMR (400 MHz, $CDCl_3$) : δ 1.17 (d, *J* = 6.1 Hz, 3H), 2.85 (dd, *J* = 12.3, 10.5 Hz, 1H), 2.92-2.97 (m, 1H), 3.00 (dd, *J* = 11.9, 3.3 Hz, 1H), 3.11-3.16 (m, 1H), 3.23 (td, *J* = 12.3, 3.3 Hz, 1H), 3.96-4.05 (m, 2H), 7.53 (dd, *J* = 8.5, 1.4 Hz, 1H), 7.57 (d, *J* = 8.5 Hz, 1H), 7.85 (br s, 1H).

Compound **6_12f**

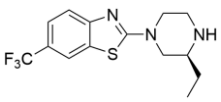

White solid, 76% yield. ^{1}H NMR (400 MHz, $CDCl_3$) : δ 1.02 (t, *J* = 7.5 Hz, 3H), 1.42-1.58 (m, 2H), 2.69-2.76 (m, 1H), 2.88 (dd, *J* = 12.2, 10.4 Hz, 1H), 2.97 (td, *J* = 11.9, 3.4

Hz, 1H), 3.12-3.17 (m, 1H), 3.25 (td, *J* = 12.2, 3.4 Hz, 1H), 3.97-4.07 (m, 2H), 7.52 (dd, *J* = 8.5, 1.4 Hz, 1H), 7.57 (d, *J* = 8.5 Hz, 1H), 7.85 (br s, 1H).

Typical procedure for synthesis of compounds **6_22a–b**

A mixture of 2,6-dichlorobenzothiazole (500 mg, 2.45 mmol), (*R*/*S*)-1-Boc-3-methylpiperazine (589 mg, 2.94 mmol), K_2CO_3 (1.02 g, 7.35 mmol) and anhydrous DMF (5 mL) was stirred at 100 °C for 18 hours. Water was added, and the mixture was extracted with EtOAc. The extract was washed with brine, dried over Na_2SO_4, and concentrated under reduced pressure. The residue was purified by silica gel column chromatography to give the target compound.

Compound **6_22a**

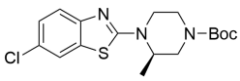

Yellow oil, 69% yield. ^{1}H NMR (400 MHz, $CDCl_3$) : δ 1.30 (d, *J* = 6.8 Hz, 3H), 1.49 (s, 9H), 2.95-3.22 (m, 2H), 3.40 (td, *J* = 12.6, 3.5 Hz, 1H), 3.80-4.28 (m, 4H), 7.25 (dd, *J* = 8.5, 2.1 Hz, 2H), 7.44 (d, *J* = 8.5 Hz, 1H), 7.57 (d, *J* = 2.1 Hz, 1H).

Compound **6_22b**

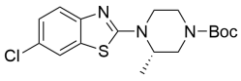

Yellow oil, 68% yield. ^{1}H NMR (400 MHz, $CDCl_3$) : δ 1.30 (d, *J* = 6.7 Hz, 3H), 1.49 (s, 9H), 2.95-3.22 (m, 2H), 3.40 (td, *J* = 12.6, 3.5 Hz, 1H), 3.82-4.28 (m, 4H), 7.25 (dd, *J* = 8.7, 2.1 Hz, 1H), 7.44 (d, *J* = 8.7 Hz, 1H), 7.57 (d, *J* = 2.1 Hz, 1H).

Typical procedure for synthesis of compounds **6_23a–b**

To 4 M solution of hydrochloric acid-dioxane was added **6_22** (500 mg, 1.36 mmol). After stirring at room temperature for 3 hours, the reaction mixture was concentrated under reduced pressure and the residue was washed with IPE to give the target compound.

Compound **6_23a**

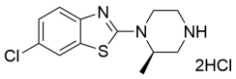

Yellow solid, 99% yield. ^{1}H NMR (400 MHz, DMSO-d_6) : δ 1.40 (d, J = 6.9 Hz, 3H), 3.03-3.14 (m, 1H), 3.21-3.36 (m, 3H), 3.48-3.57 (m, 1H), 3.99-4.05 (m, 1H), 4.44-4.50 (m, 1H), 7.33 (dd, J = 8.5, 2.2 Hz, 1H), 7.48 (d, J = 8.5 Hz, 1H), 7.97 (d, J = 2.1 Hz, 1H), 9.22 (br s, 1H), 9.68 (br s, 1H).

Compound **6_23b**

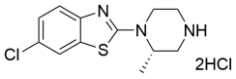

Yellow solid, 99% yield. ^{1}H NMR (400 MHz, DMSO-d_6) : δ 1.41 (d, J = 7.0 Hz, 3H), 3.02-3.13 (m, 1H), 3.20-3.35 (m, 3H), 3.49-3.57 (m, 1H), 4.00-4.04 (m, 1H), 4.44-4.48 (m, 1H), 7.33 (dd, J = 8.5, 2.2 Hz, 1H), 7.48 (d, J = 8.5 Hz, 1H), 7.98 (d, J = 2.1 Hz, 1H), 9.32 (br s, 1H), 9.78 (br s, 1H).

Typical procedure for synthesis of compounds **6_13a–h**

Compound **6_12** or **6_23** (2.01 mmol) was dissolved in anhydrous DMF (5 mL). After addition of K_2CO_3 (335 mg, 2.42 mmol) and methyl 2-bromoacetate (205 μL, 2.22 mmol),

the solution was stirred at 60 °C for 1 hour. Water was added, and the mixture was extracted with EtOAc. The extract was washed with brine, dried over Na_2SO_4, and concentrated under reduced pressure. The residue was purified by silica gel column chromatography to give the target compound.

Compound **6_13a**

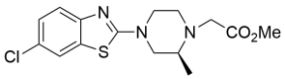

White solid, 99% yield. ^{1}H NMR (300 MHz, $CDCl_3$) : δ 1.15 (d, J = 6.4 Hz, 3H), 2.77-2.97 (m, 3H), 3.00-3.08 (m, 1H), 3.41 (d, J = 16.8 Hz, 1H), 3.39-3.48 (m, 1H), 3.49 (d, J = 16.8 Hz, 1H), 3.72 (s, 3H), 3.84-3.92 (m, 2H), 7.24 (dd, J = 8.8, 2.0 Hz, 1H), 7.43 (d, J = 8.8 Hz, 1H), 7.55 (d, J = 2.0 Hz, 1H).

Compound **6_13b**

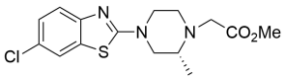

Yellow solid, 100% yield. ^{1}H NMR (300 MHz, $CDCl_3$) : δ 1.15 (d, J = 6.3 Hz, 3H), 2.78-2.99 (m, 3H), 3.02-3.10 (m, 1H), 3.39-3.53 (m, 3H), 3.73 (s, 3H), 3.84-3.93 (m, 2H), 7.24 (dd, J = 8.6, 2.2 Hz, 1H), 7.44 (d, J = 8.6 Hz, 1H), 7.56 (d, J = 2.2 Hz, 1H).

Compound **6_13c**

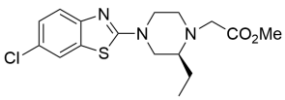

Colorless oil, 94% yield. ^{1}H NMR (300 MHz, $CDCl_3$) : δ 0.99 (t, J = 7.2 Hz, 3H), 1.46-1.56 (m, 1H), 1.62-1.70 (m, 1H), 2.72-2.80 (m, 1H), 2.83-2.96 (m, 2H), 3.18 (dd, J = 12.8,

9.2 Hz, 1H), 3.40-3.51 (m, 3H), 3.72 (s, 3H), 3.80-3.91 (m, 2H), 7.24 (dd, *J* = 8.8, 2.0 Hz, 1H), 7.43 (d, *J* = 8.8 Hz, 1H), 7.55 (d, *J* = 2.0 Hz, 1H).

Compound **6_13d**

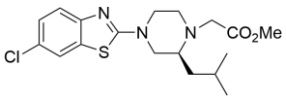

White solid, 98% yield. ^{1}H NMR (300 MHz, $CDCl_3$) : δ 0.94 (d, *J* = 6.4 Hz, 3H), 0.96 (d, *J* = 6.4 Hz, 3H), 1.29-1.43 (m, 2H), 1.65-1.75 (m, 1H), 2.80-2.95 (m, 3H), 3.18 (dd, *J* = 12.8, 8.0 Hz, 1H), 3.43 (ABq, *J* = 12.9 Hz, 2H), 3.50-3.58 (m, 1H), 3.72 (s, 3H), 3.76-3.88 (m, 2H), 7.24 (dd, *J* = 8.8, 2.0 Hz, 1H), 7.43 (d, *J* = 8.8 Hz, 1H), 7.55 (d, *J* = 2.0 Hz, 1H).

Compound **6_13e**

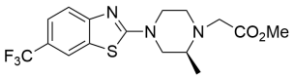

White solid, 96% yield. ^{1}H NMR (400 MHz, $CDCl_3$) : δ 1.16 (d, *J* = 6.3 Hz, 3H), 2.81-2.98 (m, 3H), 3.08 (dd, *J* = 12.7, 9.8 Hz, 1H), 3.40-3.52 (m, 3H), 3.73 (s, 3H), 3.90-3.97 (m, 2H), 7.53 (dd, *J* = 8.6, 1.6 Hz, 1H), 7.57 (d, *J* = 8.6 Hz, 1H), 7.85 (br s, 1H).

Compound **6_13f**

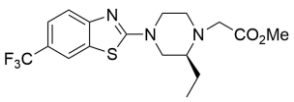

White solid, 99% yield. ^{1}H NMR (400 MHz, $CDCl_3$) : δ 1.00 (t, *J* = 7.5 Hz, 3H), 1.47-1.55 (m, 1H), 1.62-1.70 (m, 1H), 2.75-2.81 (m, 1H), 2.84-2.97 (m, 2H), 3.24 (dd, *J* = 12.7, 9.0 Hz, 1H), 3.46 (d, *J* = 2.8 Hz, 2H), 3.47-3.55 (m, 1H), 3.73 (s, 3H), 3.85-3.96 (m, 2H),

7.52 (dd, J = 8.5, 1.4 Hz, 1H), 7.57 (d, J = 8.5 Hz, 1H), 7.84 (br s, 1H).

Compound **6_13g**

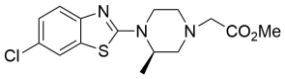

Yellow oil, quantitative yield. ^{1}H NMR (300 MHz, $CDCl_3$) : δ 1.45 (d, J = 6.6 Hz, 3H), 2.55 (dt, J = 11.4, 3.6 Hz, 1H), 2.62 (dd, J = 11.1, 3.6 Hz, 1H), 2.84 (d, J = 11.1, 1H), 2.97 (m, 1H), 3.29 (ABq, J = 16.5 Hz, 2H), 3.55 (dt, J = 12.6, 3.3 Hz, 1H), 3.74 (s, 3H), 3.85-3.92 (m, 1H), 4.18-4.27 (m, 1H), 7.24 (dd, J = 8.6, 2.0 Hz, 1H), 7.44 (d, J = 8.6 Hz, 1H), 7.56 (d, J = 2.0 Hz, 1H).

Compound **6_13h**

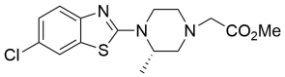

Yellow oil, 75% yield. ^{1}H NMR (300 MHz, $CDCl_3$) : δ 1.45 (d, J = 6.6 Hz, 3H), 2.50 (dt, J = 11.7, 3.6 Hz, 1H), 2.62 (dd, J = 10.8, 3.9 Hz, 1H), 2.84 (d, J = 11.7, 1H), 2.97 (dd, J = 11.1, 3.9 Hz, 1H), 3.25 (d, J = 16.8 Hz, 1H), 3.31 (d, J = 16.8 Hz, 1H), 3.55 (dt, J = 12.3, 3.6 Hz, 1H), 3.74 (s, 3H), 3.88 (d, J = 12.3 Hz, 1H), 4.18-4.27 (m, 1H), 7.24 (dd, J = 8.7, 2.4 Hz, 1H), 7.44 (d, J = 8.7 Hz, 1H), 7.56 (d, J = 2.4 Hz, 1H).

Typical procedure for synthesis of compounds **6_14a–h**

To a suspension of lithium aluminium hydride (148 mg, 3.90 mmol) in anhydrous THF (7 mL) was added dropwise a solution of **6_13** (1.95 mmol) in anhydrous THF (7 mL) under ice-cooling, and the mixture was stirred at the same temperature for 1 hour. Water

(0.15 mL), 10% aqueous sodium hydroxide solution (0.15 mL) and water (0.40 mL) were added dropwise sequentially under ice-cooling. After filtration of aluminium hydroxide, the filtrate was extracted with EtOAc. The extract was washed with brine, dried over Na_2SO_4, and concentrated under reduced pressure. The obtained solid was collected by filtration, washed with diisopropyl ether, and dried under high vacuum to give the target compound.

Compound **6_14a**

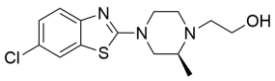

White solid, 84% yield. ^{1}H NMR (300 MHz, $CDCl_3$) : δ 1.15 (d, J = 6.4 Hz, 3H), 2.37-2.53 (m, 2H), 2.57 (br s, 1H), 2.71-2.78 (m, 1H), 2.95-3.02 (m, 2H), 3.19 (dd, J = 12.8, 8.4 Hz, 1H), 3.47-3.83 (m, 5H), 7.24 (dd, J = 8.4, 2.0 Hz, 1H), 7.43 (d, J = 8.4 Hz, 1H), 7.56 (d, J = 2.0 Hz, 1H).

Compound **6_14b**

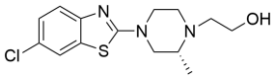

White solid, 82% yield. ^{1}H NMR (300 MHz, $CDCl_3$) : δ 1.19 (d, J = 6.3 Hz, 3H), 2.40-2.58 (m, 2H), 2.75-2.84 (m, 2H), 2.98-3.09 (m, 2H), 3.24 (dd, J = 12.6, 8.1 Hz, 1H), 3.54-3.87 (m, 5H), 7.25 (dd, J = 8.4, 2.1 Hz, 1H), 7.44 (d, J = 8.4 Hz, 1H), 7.57 (d, J = 2.1 Hz, 1H).

Compound **6_14c**

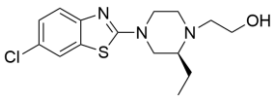

Colorless oil, 95% yield. ^{1}H NMR (300 MHz, $CDCl_3$) : δ 0.99 (t, J = 7.2 Hz, 3H), 1.50-1.68 (m, 2H), 2.49-2.68 (m, 4H), 2.89-3.02 (m, 2H), 3.46 (dd, J = 12.8, 6.4 Hz, 1H), 3.58-3.73 (m, 5H), 7.24 (dd, J = 8.4, 2.0 Hz, 1H), 7.43 (d, J = 8.4 Hz, 1H), 7.55 (d, J = 2.0 Hz, 1H).

Compound **6_14d**

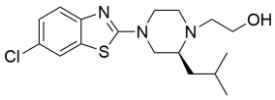

Colorless oil, 86% yield. ^{1}H NMR (300 MHz, $CDCl_3$) : δ 0.94 (d, J = 6.4 Hz, 3H), 0.95 (d, J = 6.4 Hz, 3H), 1.36-1.43 (m, 2H), 1.63-1.74 (m, 1H), 2.54-2.63 (m, 2H), 2.64-2.77 (m, 2H), 2.82-2.90 (m, 1H), 2.91-2.99 (m, 1H), 3.45 (dd, J = 12.8, 5.6 Hz, 1H), 3.52-3.68 (m, 4H), 3.72-3.79 (m, 1H), 7.24 (dd, J = 8.8, 2.0 Hz, 1H), 7.43 (d, J = 8.8 Hz, 1H), 7.55 (d, J = 2.0 Hz, 1H).

Compound **6_14e**

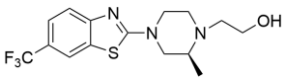

Colorless oil, 99% yield. ^{1}H NMR (400 MHz, $CDCl_3$) : δ 1.16 (d, J = 6.3 Hz, 3H), 2.39-2.45 (m, 1H), 2.47-2.53 (m, 1H), 2.59 (br s, 1H), 2.73-2.78 (m, 1H), 2.96-3.03 (m, 2H), 3.24 (dd, J = 12.7, 8.1 Hz, 1H), 3.54-3.63 (m, 2H), 3.67-3.72 (m, 1H), 3.78-3.88 (m, 2H), 7.53 (dd, J = 8.6, 1.3 Hz, 1H), 7.57 (d, J = 8.6 Hz, 1H), 7.85 (br s, 1H).

Compound **6_14f**

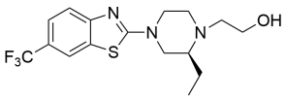

Colorless oil, 99% yield. ^{1}H NMR (400 MHz, $CDCl_3$) : δ 1.00 (t, J = 7.5 Hz, 3H), 1.52-1.69 (m, 2H), 2.52-2.63 (m, 3H), 2.66 (br s, 1H), 2.90-3.02 (m, 2H), 3.53 (dd, J = 12.9, 6.3 Hz, 1H), 3.63-3.76 (m, 5H), 7.53 (dd, J = 8.5, 1.5 Hz, 1H), 7.57 (d, J = 8.5 Hz, 1H), 7.85 (br s, 1H).

Typical procedure for synthesis of compounds **6_15a–i**

To a solution of **6_14** (125 mg, 0.401 mmol) and TEA (100 μL, 0.721 mmol) in anhydrous CH_2Cl_2 (1.25 mL) was added MsCl (40 μL, 0.513 mmol) under ice-cooling. After stirring at the same temperature for 1 hour, water was added, and the mixture was extracted with EtOAc. The extract was washed with brine, dried over Na_2SO_4, and concentrated under reduced pressure. A mixture of the residue, the corresponding phenol (0.458 mmol), Cs_2CO_3 (159 mg, 0.488 mmol) and anhydrous DMF (2 mL) was stirred at 60 °C for 4 hours. Water was added, and the mixture was extracted with EtOAc. The extract was washed with brine, dried over Na_2SO_4, and concentrated under reduced pressure. The residue was purified by silica gel column chromatography to give the target compound.

Compound **6_15a**

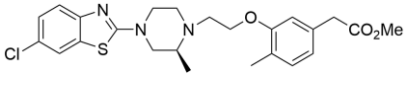

Colorless oil, 28% yield. ^{1}H NMR (300 MHz, $CDCl_3$) : δ 1.20 (d, J = 6.0 Hz, 3H), 2.19 (s, 3H), 2.54-2.80 (m, 3H), 2.90-3.20 (m, 3H) , 3.41-3.50 (m, 1H), 3.57 (m, 2H), 3.68 (s,

3H), 3.77-3.89 (m, 2H), 4.09-4.26 (m, 2H), 6.74-6.78 (m, 2H), 7.07 (d, J = 8.0 Hz, 1H), 7.23 (dd, J = 8.8, 2.0 Hz, 1H), 7.43 (d, J = 8.8 Hz, 1H), 7.55 (d, J = 2.0 Hz, 1H).

Compound **6_15b**

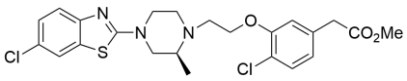

Yellow oil, 87% yield. ^{1}H NMR (300 MHz, $CDCl_3$) : δ 1.23 (d, J = 6.3 Hz, 3H), 2.72-2.88 (m, 2H), 2.95-3.23 (m, 4H), 3.42-3.52 (m, 1H), 3.58 (s, 2H), 3.70 (s, 3H), 3.80-3.89 (m, 2H), 4.13-4.20 (m, 2H), 6.81 (dd, J = 8.1, 1.9 Hz, 1H), 6.87 (d, J = 1.9 Hz, 1H), 7.23 (dd, J = 8.6, 2.2 Hz, 1H), 7.30 (d, J = 8.1 Hz, 1H) , 7.43 (d, J = 8.6 Hz, 1H), 7.55 (d, J = 2.2 Hz, 1H).

Compound **6_15c**

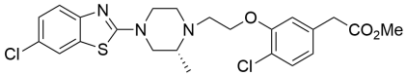

Yellow oil, 84% yield. ^{1}H NMR (300 MHz, $CDCl_3$) : δ 1.23 (d, J = 6.0 Hz, 3H), 2.70-2.88 (m, 2H), 2.95-3.24 (m, 4H), 3.42-3.50 (m, 1H), 3.58 (s, 2H), 3.70 (s, 3H), 3.80-3.89 (m, 2H), 4.13-4.20 (m, 2H), 6.81 (dd, J = 8.1, 1.8 Hz, 1H), 6.87 (d, J = 1.8 Hz, 1H), 7.24 (dd, J = 8.6, 2.2 Hz, 1H), 7.30 (d, J = 8.1 Hz, 1H) , 7.43 (d, J = 8.6 Hz, 1H), 7.55 (d, J = 2.2 Hz, 1H).

Compound **6_15d**

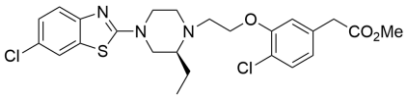

Colorless oil, 46% yield. ^{1}H NMR (300 MHz, $CDCl_3$) : δ 1.01 (t, J = 7.6 Hz, 3H), 1.54-

1.65 (m, 1H), 1.69-1.80 (m, 1H), 2.62-2.70 (m, 1H), 2.72-2.80 (m, 1H), 2.93-3.01 (m, 1H), 3.06-3.20 (m, 2H), 3.30 (dd, *J* = 12.8, 7.6 Hz, 1H), 3.50-3.60 (m, 1H), 3.58 (s, 2H), 3.70 (s, 3H), 3.66-3.81 (m, 2H), 4.11-4.19 (m, 2H), 6.81 (dd, *J* = 8.0, 2.0 Hz, 1H), 6.87 (d, *J* = 2.0 Hz, 1H), 7.23 (dd, *J* = 8.4, 2.0 Hz, 1H), 7.30 (d, *J* = 8.0 Hz, 1H) , 7.43 (d, *J* = 8.4 Hz, 1H), 7.55 (d, *J* = 2.0 Hz, 1H).

Compound **6_15e**

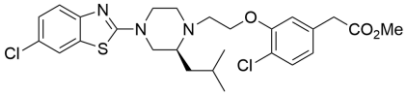

Colorless oil, 65% yield. ^{1}H NMR (300 MHz, $CDCl_3$) : δ 0.96 (d, *J* = 6.4 Hz, 6H), 1.35-1.53 (m, 2H), 1.65-1.77 (m, 1H), 2.73-2.82 (m, 2H), 2.86-2.94 (m, 1H), 3.07-3.15 (m, 2H), 3.30 (dd, *J* = 12.4, 2.8 Hz, 1H), 3.58 (s, 2H), 3.62-3.67 (m, 2H), 3.70 (s, 3H), 3.74 (dd, *J* = 12.4, 3.6 Hz, 1H), 4.13 (t, *J* = 6.0 Hz, 2H), 6.81 (dd, *J* = 8.0, 1.6 Hz, 1H), 6.88 (d, *J* = 1.6 Hz, 1H), 7.23 (dd, *J* = 8.8, 2.0 Hz, 1H), 7.30 (d, *J* = 8.0 Hz, 1H) , 7.42 (d, *J* = 8.8 Hz, 1H), 7.55 (d, *J* = 2.0 Hz, 1H).

Compound **6_15f**

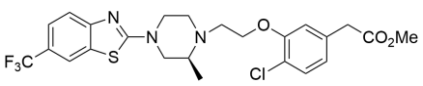

White solid, 68% yield. ^{1}H NMR (400 MHz, $CDCl_3$) : δ 1.23 (d, *J* = 6.1 Hz, 3H), 2.72-2.79 (m, 1H), 2.80-2.85 (m, 1H), 2.95-3.02 (m, 1H), 3.10-3.21 (m, 3H), 3.47-3.53 (m, 1H), 3.58 (s, 2H), 3.70 (s, 3H), 3.85-3.91 (m, 2H), 4.14-4.17 (m, 2H), 6.81 (dd, *J* = 8.0, 1.8 Hz, 1H), 6.87 (d, *J* = 1.8 Hz, 1H), 7.30 (d, *J* = 8.0 Hz, 1H), 7.52 (dd, *J* = 8.5, 1.4 Hz, 1H), 7.56 (d, *J* = 8.5 Hz, 1H), 7.84 (br s, 1H).

Compound **6_15g**

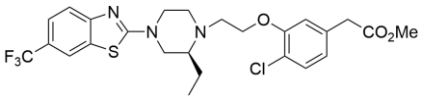

White solid, 50% yield. ^{1}H NMR (400 MHz, $CDCl_3$) : δ 1.02 (t, J = 7.5 Hz, 3H), 1.55-1.65 (m, 1H), 1.71-1.80 (m, 1H), 2.65-2.71 (m, 1H), 2.75-2.81 (m, 1H), 2.95-3.02 (m, 1H), 3.09-3.19 (m, 2H), 3.36 (dd, J = 12.8, 7.8 Hz, 1H), 3.57-3.63 (m, 1H), 3.59 (s, 2H), 3.70 (s, 3H), 3.74-3.79 (m, 1H), 3.83 (dd, J = 12.8, 3.0 Hz, 1H), 4.12-4.19 (m, 2H), 6.81 (dd, J = 8.0, 1.8 Hz, 1H), 6.87 (d, J = 1.8 Hz, 1H), 7.30 (d, J = 8.0 Hz, 1H), 7.52 (dd, J = 8.4, 1.4 Hz, 1H), 7.56 (d, J = 8.4 Hz, 1H), 7.84 (br s, 1H).

Compound **6_15h**

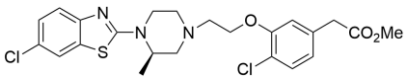

Colorless oil, 47% yield (2 steps). ^{1}H NMR (400 MHz, $CDCl_3$) : δ 1.39 (d, J = 6.7 Hz, 3H), 2.41 (td, J = 11.7, 3.5 Hz, 1H), 2.58 (dd, J = 11.3, 3.8 Hz, 1H), 2.86-2.90 (m, 2H), 2.92-2.95 (m, 1H), 3.05-3.09 (m, 1H), 3.47 (td, J = 12.5, 3.5 Hz, 1H), 3.59 (s, 2H), 3.70 (s, 3H), 3.85-3.89 (m, 1H), 4.19 (t, J = 5.4 Hz, 3H), 6.82 (dd, J = 8.0, 1.8 Hz, 1H), 6.88 (d, J = 1.8 Hz, 1H), 7.23 (dd, J = 8.7, 2.1 Hz, 1H), 7.31 (d, J = 8.0 Hz, 1H), 7.42 (d, J = 8.7 Hz, 1H), 7.55 (d, J = 2.1 Hz, 1H).

Compound **6_15i**

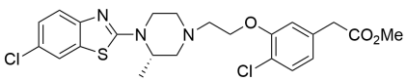

Colorless oil, 50% yield (2 steps). ^{1}H NMR (400 MHz, $CDCl_3$) : δ 1.39 (d, J = 6.7 Hz, 3H), 2.41 (td, J = 11.7, 3.5 Hz, 1H), 2.58 (dd, J = 11.2, 3.7 Hz, 1H), 2.86-2.90 (m, 2H), 2.92-2.95 (m, 1H), 3.05-3.09 (m, 1H), 3.47 (td, J = 12.5, 3.4 Hz, 1H), 3.59 (s, 2H), 3.71

(s, 3H), 3.85-3.89 (m, 1H), 4.19 (t, *J* = 5.4 Hz, 3H), 6.82 (dd, *J* = 8.0, 1.8 Hz, 1H), 6.88 (d, *J* = 1.8 Hz, 1H), 7.23 (dd, *J* = 8.7, 2.1 Hz, 1H), 7.31 (d, *J* = 8.0 Hz, 1H), 7.42 (d, *J* = 8.7 Hz, 1H), 7.55 (d, *J* = 2.1 Hz, 1H).

Typical procedure for synthesis of compounds **3_2–4** and **3_6–11**

To a solution of **6_15** (0.111 mmol) in THF (0.5 mL) and MeOH (0.5 mL) was added 2 M aqueous NaOH solution (0.2 mL), and the mixture was stirred at 60 °C for 1 hour. To the reaction mixture was added 2 M aqueous HCl solution to be neutral, and extracted with EtOAc. The extract was washed with brine, dried over Na_2SO_4, and concentrated under reduced pressure. The obtained solid was washed with IPE to give the target compound.

Compound **3_2**

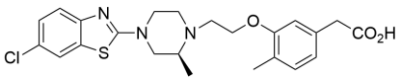

White solid, 41% yield. ^{1}H NMR (400 MHz, DMSO-d_6) : δ 1.12 (d, *J* = 6.3 Hz, 3H), 2.12 (s, 3H), 2.56-2.62 (m, 1H), 2.68-2.74 (m, 1H), 2.82 (dt, *J* = 13.9, 5.6 Hz, 1H), 2.99-3.09 (m, 3H), 3.34-3.40 (m, 1H), 3.50 (s, 2H), 3.73-3.80 (m, 2H), 4.05 (t, *J* = 5.4 Hz, 2H), 6.72 (d, *J* = 7.5 Hz, 1H), 6.85 (s, 1H), 7.05 (d, *J* = 7.5 Hz, 1H), 7.28 (dd, *J* = 8.6, 2.1 Hz, 1H), 7.41 (d, *J* = 8.6 Hz, 1H), 7.89 (d, *J* = 2.1 Hz, 1H), 12.26 (br s, 1H). ^{13}C NMR (100 MHz, DMSO-d_6) : δ 15.11, 15.68, 40.58, 48.12, 50.01, 51.37, 53.54, 54.22, 65.67, 112.29, 119.28, 120.74, 120.99, 123.75, 124.72, 126.04, 129.97, 131.85, 133.69, 151.32, 156.24, 168.34, 172.64. HRMS (ESI) : m/z $[M + H]^+$ calcd. for $C_{23}H_{27}ClN_3O_3S^+$, 460.1456; found, 460.1450.

Compound **3_3**

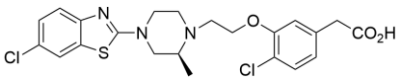

White solid, 75% yield. ^{1}H NMR (400 MHz, DMSO-d$_6$, 145 °C) : δ 1.16 (d, J = 6.2 Hz, 3H), 2.75-2.81 (m, 1H), 2.92-2.98 (m, 2H), 3.10-3.23 (m, 3H), 3.47-3.53 (m, 1H), 3.53 (s, 2H), 3.73-3.80 (m, 2H), 4.22 (t, J = 5.6 Hz, 2H), 6.85 (dd, J = 8.0, 1.6 Hz, 1H), 7.07 (d, J = 1.6 Hz, 1H), 7.23 (dd, J = 8.6, 2.0 Hz, 1H), 7.28 (d, J = 8.0 Hz, 1H), 7.38 (d, J = 8.6 Hz, 1H), 7.74 (d, J = 2.0 Hz, 1H). ^{13}C NMR (100 MHz, DMSO-d$_6$) : δ 15.08, 40.12, 48.06, 50.01, 51.07, 53.53, 54.19, 66.75, 114.99, 119.34, 119.43, 120.79, 122.49, 124.79, 126.08, 129.35, 131.91, 135.46, 151.28, 153.33, 168.30, 172.21. HRMS (ESI) : m/z [M + H]$^+$ calcd. for $C_{22}H_{24}Cl_2N_3O_3S^+$, 480.0910; found, 480.0914.

Compound **3_4**

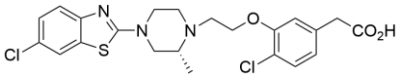

White solid, 82% yield. ^{1}H NMR (400 MHz, DMSO-d$_6$) : δ 1.12 (d, J = 6.3 Hz, 3H), 2.59-2.65 (m, 1H), 2.70-2.75 (m, 1H), 2.84 (dt, J = 14.2, 5.7 Hz, 1H), 3.00-3.10 (m, 1H), 3.34-3.40 (m, 1H), 3.57 (s, 2H), 3.71-3.79 (m, 2H), 4.14 (t, J = 5.6 Hz, 2H), 6.84 (dd, J = 8.0, 1.5 Hz, 1H), 7.09 (d, J = 1.5 Hz, 1H), 7.28 (dd, J = 8.5, 2.1 Hz, 1H), 7.34 (d, J = 8.0 Hz, 1H), 7.41 (d, J = 8.5 Hz, 1H), 7.89 (d, J = 2.1 Hz, 1H), 12.36 (br s, 1H). ^{13}C NMR (100 MHz, DMSO-d$_6$) : δ 15.13, 40.17, 48.09, 49.97, 51.10, 53.49, 54.21, 66.74, 114.98, 119.28, 119.41, 120.74, 122.41, 124.72, 126.04, 129.32, 131.85, 135.47, 151.33, 153.39, 168.33, 172.24. HRMS (ESI) : m/z [M + H]$^+$ calcd. for $C_{22}H_{24}Cl_2N_3O_3S^+$, 480.0910; found, 480.0920.

Compound **3_6**

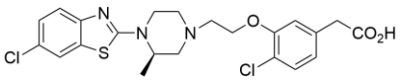

White solid, quantitative yield. ^{1}H NMR (400 MHz, DMSO-d$_6$) : δ 1.29 (d, J = 6.5 Hz, 3H), 2.26 (td, J = 11.6, 3.3 Hz, 1H), 2.43 (dd, J = 11.6, 3.7 Hz, 1H), 2.76-2.82 (m, 2H), 2.92 (d, J = 11.2 Hz, 1H), 3.06 (d, J = 11.2 Hz, 1H), 3.35 (td, J = 12.5, 3.3 Hz, 2H), 3.57 (s, 2H), 3.77 (d, J = 12.5 Hz, 1H), 4.17-4.21 (m, 3H), 6.85 (dd, J = 8.2, 1.5 Hz, 1H), 7.11 (d, J = 1.5 Hz, 1H), 7.28 (dd, J = 8.5, 2.2 Hz, 1H), 7.34 (d, J = 8.2 Hz, 1H), 7.41 (d, J = 8.5 Hz, 1H), 7.89 (d, J = 2.2 Hz, 1H), 12.39 (br s, 1H). ^{13}C NMR (100 MHz, DMSO-d$_6$) : δ 14.44, 40.28, 43.58, 51.85, 52.50, 56.13, 57.16, 66.90, 115.26, 119.23, 119.55, 120.71, 12.52, 124.62, 125.98, 129.32, 131.65, 135.59, 151.32, 153.38, 167.78, 172.28. HRMS (ESI) : m/z [M + H]$^+$ calcd. for $C_{22}H_{24}Cl_2N_3O_3S^+$, 480.0910; found, 480.0881.

Compound **3_7**

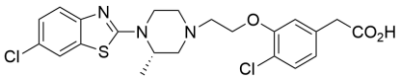

White solid, 29% yield. ^{1}H NMR (400 MHz, DMSO-d$_6$) : δ 1.29 (d, J = 6.7 Hz, 3H), 2.26 (td, J = 11.7, 3.2 Hz, 1H), 2.43 (dd, J = 11.4, 3.5 Hz, 1H), 2.76-2.83 (m, 2H), 2.93 (d, J = 11.2 Hz, 1H), 3.06 (d, J = 10.9 Hz, 1H), 3.32-3.39 (m, 1H), 3.58 (s, 2H), 3.77 (d, J = 12.4 Hz, 1H), 4.19 (t, J = 5.3 Hz, 3H), 6.85 (dd, J = 8.0, 1.3 Hz, 1H), 7.12 (d, J = 1.3 Hz, 1H), 7.28 (dd, J = 8.6, 2.1 Hz, 1H), 7.35 (d, J = 8.0 Hz, 1H), 7.41 (d, J = 8.6 Hz, 1H), 7.89 (d, J = 2.1 Hz, 1H), 12.41 (br s, 1H). ^{13}C NMR (100 MHz, DMSO-d$_6$) : δ 14.44, 40.13, 43.59, 51.85, 52.50, 56.14, 57.16, 66.91, 115.28, 119.24, 119.61, 120.72, 122.53, 124.62, 125.99, 129.35, 131.65, 135.44, 151.33, 153.40, 167.79, 172.25. HRMS (ESI) : m/z [M + H]$^+$

calcd. for $C_{22}H_{24}Cl_2N_3O_3S^+$, 480.0910; found, 480.0923.

Compound **3_8**

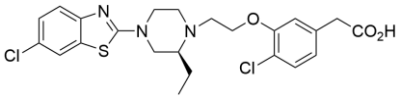

White solid, 90% yield. ^{1}H NMR (400 MHz, DMSO-d_6, 145 °C) : δ 0.96 (t, J = 7.5 Hz, 3H), 1.52-1.61 (m, 1H), 1.70-1.78 (m, 1H), 2.83-2.91 (m, 2H), 3.03-3.10 (m, 1H), 3.16-3.24 (m, 2H), 3.43 (dd, J = 13.2, 7.0 Hz, 1H), 3.54 (s, 2H), 3.55-3.60 (m, 1H), 3.69-3.74 (m, 1H), 3.78 (dd, J = 13.2, 3.1 Hz, 1H), 4.25 (t, J = 5.6 Hz, 2H), 6.86 (dd, J = 8.0, 1.8 Hz, 1H), 7.07 (d, J = 1.8 Hz, 1H), 7.23 (dd, J = 8.6, 1.8 Hz, 1H), 7.28 (d, J = 8.0 Hz, 1H), 7.39 (d, J = 8.6 Hz, 1H), 7.74 (d, J = 1.8 Hz, 1H). ^{13}C NMR (100 MHz, DMSO-d_6) : δ 9.73, 20.31, 40.11, 47.28, 49.14, 50.74, 50.79, 59.06, 67.06, 114.98, 119.40, 119.51, 120.82, 122.52, 124.75, 126.11, 129.38, 131.87, 135.49, 151.29, 153.37, 168.44, 172.21. HRMS (ESI) : m/z $[M + H]^+$ calcd. for $C_{23}H_{26}Cl_2N_3O_3S^+$, 494.1066; found, 494.1053.

Compound **3_9**

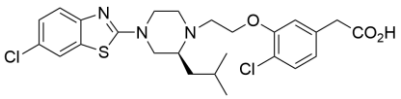

White solid, 77% yield. ^{1}H NMR (400 MHz, DMSO-d_6) : δ 0.90 (dd, J = 6.4, 0.9 Hz, 6H), 1.24-1.31 (m, 1H), 1.42-1.49 (m, 1H), 1.63-1.69 (m, 1H), 2.69-2.77 (m, 2H), 2.85 (dt, J = 13.8, 5.7 Hz, 1H), 2.97-3.05 (m, 2H), 3.27-3.34 (m, 1H), 3.55-3.59 (m, 4H), 3.65 (dd, J = 12.8, 2.9 Hz, 1H), 4.13 (t, J = 5.6 Hz, 2H), 6.85 (dd, J = 8.1, 1.5 Hz, 1H), 7.10 (d, J = 1.5 Hz, 1H), 7.28 (dd, J = 8.6, 2.2 Hz, 1H), 7.34 (d, J = 8.1 Hz, 1H), 7.41 (d, J = 8.6 Hz, 1H), 7.89 (d, J = 2.2 Hz, 1H), 12.35 (br s, 1H). ^{13}C NMR (100 MHz, DMSO-d_6) : δ

21.93, 23.38, 24.77, 36.22, 40.14, 46.66, 48.42, 50.69, 51.05, 56.27, 67.53, 115.09, 119.24, 119.49, 120.75, 122.44, 124.64, 126.05, 129.34, 131.70, 135.44, 151.40, 153.42, 168.58, 172.25. HRMS (ESI) : m/z $[M + H]^+$ calcd. for $C_{25}H_{30}Cl_2N_3O_3S^+$, 522.1379; found, 522.1384.

Compound **3_10**

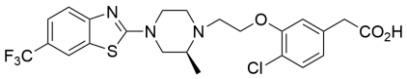

White solid, 81% yield. ^{1}H NMR (400 MHz, DMSO-d_6) : δ 1.13 (d, J = 6.1 Hz, 3H), 2.60-2.67 (m, 1H), 2.72-2.78 (m, 1H), 2.86 (dt, J = 14.1, 5.6 Hz, 1H), 3.02-3.13 (m, 3H), 3.40-3.47 (m, 1H), 3.57 (s, 2H), 3.78-3.85 (m, 2H), 4.15 (t, J = 5.5 Hz, 2H), 6.84 (dd, J = 8.2, 1.5 Hz, 1H), 7.10 (d, J = 1.5 Hz, 1H), 7.34 (d, J = 8.0 Hz, 1H), 7.54-7.59 (m, 2H), 8.23 (s, 1H), 12.40 (br s, 1H). ^{13}C NMR (100 MHz, DMSO-d_6) : δ 15.03, 40.16, 48.15, 49.91, 51.09, 53.53, 54.22, 66.76, 114.99, 118.16, 118,85 (q, J = 3.7 Hz), 119.42, 121.03 (q, J = 32.3 Hz), 122.43, 122.97 (q, J = 3.7 Hz), 124.65 (q, J = 271.4 Hz), 129.33, 130.79, 135.46, 153.39, 155.43, 170.05, 172.25. HRMS (ESI) : m/z $[M + H]^+$ calcd. for $C_{23}H_{24}ClF_3N_3O_3S^+$, 514.1174; found, 514.1183.

Compound **3_11**

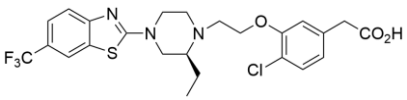

White solid, 93% yield. ^{1}H NMR (400 MHz, DMSO-d_6) : δ 0.93 (t, J = 7.4 Hz, 3H), 1.48-1.55 (m, 1H), 1.63-1.71 (m, 1H), 2.62-2.71 (m, 2H), 2.88 (dt, J = 14.1, 5.6 Hz, 1H), 3.02-3.09 (m, 2H), 3.36 (dd, J = 12.9, 7.6 Hz, 1H), 3.49-3.55 (m, 1H), 3.56 (s, 2H), 3.69-3.77

(m, 2H), 4.15 (t, J = 5.5 Hz, 2H), 6.84 (dd, J = 8.1, 1.4 Hz, 1H), 7.10 (d, J = 1.4 Hz, 1H), 7.33 (d, J = 8.1 Hz, 1H), 7.53-7.59 (m, 2H), 8.22 (s, 1H), 12.22 (br s, 1H). ^{13}C NMR (100 MHz, DMSO-d_6) : δ 9.46, 20.32, 40.44, 47.51, 49.11, 50.66, 50.86, 59.15, 67.13, 115.07, 118.24, 118,95 (q, J = 3.7 Hz), 119.46, 121.08 (q, J = 32.3 Hz), 122.53, 123.08 (q, J = 3.7 Hz), 124.77 (q, J = 271.4 Hz), 129.42, 130.82, 135.74, 153.50, 155.59, 170.32, 172.40. HRMS (ESI) : m/z $[M + H]^+$ calcd. for $C_{24}H_{26}ClF_3N_3O_3S^+$, 528.1330; found, 528.1356.

Synthesis of compound **6_17**

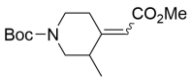

A mixture of trimethyl phosphonoacetate (376 μL, 2.32 mmol), 28% NaOMe solution in MeOH (471 μL, 2.32 mmol) and anhydrous THF (10 mL) was stirred at 0 °C for 1 hour. Then a solution of **6_16** (450 mg, 2.11 mmol) in THF (5 mL) was added dropwise thereto at 0 °C. After stirring at room temperature for 2 h, to the reaction mixture was added water and extracted with EtOAc. The extract was washed with brine, dried over Na_2SO_4, and concentrated under reduced pressure. The residue was purified by silica gel column chromatography to give compound **6_17** (564 mg, 99%) as a mixture of stereoisomers (E:Z = ca. 4:3). A colorless oil. ^{1}H-NMR (400 MHz, $CDCl_3$) : δ 1.09 (d, J = 6.7 Hz, 1.7H), 1.15 (d, J = 7.0 Hz, 1.3H), 1.47 (s, 9H), 2.05 (d, J = 13.8 Hz, 0.4H), 2.37-2.41 (m, 0.6H), 2.55-3.68 (m, 4H), 3.69 (s, 1.3H), 3.70 (s, 1.7H), 3.71-4.35 (m, 2H), 5.63 (d, J = 1.4 Hz, 0.4H), 5.69 (br s, 0.6H).

Synthesis of compound **6_18**

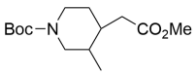

To a solution of **6_17** (200 mg, 0.743 mmol) in MeOH (6 mL) was added Pd/C (10%, 20.0 mg) at room temperature. After stirring under a hydrogen atmosphere at the same temperature for 2 hours, the insoluble material was filtrated and the filtrate was concentrated under reduced pressure to give compound **6_18** (197 mg, 98%) as a mixture of stereoisomers (ca. 3:1). A colorless oil. ^{1}H-NMR (400 MHz, $CDCl_3$) : δ 0.86 (d, J = 7.0 Hz, 2.25H), 0.90 (d, J = 6.7 Hz, 0.75H), 1.15-1.39 (m, 0.75H), 1.41-1.44 (m, 1H), 1.45 (s, 9H), 1.53-1.62 (m, 0.25H), 1.67-1.72 (m, 0.25H), 1.82 (br s, 0.75H), 2.04-2.40 (m, 3H), 2.57 (dd, J = 15.1, 4.3 Hz, 0.25H), 2.67-2.95 (m, 1H), 2.99 (dd, J = 13.2, 3.1 Hz, 0.75H), 3.68 (s, 3H), 3.73-3.78 (m, 0.75H), 3.86 (br s, 0.25H), 4.04 (br s, 1H).

Synthesis of compound **6_19**

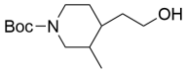

To a suspension of lithium aluminium hydride (66.4 mg, 1.75 mmol) in anhydrous THF (5 mL) was added dropwise a solution of **6_18** (475 mg, 1.75 mmol) in anhydrous THF (5 mL) under ice-cooling, and the mixture was stirred at the same temperature for 1 hour. Water (70 μL), 10% aqueous sodium hydroxide solution (70 μL) and water (210 μL) were added dropwise sequentially under ice-cooling. After filtration of aluminium hydroxide, the filtrate was concentrated under reduced pressure. The residue was purified by silica gel column chromatography to give compoound **6_19** (423 mg, 99%) as a mixture of stereoisomers. A colorless oil. ^{1}H NMR (300 MHz, $CDCl_3$) : δ 0.86 (d, J = 6.9 Hz, 2.25H),

0.91 (d, *J* = 6.7 Hz, 0.75H), 1.10-1.60 (m, 6H), 1.45 (s, 9H), 1.70-1.98 (m, 1.75H), 2.30-2.38 (dd, *J* = 13.2, 10.8 Hz, 0.25H), 2.64-2.82 (m, 1H), 2.93 (dd, *J* = 13.2, 2.4 Hz, 0.75H), 3.64-3.74 (m, 2H), 3.78-3.84 (m, 0.75H), 3.94-4.08 (m, 1H).

Synthesis of compound **6_20**

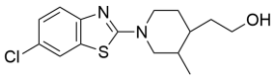

To 4 M solution of hydrochloric acid-dioxane (4 mL) was added **6_19** (410 mg, 1.69 mmol). After stirring at room temperature for 2 hours, the reaction mixture was concentrated under reduced pressure. To the obtained residue was added anhydrous DMF (5 mL), K_2CO_3 (699 mg, 5.06 mmol) and 2,6-dichlorobenzothiazole (344 mg, 1.69 mmol), and the mixture was stirred at 60 °C for 6 h. Water was added, and the mixture was extracted with EtOAc. The extract was washed with brine, dried over $MgSO_4$, and concentrated under reduced pressure. The residue was purified by silica gel column chromatography to give compound **6_20** (510 mg, 97%) as a mixture of stereoisomers. A colorless oil. ^{1}H NMR (300 MHz, $CDCl_3$) : δ 0.96 (d, *J* = 6.9 Hz, 2.25H), 1.01 (d, *J* = 6.6 Hz, 0.75H), 1.44-1.68 (m, 4H), 1.84-2.02 (m, 3H), 2.78 (dd, *J* = 12.4, 10.8 Hz, 0.25H), 3.08-3.23 (m, 1H), 3.36 (dd, *J* = 12.9, 2.4 Hz, 0.75H), 3.68-3.80 (m, 3H), 4.02-4.16 (m, 1H), 7.20-7.24 (m, 1H), 7.40-7.46 (m, 1H), 7.52-7.54 (m, 1H).

Synthesis of compound **6_21**

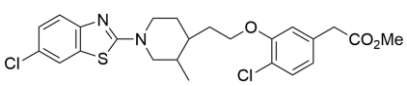

To a solution of **6_20** (150 mg, 0.483 mmol) and TEA (202 μL, 1.45 mmol) in anhydrous

CH_2Cl_2 (2 mL) was added MsCl (56 μL, 0.725 mmol) under ice-cooling. After stirring at room temperature for 1 hour, water was added, and the mixture was extracted with EtOAc. The extract was washed with brine, dried over $MgSO_4$, and concentrated under reduced pressure. A mixture of the residue, methyl 2-(4-chloro-3-hydroxyphenyl)acetate (107 mg, 0.531 mmol), Cs_2CO_3 (173 mg, 0.531 mmol) and anhydrous DMF (2 mL) was stirred at 60 °C for 3 hours. Water was added, and the mixture was extracted with EtOAc. The extract was washed with brine, dried over $MgSO_4$, and concentrated under reduced pressure. The residue was purified by silica gel column chromatography to give compound **6_21** (237 mg, 99%) as a mixture of stereoisomers. A colorless oil. ^{1}H NMR (300 MHz, $CDCl_3$) : δ 1.01 (d, J = 6.6 Hz, 2.25H), 1.06 (d, J = 6.0 Hz, 0.75H), 1.66-1.90 (m, 3H), 1.96-2.12 (m, 2H), 3.10-3.24 (m, 1H), 3.38-3.48 (m, 1H), 3.56-3.60 (m, 3H), 3.69-3.71 (m, 4H), 4.05-4.16 (m, 3H), 6.79-6.96 (m, 3H), 7.20-7.33 (m, 2H), 7.52-7.54 (m, 1H).

Synthesis of compound **3_5**

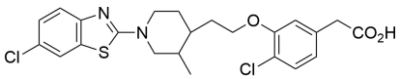

To a solution of **6_21** (205 mg, 0.415 mmol) in THF (1 mL) and MeOH (1 mL) was added 2 M aqueous NaOH solution (0.5 mL), and the mixture was stirred at room temperature for 1 hour. To the reaction mixture was added 2 M aqueous HCl solution to be acidic, and extracted with EtOAc. The extract was washed with brine, dried over Na_2SO_4, and concentrated under reduced pressure. The obtained solid was washed with n-hexane to give compound **3_5** (155 mg, 78%) as a mixture of stereoisomers. A white solid. ^{1}H NMR (400 MHz, DMSO-d_6) : δ 0.90 (d, J = 6.8 Hz, 2.1H), 0.98 (d, J = 5.9 Hz, 0.9H), 1.35-1.66

(m, 2.6H), 1.71-1.76 (m, 1.4H), 1.89-2.12 (m, 2H), 2.84 (dd, *J* = 12.7, 10.7 Hz, 0.3H), 3.12-3.24 (m, 1H), 3.37 (dd, *J* = 13.0, 2.7 Hz, 0.7H), 3.54-3.55 (m, 2H), 3.70-3.74 (m, 0.7H), 3.92-4.02 (m, 1.3H), 4.05-4.12 (m, 2H), 6.81-6.85 (m, 1H), 7.07-7.09 (m, 1H), 7.24-7.28 (m, 1H), 7.31-7.41 (m, 2H), 7.85 (d, *J* = 2.1 Hz, 0.7H), 7.87 (d, J = 2.3 Hz, 0.3H). ^{13}C NMR (100 MHz, DMSO-d_6) : δ 11.54, 16.25, 25.77, 29.58, 30.59, 31.26, 31.61, 34.63, 34.90, 40.56, 47.55, 48.51, 54.49, 54.77, 66.28, 66.74, 115.03, 118.97, 119.11, 119.33, 119.35, 119.37, 119.39, 120.58, 120.66, 122.32, 122.36, 124.37, 124.50, 125.94, 125.97, 129.27, 131.72, 131.88, 138.81, 135.84, 135.89, 151.54, 151.56, 153.40, 135.43, 168.01, 168.81, 172.35. HRMS (ESI) : m/z $[M + H]^+$ calcd. for $C_{23}H_{25}Cl_2N_2O_3S^+$, 479.0957; found, 479.0966.

Typical procedure for synthesis of compounds **6_24a–k**

A mixture of 2-chloro-6-(trifluoromethyl)benzothiazole (300 mg, 1.26 mmol), the corresponding *N*-Boc-piperazine (1.52 mmol), K_2CO_3 (523 mg, 3.79 mmol) and anhydrous DMF (3 mL) was stirred at 50 °C for 3 hours. Water was added, and the mixture was extracted with EtOAc. The extract was washed with brine, dried over Na_2SO_4, and concentrated under reduced pressure. The residue was purified by silica gel column chromatography to give the target compound.

Compound **6_24a**

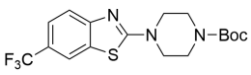

White solid, 75% yield. ^{1}H NMR (400 MHz, $CDCl_3$) : δ 1.49 (s, 9H), 3.58-3.62 (m, 4H), 3.64-3.68 (m, 4H), 7.54 (dd, *J* = 8.5, 1.4 Hz, 1H), 7.59 (d, *J* = 8.5 Hz, 1H), 7.87 (s, 1H).

Compound **6_24b**

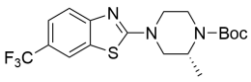

White solid, 70% yield. ^{1}H NMR (400 MHz, $CDCl_3$) : δ 1.24 (d, J = 6.8 Hz, 3H), 1.49 (s, 9H), 3.20-3.31 (m, 2H), 3.48 (dd, J = 13.1, 4.0 Hz, 1H), 3.84 (d, J = 13.1 Hz, 1H), 3.97-4.15 (m, 2H), 4.40-4.45 (m, 1H), 7.54 (dd, J = 8.5, 1.5 Hz, 1H), 7.57 (d, J = 8.5 Hz, 1H), 7.86 (s, 1H).

Compound **6_24c**

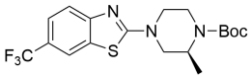

White solid, 74% yield. ^{1}H NMR (400 MHz, $CDCl_3$) : δ 1.24 (d, J = 6.8 Hz, 3H), 1.49 (s, 9H), 3.21-3.31 (m, 2H), 3.48 (dd, J = 13.2, 4.0 Hz, 1H), 3.84 (d, J = 13.1 Hz, 1H), 3.97-4.15 (m, 2H), 4.40-4.45 (m, 1H), 7.54 (dd, J = 8.5, 1.6 Hz, 1H), 7.57 (d, J = 8.5 Hz, 1H), 7.86 (s, 1H).

Compound **6_24d**

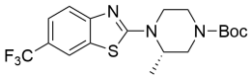

White solid, 50% yield. ^{1}H NMR (300 MHz, $CDCl_3$) : δ 1.32 (d, J = 6.5 Hz, 3H), 1.50 (s, 9H), 2.85-3.27 (m, 2H), 3.32-3.52 (m, 1H), 3.82-4.38 (m, 4H), 7.54 (d, J = 8.5 Hz, 1H), 7.58 (d, J = 8.5 Hz, 1H), 7.86 (s, 1H).

Compound **6_24e**

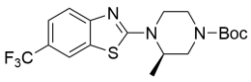

White solid, 65% yield. ^{1}H NMR (300 MHz, $CDCl_3$) : δ 1.31 (d, J = 6.5 Hz, 3H), 1.50 (s, 9H), 2.90-3.30 (m, 2H), 3.44 (td, J = 12.5, 3.5 Hz, 1H), 3.85-4.35 (m, 4H), 7.53 (dd, J = 8.5, 1.5 Hz, 1H), 7.58 (d, J = 8.5 Hz, 1H), 7.86 (d, J = 1.5 Hz, 1H).

Compound **6_24f**

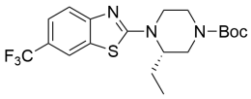

White solid, 67% yield. ^{1}H NMR (300 MHz, $CDCl_3$) : δ 1.01 (t, J = 7.5 Hz, 3H), 1.49 (s, 9H), 1.68-1.80 (m, 2H), 2.90-3.20 (m, 2H), 3.32-3.46 (m, 1H), 3.90-4.32 (m, 4H), 7.54 (d, J = 8.5 Hz, 1H), 7.55 (d, J = 8.5 Hz, 1H), 7.85 (s, 1H).

Compound **6_24g**

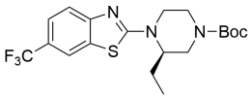

White solid, 60% yield. ^{1}H NMR (300 MHz, $CDCl_3$) : δ 1.01 (t, J = 7.5 Hz, 3H), 1.49 (s, 9H), 1.74 (q, J = 7.5 Hz, 2H), 2.90-3.20 (m, 2H), 3.33-3.46 (m, 1H), 3.92-4.31 (m, 4H), 7.50-7.58 (m, 2H), 7.85 (s, 1H).

Compound **6_24h**

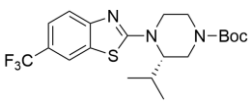

White solid, 31% yield. ^{1}H NMR (300 MHz, $CDCl_3$) : δ 0.91 (d, J = 6.5 Hz, 3H), 1.13 (d, J = 6.5 Hz, 3H), 1.49 (s, 9H), 2.12-2.24 (m, 1H), 2.84-3.13 (m, 2H), 3.27-3.43 (m, 1H), 3.60-3.75 (m, 1H), 4.02-4.40 (m, 3H), 7.53 (s, 2H), 7.83 (s, 1H).

Compound **6_24i**

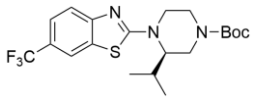

White solid, 11% yield. ^{1}H NMR (300 MHz, $CDCl_3$) : δ 0.92 (d, J = 6.5 Hz, 3H), 1.13 (d, J = 6.5 Hz, 3H), 1.49 (s, 9H), 2.07-2.27 (m, 1H), 2.70-3.15 (m, 2H), 3.25-3.44 (m, 1H), 3.59-3.75 (m, 1H), 3.95-4.46 (m, 3H), 7.52 (s, 1H), 7.53 (s, 1H), 7.83 (s, 1H).

Compound **6_24j**

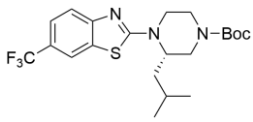

White solid, 57% yield. ^{1}H NMR (300 MHz, $CDCl_3$) : δ 1.00 (t, J = 6.0Hz, 6H), 1.40-1.52(m, 1H), 1.49(s, 9H), 1.60-1.69(m, 2H), 2.99 (t, J = 10.8 Hz, 1H), 3.12 (d, J = 10.8 Hz, 1H), 3.40 (dt, J = 3.6, 12.9 Hz, 1H), 3.98-4.13 (m, 4H), 7.49-7.56 (m, 2H), 7.84 (s, 1H).

Compound **6_24k**

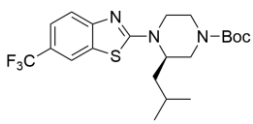

White solid, 43% yield. ^{1}H NMR (300 MHz, $CDCl_3$) : δ 0.99 (d, J = 6.5 Hz, 3H), 1.00 (d,

J = 6.5 Hz, 3H), 1.37-1.52 (m, 1H), 1.49 (s, 9H), 1.57-1.75 (m, 2H), 2.84-3.23 (m, 2H), 3.40 (td, *J* = 13.0, 3.5 Hz, 1H), 3.94-4.35 (m, 4H), 7.48-7.58 (m, 2H), 7.85 (s, 1H).

Typical procedure for synthesis of compounds **6_25a–k**

To 4 M solution of hydrochloric acid-dioxane (3 mL, 12 mmol) was added **6_24** (0.774 mmol). After stirring at room temperature for 3 hours, the reaction mixture was concentrated under reduced pressure and the residue was washed with IPE to give the target compound.

Compound **6_25a**

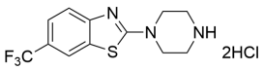

White solid, 100% yield. ^{1}H NMR (400 MHz, DMSO-d$_6$) : δ 3.26 (br s, 4H), 3.85-3.90 (m, 4H), 4.55 (br s, 1H), 7.63 (s, 2H), 8.33 (s, 1H), 9.50 (br s, 2H).

Compound **6_25b**

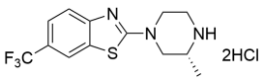

White solid, 100% yield. ^{1}H NMR (400 MHz, DMSO-d$_6$) : δ 1.33 (d, *J* = 6.3 Hz, 3H), 3.12-3.23 (m, 1H), 3.32-3.47 (m, 3H), 3.55-3.63 (m, 2H), 4.10-4.22 (m, 1H), 4.49 (br s, 1H), 7.63 (s, 2H), 8.33 (s, 1H), 9.48-9.56 (m, 1H), 9.58-9.65 (m, 1H).

Compound **6_25c**

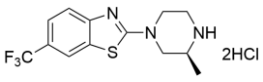

White solid, 98% yield. ^{1}H NMR (400 MHz, DMSO-d_6) : δ 1.33 (d, J = 6.1 Hz, 3H), 3.12-3.22 (m, 1H), 3.33-3.46 (m, 3H), 3.56-3.64 (m, 2H), 4.10-4.22 (m, 1H), 4.38 (br s, 1H), 7.63 (s, 2H), 8.33 (s, 1H), 9.54-9.61 (m, 1H), 9.64-9.69 (m, 1H).

Compound **6_25d**

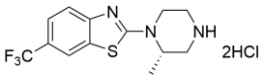

White solid, 80% yield. ^{1}H NMR (300 MHz, DMSO-d_6) : δ 1.41 (d, J = 7.0 Hz, 3H), 3.00-3.17 (m, 1H), 3.18-3.38 (m, 3H), 3.49-3.64 (m, 1H), 4.05-4.14 (m, 1H), 4.45-4.58 (m, 1H), 6.03 (br s, 1H) 7.61 (m, 2H), 8.31 (s, 1H), 9.25-9.50 (m, 1H), 9.73-9.92 (m, 1H).

Compound **6_25e**

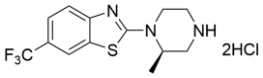

White solid, 100% yield. ^{1}H NMR (300 MHz, $CDCl_3$) : δ 1.40 (d, J = 7.0 Hz, 3H), 2.84-2.96 (m, 2H), 3.05-3.15 (m, 2H), 3.39 (dt, J = 12.5, 3.5 Hz, 1H), 3.88 (dd, J = 12.5, 2.5 Hz, 1H), 4.15-4.25 (m, 1H), 7.52 (dd, J = 8.5, 1.5 Hz, 1H), 7.56 (d, J = 8.5 Hz, 1H), 7.85 (d, J = 1.5 Hz, 1H).

Compound **6_25f**

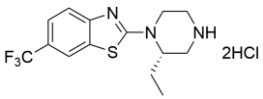

White solid, quantitative yield. ^{1}H NMR (300 MHz, $CDCl_3$) : δ 0.98 (t, J = 7.5 Hz, 3H), 1.72 (br s, 1H), 1.91 (q, J = 7.5 Hz, 2H), 2.89 (td, J = 12.5, 3.5 Hz, 1H), 2.95-3.13 (m,

3H), 3.38 (td, *J* = 12.5, 3.5 Hz, 1H), 3.84-3.95 (m, 1H), 3.95-4.08 (m, 1H), 7.50 (d, *J* = 8.5 Hz, 1H), 7.54 (d, *J* = 8.5 Hz, 1H), 7.83 (s, 1H).

Compound **6_25g**

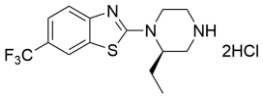

White solid, quantitative yield. ^{1}H NMR (300 MHz, $CDCl_3$) : δ 0.98 (t, *J* = 7.5 Hz, 3H), 1.61 (br s, 1H), 1.90 (q, *J* = 7.5 Hz, 2H), 2.89 (td, *J* = 12, 3.5 Hz, 1H), 2.95-3.13 (m, 3H), 3.37 (td, *J* = 12.5, 3.5 Hz, 1H), 3.83-3.94 (m, 1H), 3.95-4.06 (m, 1H), 7.45-7.56 (m, 2H), 7.83 (s, 1H).

Compound **6_25h**

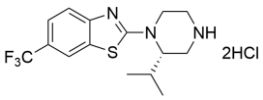

White solid, 93% yield. ^{1}H NMR (300 MHz, DMSO-d_6) : δ 0.86 (d, *J* = 6.5 Hz, 3H), 1.00 (d, *J* = 6.5 Hz, 3H), 2.50-2.60 (m, 1H), 3.03-3.31 (m, 3H), 3.44-3.60 (m, 2H), 3.90-4.00 (m, 1H), 4.20-4.30 (m, 1H), 7.54-7.63 (m, 2H), 8.29 (s, 1H), 9.23 (br s, 1H), 9.48 (br s, 1H).

Compound **6_25i**

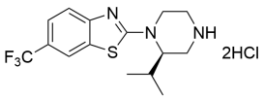

White solid, quantitative yield. ^{1}H NMR (300 MHz, DMSO-d_6) : δ 0.86 (d, *J* = 6.5 Hz, 3H), 1.04 (d, *J* = 6.5 Hz, 3H), 3.00-3.35 (m, 4H), 3.38-3.60 (m, 2H), 3.87-4.02 (m, 1H),

4.16-4.31 (m, 1H), 5.20 (br s, 1H), 7.57 (d, J = 8.5 Hz, 1H), 7.61 (d, J = 8.5 Hz, 1H), 8.29 (s, 1H), 9.05-9.22 (m, 1H), 9.37-9.50 (m, 1H).

Compound **6_25j**

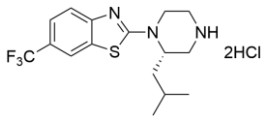

White solid, 97% yield. ^{1}H NMR (300 MHz, $CDCl_3$) : δ 1.04 (s, 6H), 1.68 (br s, 1H), 1.98 (br s, 1H), 2.07 (br s, 1H), 3.54 (br s, 3H), 3.71 (br s, 1H), 3.98 (s, 1H), 4.46 (br s, 2H), 7.52 (d, J = 7.5 Hz, 1H), 7.65 (d, J = 7.5 Hz, 1H), 7.90 (s, 1H).

Compound **6_25k**

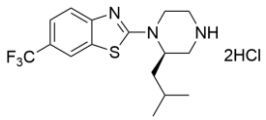

White solid, quantitative yield. ^{1}H NMR (300 MHz, DMSO-d_6) : δ 0.96 (d, J = 6.5 Hz, 6H), 1.50-1.90 (m, 3H), 2.99-3.39 (m, 4H), 3.46-3.63 (m, 1H), 4.08-4.22 (m, 1H), 4.35-4.48 (m, 1H), 6.11 (br s, 1H), 7.60 (s, 2H), 8.31 (s, 1H), 9.10-9.29 (m, 1H), 9.54-9.67 (m, 1H).

Typical procedure for synthesis of compounds **6_26a–k**

A mixture of **6_25** (0.555 mmol), ethyl 2-(3-(bromomethyl)-5-methylphenyl)acetate (166 mg, 0.611 mmol), K_2CO_3 (230 mg, 1.67 mmol) and anhydrous DMF (2 mL) was stirred at 60 °C for 3 hours. Water was added, and the mixture was extracted with EtOAc. The extract was washed with brine, dried over $MgSO_4$, and concentrated under reduced

pressure. The residue was purified by silica gel column chromatography to give the target compound.

Compound **6_26a**

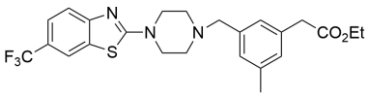

Colorless oil, 89% yield. ^{1}H NMR (400 MHz, $CDCl_3$) : δ 1.26 (t, J = 7.1 Hz, 5H), 2.35 (s, 3H), 2.57-2.60 (m, 4H), 3.52 (s, 2H), 3.58 (s, 2H), 3.67-3.70 (m, 4H), 4.16 (q, J = 7.1 Hz, 2H), 7.02 (br s, 1H), 7.06 (br s, 2H), 7.51-7.58 (m, 2H), 7.84 (br s, 1H).

Compound **6_26b**

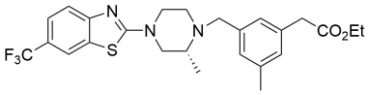

Colorless oil, 92% yield. ^{1}H NMR (400 MHz, $CDCl_3$) : δ 1.24 (t, J = 6.4 Hz, 3H), 1.26 (t, J = 7.1 Hz, 3H), 2.25-2.31 (m, 1H), 2.34 (s, 3H), 2.62-2.67 (m, 1H), 2.80-2.85 (m, 1H), 3.15-3.24 (m, 2H), 3.40-3.47 (m, 1H), 3.58 (s, 2H), 3.73-3.78 (m, 1H), 3.89-3.94 (m, 1H), 4.02 (d, J = 13.3 Hz, 1H), 4.16 (q, J = 7.1 Hz, 2H), 7.01 (s, 1H), 7.05 (s, 2H), 7.50-7.57 (m, 2H), 7.83 (s, 1H).

Compound **6_26c**

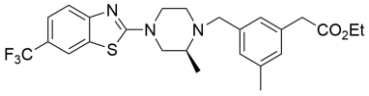

Colorless oil, 88% yield. ^{1}H NMR (400 MHz, $CDCl_3$) : δ 1.24 (t, J = 6.4 Hz, 3H), 1.26 (t, J = 7.1 Hz, 3H), 2.25-2.31 (m, 1H), 2.34 (s, 3H), 2.62-2.67 (m, 1H), 2.80-2.85 (m, 1H),

3.15-3.24 (m, 2H), 3.40-3.47 (m, 1H), 3.58 (s, 2H), 3.73-3.79 (m, 1H), 3.89-3.94 (m, 1H), 4.02 (d, J = 13.3 Hz, 1H), 4.16 (q, J = 7.1 Hz, 2H), 7.01 (s, 1H), 7.05 (s, 2H), 7.50-7.57 (m, 2H), 7.83 (s, 1H).

Compound **6_26d**

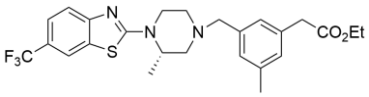

Colorless oil, 69% yield. ^{1}H NMR (300 MHz, $CDCl_3$) : δ 1.26 (t, J = 7.0 Hz, 3H), 1.43 (d, J = 6.5 Hz, 3H), 2.17-2.39 (m, 5H), 2.70-2.79 (m, 1H), 2.87-2.97 (m, 1H), 3.43 (d, J = 13.0 Hz, 1H), 3.46-3.62 (m, 4H), 3.85-3.97 (m, 1H), 4.16 (q, J = 7.0 Hz, 2H), 4.17-4.29 (m, 1H), 7.02 (s, 1H), 7.05-7.11 (m, 2H), 7.47-7.59 (m, 2H), 7.84 (s, 1H).

Compound **6_26e**

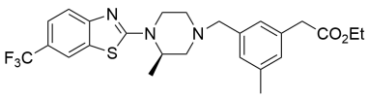

Colorless oil, 74% yield. ^{1}H NMR (300 MHz, $CDCl_3$) : δ 1.26 (t, J = 7.0 Hz, 3H), 1.42 (d, J = 6.5 Hz, 3H), 2.18-2.34 (m, 2H), 2.35 (s, 3H), 2.74 (d, J = 11.0 Hz, 1H), 2.92 (d, J = 11.5 Hz, 1H), 3.42 (d, J = 13.5 Hz, 1H), 3.53 (td, J = 11.5, 3.5 Hz, 1H), 3.56 (d, J = 13.5 Hz, 1H), 3.58 (s, 2H), 3.91 (d, J = 12.0 Hz, 1H), 4.15 (q, J = 7.0 Hz, 2H), 4.15-4.30 (m, 1H), 7.02 (s, 1H), 7.07 (s, 1H), 7.09 (s, 1H), 7.51 (d, J = 8.5 Hz, 1H), 7.55 (d, J = 8.5 Hz, 1H), 7.84 (s, 1H).

Compound **6_26f**

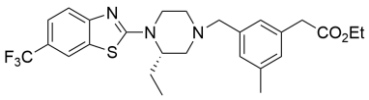

Colorless oil, 73% yield. ^{1}H NMR (300 MHz, $CDCl_3$) : δ 0.88 (t, J = 7.5 Hz, 3H), 1.26 (t, J = 7.0 Hz, 3H), 1.95 (q, J = 7.5 Hz, 2H), 2.15-2.28 (m, 2H), 2.34 (s, 3H), 2.82-2.93 (m, 2H), 3.39 (d, J = 13.5 Hz, 1H), 3.48 (td, J = 12.5, 3.5 Hz, 1H), 3.55 (d, J = 13.5 Hz, 1H), 3.57 (s, 2H), 3.80-3.95 (m, 1H), 3.98-4.10 (m, 1H), 4.15 (q, J = 7.0 Hz, 2H), 7.01 (s, 1H), 7.06 (s, 2H), 7.52 (s, 2H), 7.82 (s, 1H).

Compound **6_26g**

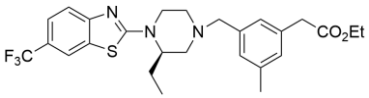

Colorless oil, 53% yield. ^{1}H NMR (300 MHz, $CDCl_3$) : δ 0.89 (t, J = 7.5 Hz, 3H), 1.20 (t, J = 7.0 Hz, 3H), 1.87-2.03 (m, 2H), 2.24 (td, J = 11.0, 3.5 Hz, 2H), 2.34 (s, 3H), 2.82-2.95 (m, 2H), 3.38 (d, J = 13.0 Hz, 1H), 3.49 (td, J = 13.0, 3.5 Hz, 1H), 3.56 (d, J = 13 Hz, 1H), 3.57 (s, 2H), 3.80-3.95 (m, 1H), 4.00-4.10 (m, 1H), 4.16 (q, J = 7.0 Hz, 2H), 7.01 (s, 1H), 7.05 (s, 1H), 7.06 (s, 1H), 7.48-7.55 (m, 2H), 7.82 (s, 1H).

Compound **6_26h**

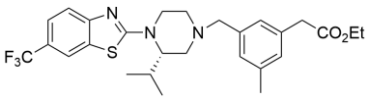

Colorless oil, 70% yield. ^{1}H NMR (300 MHz, $CDCl_3$) : δ 0.90 (d, J = 2.5 Hz, 3H), 0.91 (d, J = 2.5 Hz, 3H), 1.26 (t, J = 7.0 Hz, 3H), 2.12 (dd, J = 11.5, 3.5 Hz, 1H), 2.23 (td, J = 11.5, 3.5 Hz, 1H), 2.34 (s, 3H), 2.55-2.73 (m, 1H), 2.88 (d, J = 9.5 Hz, 1H), 2.98 (d, J =

9.5 Hz, 1H), 3.34 (d, *J* = 13.0 Hz, 1H), 3.40-3.54 (m, 1H), 3.56 (d, *J* = 13.0 Hz, 1H), 3.57 (s, 2H), 3.57-3.60 (m, 1H), 4.11-4.15 (m, 1H), 4.16 (q, *J* = 7.0 Hz, 2H), 7.01 (s, 1H), 7.04 (s, 1H), 7.05 (s, 1H), 7.49-7.50 (m, 2H), 7.79 (s, 1H).

Compound **6_26i**

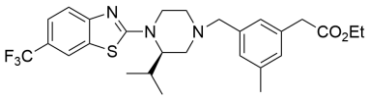

Colorless oil, 44% yield. ^{1}H NMR (300 MHz, $CDCl_3$) : δ 0.90 (d, *J* = 6.5 Hz, 3H), 0.91 (d, *J* = 6.5 Hz, 3H), 1.26 (t, *J* = 7.0 Hz, 3H), 2.12 (dd, *J* = 11.5, 3.5 Hz, 1H), 2.23 (td, *J* = 11.5, 3.5 Hz, 1H), 2.34 (s, 3H), 2.56-2.72 (m, 1H), 2.88 (d, *J* = 11.5 Hz, 1H), 2.98 (d, *J* = 11.5 Hz, 1H), 3.34 (d, *J* = 13.0 Hz, 1H), 3.40-3.65 (m, 2H), 3.56 (d, *J* = 13.0 Hz, 1H), 3.57 (s, 2H), 4.08-4.22 (m, 1H), 4.15 (q, *J* = 7.0 Hz, 2H), 7.01 (s, 1H), 7.05 (s, 2H), 7.49 (s, 2H), 7.79 (s, 1H).

Compound **6_26j**

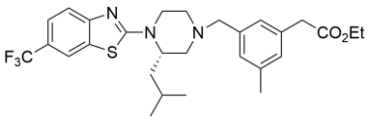

Colorless oil, 80% yield. ^{1}H NMR (300 MHz, $CDCl_3$) : δ 0.94 (dd, *J* = 6.3, 3.0 Hz, 6H), 1.26 (t, *J* = 7.2 Hz, 3H), 1.44-1.48 (m, 1H), 1.56-1.62 (m, 1H), 1.91-2.00 (m, 1H), 2.18-2.26 (m, 2H), 2.34 (s, 3H), 2.80 (d, *J* = 11.4 Hz, 1H), 2.91 (d, *J* = 11.4 Hz, 1H), 3.36 (d, *J* = 13.2 Hz, 1H), 3.52 (dt, *J* = 12.6, 3.6 Hz, 1H), 3.57 (s, 2H), 3.60 (d, *J* = 13.2 Hz, 1H), 4.04 (br s, 2H), 4.16 (q, *J* = 7.2 Hz, 2H), 7.01 (s, 1H), 7.04 (s, 1H), 7.06 (s, 1H), 7.2 (s, 2H), 7.83 (s, 1H).

Compound **6_26k**

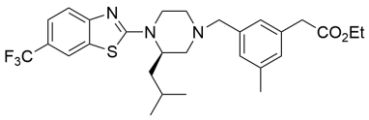

Colorless oil, 47% yield. ^{1}H NMR (300 MHz, $CDCl_3$) : δ 0.94 (d, J = 6.5 Hz, 3H), 0.95 (d, J = 6.5 Hz, 3H), 1.27 (t, J = 7.0 Hz, 3H), 1.38-1.67 (m, 2H), 1.89-2.04 (m, 1H), 2.14-2.38 (m, 2H), 2.34 (s, 3H), 2.80 (d, J = 11.5 Hz, 1H), 2.90 (d, J = 11.5 Hz, 1H), 3.35 (d, J = 13.5 Hz, 1H), 3.44-3.64 (m, 2H), 3.57 (s, 2H), 3.94-4.21 (m, 2H), 4.16 (q, J = 7.0 Hz, 2H), 7.01 (s, 1H), 7.06 (s, 2H), 7.49 (d, J = 8.5 Hz, 1H), 7.53 (d, J = 8.5 Hz, 1H), 7.82 (s, 1H).

Typical procedure for synthesis of compounds **3_12–22**

To a solution of **6_26** (0.209 mmol) in THF (0.5 mL) and MeOH (0.5 mL) was added 2 M aqueous NaOH solution (0.5 mL), and the mixture was stirred at 60 °C for 1 hour. To the reaction mixture was added 2 M aqueous HCl solution to be neutral, and extracted with EtOAc. The extract was washed with brine, dried over Na_2SO_4, and concentrated under reduced pressure. The obtained solid was washed with IPE to give the target compound.

Compound **3_12**

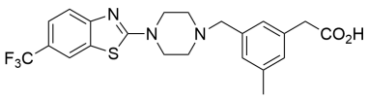

White solid, 64% yield. ^{1}H NMR (400 MHz, DMSO-d_6, 145 °C) : δ 2.29 (s, 3H), 2.61 (t, J = 5.1 Hz, 4H), 3.50 (s, 2H), 3.57 (s, 2H), 3.66 (t, J = 5.1 Hz, 4H), 6.98 (s, 1H), 7.04 (d,

J = 6.7 Hz, 2H), 7.51-7.53 (m, 2H), 8.06 (s, 1H). ^{13}C NMR (100 MHz, DMSO-d_6) : δ 20.81, 40.55, 47.85, 51.59, 61.55, 115.54, 118.29, 118,92 (q, *J* = 3.7 Hz), 121.14 (q, *J* = 32.3 Hz), 122.97 (q, *J* = 3.7 Hz), 124.65 (q, *J* = 271.4 Hz), 127.08, 127.95, 128.86, 130.86, 134.79, 137.70, 155.37, 170.17, 172.61. HRMS (ESI) : m/z [M + H]$^+$ calcd. for $C_{22}H_{23}F_3N_3O_2S^+$, 450.1458; found, 450.1483.

Compound **3_13**

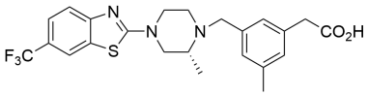

White solid, 57% yield. ^{1}H NMR (400 MHz, DMSO-d_6) : δ 1.16 (d, *J* = 6.0 Hz, 3H), 2.19-2.25 (m, 1H), 2.28 (s, 3H), 2.57-2.62 (m, 1H), 2.71-2.76 (m, 1H), 3.16-3.23 (m, 2H), 3.37-3.44 (m, 1H), 3.50 (s, 2H), 3.73 (d, *J* = 12.0 Hz, 1H), 3.84 (d, *J* = 12.0 Hz, 1H), 3.93 (d, *J* = 13.4 Hz, 1H), 6.96 (s, 1H), 7.02 (br s, 2H), 7.54-7.58 (m, 2H), 8.23 (s, 1H), 11.66 (br s, 1H). ^{13}C NMR (100 MHz, DMSO-d_6) : δ 14.77, 20.83, 40.84, 48.00, 48.87, 53.96, 54.05, 56.81, 118.16, 118.86 (q, *J* = 3.7 Hz), 121.03 (q, *J* = 32.3 Hz), 122.96 (q, *J* = 3.7 Hz), 124.65 (q, *J* = 271.4 Hz), 126.85, 127.60, 128.57, 130.81, 134.96, 137.05, 138.32, 155.44, 170.06, 172.71. HRMS (ESI) : m/z [M + H]$^+$ calcd. for $C_{23}H_{25}F_3N_3O_2S^+$, 464.1614; found, 464.1625.

Compound **3_14**

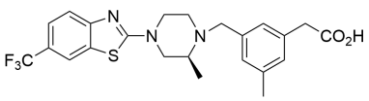

White solid, 60% yield. ^{1}H NMR (400 MHz, DMSO-d_6) : δ 1.16 (d, *J* = 5.9 Hz, 3H), 2.20-2.25 (m, 1H), 2.29 (s, 3H), 2.58-2.63 (m, 1H), 2.72-2.77 (m, 1H), 3.17-3.23 (m, 2H),

3.38-3.44 (m, 1H), 3.51 (s, 2H), 3.74 (d, J = 11.8 Hz, 1H), 3.85 (d, J = 11.8 Hz, 1H), 3.94 (d, J = 13.3 Hz, 1H), 6.96 (s, 1H), 7.03 (d, J = 4.3 Hz, 2H), 7.54-7.58 (m, 2H), 8.23 (s, 1H), 12.25 (br s, 1H). ^{13}C NMR (100 MHz, DMSO-d_6) : δ 14.76, 20.83, 40.58, 47.98, 48.87, 53.99, 54.10, 56.78, 118.18, 118.86 (q, J = 3.7 Hz), 121.06 (q, J = 32.3 Hz), 122.97 (q, J = 3.7 Hz), 124.66 (q, J = 271.4 Hz), 126.88, 127.71, 128.60, 130.82, 134.73, 137.13, 138.36, 155.44, 170.07, 172.63. HRMS (ESI) : m/z $[M + H]^+$ calcd. for $C_{23}H_{25}F_3N_3O_2S^+$, 464.1614; found, 464.1624.

Compound **3_15**

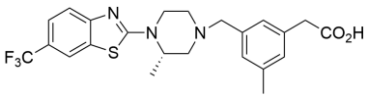

White solid, 72% yield. ^{1}H NMR (400 MHz, DMSO-d_6) : δ 1.33 (d, J = 6.7 Hz, 3H), 2.14 (td, J = 11.8, 3.5 Hz, 1H), 2.21 (dd, J = 11.4, 3.7 Hz, 1H), 2.28 (s, 3H), 2.71 (d, J = 11.2 Hz, 1H), 2.92 (d, J = 11.2 Hz, 1H), 3.36-3.46 (m, 2H), 3.48 (s, 2H), 3.54 (d, J = 13.4 Hz, 1H), 3.85 (d, J = 11.9 Hz, 1H), 4.25 (br s, 1H), 6.97 (s, 1H), 7.02 (s, 1H), 7.05 (s, 1H), 7.56 (s, 2H), 8.23 (s, 1H). ^{13}C NMR (100 MHz, DMSO-d_6) : δ 14.64, 20.85, 41.30, 43.75, 52.03, 52.21, 56.41, 61.51, 118.18, 118.84 (q, J = 3.7 Hz), 120.98 (q, J = 32.3 Hz), 122.93 (q, J = 3.7 Hz), 124.68 (q, J = 271.4 Hz), 126.55, 127.20, 128.69, 130.62, 135.44, 137.03, 137.74, 155.43, 169.60, 172.91. HRMS (ESI) : m/z $[M + H]^+$ calcd. for $C_{23}H_{25}F_3N_3O_2S^+$, 464.1614; found, 464.1628

Compound **3_16**

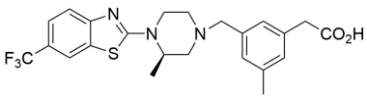

White solid, 98% yield. ^{1}H NMR (400 MHz, DMSO-d_6) : δ 1.33 (d, J = 6.5 Hz, 3H), 2.13 (td, J = 11.8, 3.5 Hz, 1H), 2.20 (dd, J = 11.4, 3.7 Hz, 1H), 2.28 (s, 3H), 2.71 (d, J = 11.2 Hz, 1H), 2.91 (d, J = 11.2 Hz, 1H), 3.36-3.44 (m, 2H), 3.45 (s, 2H), 3.53 (d, J = 13.4 Hz, 1H), 3.84 (d, J = 11.9 Hz, 1H), 4.24 (br s, 1H), 6.96 (s, 1H), 7.00 (s, 1H), 7.04 (s, 1H), 7.56-7.57 (m, 2H), 8.23 (s, 1H). ^{13}C NMR (100 MHz, DMSO-d_6) : δ 14.64, 20.87, 41.90, 43.75, 52.04, 52.21, 56.41, 61.56, 118.18, 118.84 (q, J = 3.7 Hz), 120.98 (q, J = 32.3 Hz), 122.92 (q, J = 3.7 Hz), 124.68 (q, J = 271.4 Hz), 126.57, 127.01, 128.70, 130.62, 136.00, 136.90, 137.61, 155.44, 169.59, 173.08. HRMS (ESI) : m/z [M + H]$^{+}$ calcd. for $C_{23}H_{25}F_3N_3O_2S^{+}$, 464.1614; found, 464.1648.

Compound **3_17**

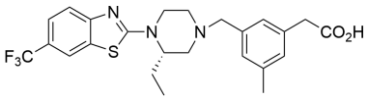

White solid, 96% yield. ^{1}H NMR (400 MHz, DMSO-d_6) : δ 0.81 (t, J = 7.5 Hz, 3H), 1.78-1.95 (m, 2H), 2.09-2.18 (m, 2H), 2.29 (s, 3H), 2.82 (d, J = 11.4 Hz, 1H), 2.91 (d, J = 11.4 Hz, 1H), 3.34-3.44 (m, 2H), 3.52 (s, 2H), 3.57 (d, J = 13.4 Hz, 1H), 3.96 (br s, 2H), 6.97 (s, 1H), 7.04 (br s, 2H), 7.51-7.57 (m, 2H), 8.21 (s, 1H), 12.29 (br s, 1H). ^{13}C NMR (100 MHz, DMSO-d_6) : δ 10.54, 20.82, 21.63, 40.63, 44.05, 52.29, 53.47, 58.36, 61.47, 118.02, 118.77 (q, J = 3.7 Hz), 120.90 (q, J = 32.3 Hz), 122.94 (q, J = 3.7 Hz), 124.70 (q, J = 271.4 Hz), 126.50, 127.41, 128.71, 130.58, 134.80, 137.16, 137.90, 155.52, 169.90, 172.62. HRMS (ESI) : m/z [M + H]$^{+}$ calcd. for $C_{24}H_{27}F_3N_3O_2S^{+}$, 478.1771; found, 478.1785.

Compound **3_18**

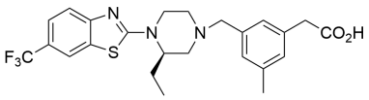

White solid, 89% yield. ^{1}H NMR (400 MHz, DMSO-d_6) : δ 0.81 (t, J = 7.5 Hz, 3H), 1.78-1.95 (m, 2H), 2.10-2.18 (m, 2H), 2.29 (s, 3H), 2.82 (d, J = 11.3 Hz, 1H), 2.91 (d, J = 11.3 Hz, 1H), 3.35-3.39 (m, 1H), 3.43 (dd, J = 12.7, 2.8 Hz, 1H), 3.52 (s, 2H), 3.57 (d, J = 13.3 Hz, 1H), 3.96 (br s, 2H), 6.98 (s, 1H), 7.04 (br s, 2H), 7.53 (d, J = 8.6 Hz, 1H), 7.56 (dd, J = 8.6, 1.6 Hz, 1H), 8.21 (br s, 1H), 12.29 (br s, 1H). ^{13}C NMR (100 MHz, DMSO-d_6) : δ 10.54, 20.82, 21.63, 40.63, 44.07, 52.29, 53.47, 58.36, 61.47, 118.02, 118.77 (q, J = 3.7 Hz), 120.90 (q, J = 32.3 Hz), 122.94 (q, J = 3.7 Hz), 124.70 (q, J = 271.4 Hz), 126.50, 127.41, 128.71, 130.59, 134.80, 137.16, 137.90, 155.52, 169.90, 172.61. HRMS (ESI) : m/z $[M + H]^+$ calcd. for $C_{24}H_{27}F_3N_3O_2S^+$, 478.1771; found, 478.1792.

Compound **3_19**

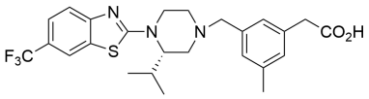

White solid, 70% yield. ^{1}H NMR (400 MHz, DMSO-d_6) : δ 0.84 (dd, J = 10.3, 6.8 Hz, 6H), 2.01 (dd, J = 11.7, 3.3 Hz, 1H), 2.13 (td, J = 11.6, 3.3 Hz, 1H), 2.29 (s, 3H), 2.54-2.61 (m, 1H), 2.89-2.96 (m, 2H), 3.32 (d, J = 13.3 Hz, 1H), 3.39-3.46 (m, 1H), 3.51 (s, 2H), 3.57 (d, J = 13.4 Hz, 1H), 3.63-3.71 (m, 1H), 4.04 (br s, 1H), 6.98 (s, 1H), 7.03 (br s, 2H), 7.50 (d, J = 8.5 Hz, 1H), 7.55 (dd, J = 8.5, 1.5 Hz, 1H), 8.18 (s, 1H), 12.32 (br s, 1H). ^{13}C NMR (100 MHz, DMSO-d_6) : δ 19.10, 19.49, 20.82, 26.50, 40.67, 44.54, 52.53, 52.62, 61.50, 63.52, 117.83, 118.66 (q, J = 3.7 Hz), 120.76 (q, J = 32.3 Hz), 122.96 (q, J = 3.7 Hz), 124.70 (q, J = 271.4 Hz), 126.58, 127.47, 128.73, 130.53, 134.81, 137.11,

137.85, 155.67, 170.10, 172.64. HRMS (ESI) : m/z $[M + H]^+$ calcd. for $C_{25}H_{29}F_3N_3O_2S^+$, 492.1927; found, 492.1940.

Compound **3_20**

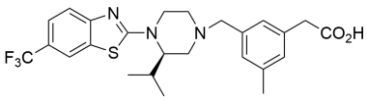

White solid, 53% yield. ^{1}H NMR (400 MHz, DMSO-d_6) : δ 0.84 (dd, J = 12.8, 6.7 Hz, 6H), 2.01 (dd, J = 11.7, 3.3 Hz, 1H), 2.12 (td, J = 11.5, 3.3 Hz, 1H), 2.27 (s, 3H), 2.55-2.60 (m, 1H), 2.90 (d, J = 11.4 Hz, 1H), 2.95 (d, J = 11.4 Hz, 1H), 3.32 (d, J = 13.3 Hz, 1H), 3.39-3.42 (m, 1H), 3.45 (s, 2H), 3.56 (d, J = 13.2 Hz, 1H), 3.65-4.10 (m, 2H), 6.96 (s, 1H), 7.01 (br s, 2H), 7.49 (d, J = 8.5 Hz, 1H), 7.54 (dd, J = 8.5, 1.3 Hz, 1H), 8.18 (br s, 1H). ^{13}C NMR (100 MHz, DMSO-d_6) : δ 19.09, 19.47, 20.82, 26.49, 41.55, 44.48, 52.48, 52.63, 61.53, 63.62, 117.80, 118.66 (q, J = 3.7 Hz), 120.71 (q, J = 32.3 Hz), 122.94 (q, J = 3.7 Hz), 124.67 (q, J = 271.4 Hz), 126.58, 127.13, 128.71, 130.49, 135.63, 136.89, 137.63, 155.64, 170.08, 172.93. HRMS (ESI) : m/z $[M + H]^+$ calcd. for $C_{25}H_{29}F_3N_3O_2S^+$, 492.1927; found, 492.1943.

Compound **3_21**

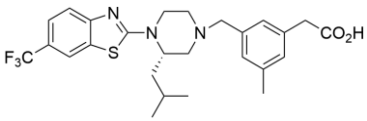

White solid, 98% yield. ^{1}H NMR (400 MHz, DMSO-d_6) : δ 0.91 (t, J = 6.4 Hz, 6H), 1.37-1.44 (m, 1H), 1.48-1.54 (m, 1H), 1.90-1.96 (m, 1H), 2.10-2.20 (m, 2H), 2.29 (s, 3H), 2.76 (d, J = 11.0 Hz, 1H), 2.93 (d, J = 11.0 Hz, 1H), 3.30-3.34 (m, 1H), 3.42-3.49 (m, 1H),

3.52 (s, 2H), 3.62 (d, J = 13.4 Hz, 1H), 3.97 (br s, 1H), 4.08 (br s, 1H), 6.98 (s, 1H), 7.03 (s, 1H), 7.04 (s, 1H), 7.52 (d, J = 8.6 Hz, 1H), 7.56 (dd, J = 8.6, 1.6 Hz, 1H), 8.22 (s, 1H), 12.30 (br s, 1H). ^{13}C NMR (100 MHz, DMSO-d_6) : δ 20.82, 21.80, 23.24, 24.46, 37.53, 40.58, 44.12, 52.45, 53.69, 55.22, 61.41, 118.07, 118.83 (q, J = 3.7 Hz), 120.93 (q, J = 32.3 Hz), 122.94 (q, J = 3.7 Hz), 124.69 (q, J = 271.4 Hz), 126.47, 127.29, 128.72, 130.61, 134.76, 137.15, 137.89, 155.47, 169.59, 172.58. HRMS (ESI) : m/z $[M + H]^+$ calcd. for $C_{26}H_{31}F_3N_3O_2S^+$, 506.2084; found, 506.2106.

Compound **3_22**

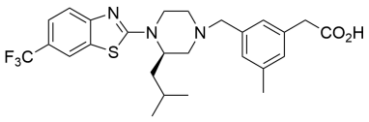

White solid, 99% yield. ^{1}H NMR (400 MHz, DMSO-d_6) : δ 0.91 (t, J = 6.5 Hz, 6H), 1.37-1.44 (m, 1H), 1.47-1.54 (m, 1H), 1.90-1.97 (m, 1H), 2.11 (dd, J = 11.5, 3.3 Hz, 1H), 2.18 (td, J = 11.7, 3.5 Hz, 1H), 2.29 (s, 3H), 2.76 (d, J = 11.3 Hz, 1H), 2.93 (d, J = 11.3 Hz, 1H), 3.32 (d, J = 13.6 Hz, 1H), 3.42-3.49 (m, 1H), 3.51 (s, 2H), 3.62 (d, J = 13.6 Hz, 1H), 3.97 (br s, 1H), 4.08 (br s, 1H), 6.98 (s, 1H), 7.02 (s, 1H), 7.04 (s, 1H), 7.52 (d, J = 8.5 Hz, 1H), 7.56 (dd, J = 8.5, 1.6 Hz, 1H), 8.22 (s, 1H), 12.31 (br s, 1H). ^{13}C NMR (100 MHz, DMSO-d_6) : δ 20.82, 21.79, 23.23, 24.45, 37.53, 40.74, 44.12, 52.44, 53.69, 55.16, 61.41, 118.07, 118.82 (q, J = 3.7 Hz), 120.92 (q, J = 32.3 Hz), 122.94 (q, J = 3.7 Hz), 124.68 (q, J = 271.4 Hz), 126.46, 127.23, 128.71, 130.59, 134.91, 137.11, 137.85, 155.46, 169.58, 172.62. HRMS (ESI) : m/z $[M + H]^+$ calcd. for $C_{26}H_{31}F_3N_3O_2S^+$, 506.2084; found, 506.2095.

Synthesis of compound **6_28**

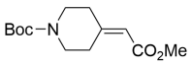

To a suspension of sodium hydride (4.02 g, 100.4 mmol) in THF (300 mL) was added trimethyl phosphonoacetate (16.3 mL, 100.4 mmol) at 0 °C, and the mixture was stirred at the same temperature for 1 hour. After addition of a solution of 1-Boc-4-piperidone (20 g, 100.4 mmol) in THF (150 mL) and stirring at 50 °C for 1.5 hours, to the reaction solution was added water and extracted with EtOAc. The organic layer was washed with water and brine, and dried over Na_2SO_4. The solvent was evaporated under reduced pressure and the residue was purified by silica gel column chromatography to give compound **6_28** (27.0 g, 100%) as a white solid. ^{1}H NMR (300 MHz, $CDCl_3$) : δ 1.47 (s, 9H), 2.28 (t, J = 5.5 Hz, 2H), 2.94 (t, J = 5.5 Hz, 2H), 3.48 (t, J = 5.5 Hz, 2H), 3.50 (t, J = 5.5 Hz, 2H), 3.70 (s, 3H), 5.72 (s, 1H).

Synthesis of compound **6_29**

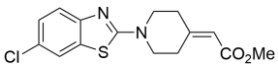

A solution of **6_28** (8.00 g, 31.3 mmol) in 4 M solution of hydrochloric acid-dioxane (80 mL) was stirred at room temperature for 1 hour. The solvent was evaporated under reduced pressure and the residue was dissolved in DMF (60 mL). K_2CO_3 (8.65 g, 62.6 mmol) and 2,6-dichlorobenzothiazole (6.39 g, 31.3 mmol) were added thereto at 0 °C. After stirring at 60 °C for 3 hours, water was added and the mixture extracted with EtOAc. The organic layer was washed with water and brine, and dried over Na_2SO_4. The solvent was evaporated under reduced pressure and the residue was purified by silica gel column chromatography to give compound **6_29** (9.48 g, 94%) as a beige solid. ^{1}H NMR (300

MHz, $CDCl_3$) : δ 2.48 (t, J = 5.4 Hz, 2H), 3.14 (t, J = 5.5 Hz, 2H), 3.70 (t, J = 5.9 Hz, 2H), 3.72 (s, 3H), 3.77 (t, J = 5.9 Hz, 2H), 5.81 (s, 1H), 7.26 (dd, J = 8.5, 2.2 Hz, 1H), 7.46 (d, J = 8.5 Hz, 1H), 7.57 (d, J = 2.2 Hz, 1H).

Typical procedure for synthesis of compounds **6_30a–h**

CuI (1.77 g, 9.30 mmol) was suspended in THF (18 mL), and the corresponding alkylmagnesium bromide (1.0 M THF solution, 18.6 mL, 18.6 mmol) was added thereto under −30 °C. After stirring at −20 °C for 30 minutes, the reaction mixture was cooled to −78 °C. To the mixture was added dropwise a solution of **6_29** (1.00 g, 3.10 mmol) in THF (10 mL), and then added TMSOTf (1.12 mL, 6.20 mmol). After stirring at −78 °C for 2 hours, aqueous $NaHCO_3$ solution was added. The insoluble material was filtered out and the filtrate was extracted with EtOAc. The organic layer was washed with water and brine, and dried over $MgSO_4$. The solvent was evaporated under reduced pressure and the residue was purified by silica gel column chromatography to give the target compound.

Compound **6_30a**

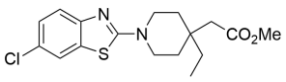

White solid, 90% yield. ^{1}H NMR (300 MHz, $CDCl_3$) : δ 0.91 (t, J = 7.6 Hz, 3H), 1.54 (q, J = 7.5 Hz, 2H), 1.65-1.72 (m, 4H), 2.39 (s, 2H), 3.59-3.66 (m, 4H), 3.67 (s, 3H), 7.24 (dd, J = 8.5, 2.2 Hz, 1H), 7.45 (d, J = 8.5 Hz, 1H), 7.55 (d, J = 2.2 Hz, 1H).

Compound **6_30b**

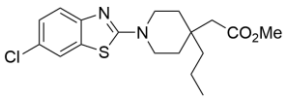

Yellow solid, 76% yield. ^{1}H NMR (300 MHz, $CDCl_3$) : δ 0.93 (t, J = 7.0 Hz, 3H), 1.26-1.39 (m, 2H), 1.42-1.48 (m, 2H), 1.62-1.76 (m, 4H), 2.40 (s, 2H), 3.57-3.66 (m, 4H), 3.67 (s, 3H), 7.23 (dd, J = 8.6, 2.2 Hz, 1H), 7.44 (d, J = 8.6 Hz, 1H), 7.55 (d, J = 2.2 Hz, 1H).

Compound **6_30c**

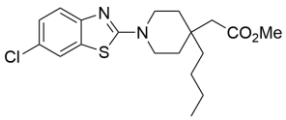

Yellow solid, 92% yield. ^{1}H NMR (300 MHz, $CDCl_3$) : δ 0.92 (t, J = 6.9 Hz, 3H), 1.26-1.34 (m, 4H), 1.44-1.50 (m, 2H), 1.63-1.75 (m, 4H), 2.40 (s, 2H), 3.57-3.66 (m, 4H), 3.67 (s, 3H), 7.23 (dd, J = 8.7, 2.2 Hz, 1H), 7.44 (d, J = 8.7 Hz, 1H), 7.55 (d, J = 2.2 Hz, 1H).

Compound **6_30d**

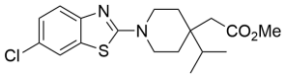

White solid, 55% yield. ^{1}H NMR (300 MHz, $CDCl_3$) : δ 0.92 (d, J = 6.9 Hz, 6H), 1.74-1.79 (m, 4H), 1.84-1.93 (m, 1H), 2.44 (s, 2H), 3.46-3.55 (m, 2H), 3.67 (s, 3H), 3.74-3.82 (m, 2H), 7.24 (dd, J = 8.8, 2.2 Hz, 1H), 7.45 (d, J = 8.8 Hz, 1H), 7.55 (d, J = 2.2 Hz, 1H).

Compound **6_30e**

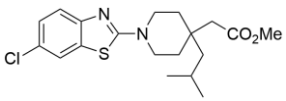

Yellow solid, 97% yield. ^{1}H NMR (300 MHz, $CDCl_3$) : δ 0.96 (d, J = 6.6 Hz, 6H), 1.43 (d, J = 5.2 Hz, 2H), 1.68-1.79 (m, 5H), 2.46 (s, 2H), 3.54-3.72 (m, 4H), 3.67 (s, 3H), 7.23 (dd, J = 8.6, 2.2 Hz, 1H), 7.45 (d, J = 8.6 Hz, 1H), 7.55 (d, J = 2.2 Hz, 1H).

Compound **6_30f**

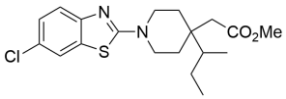

Yellow solid, 28% yield. ^{1}H NMR (300 MHz, $CDCl_3$) : δ 0.86-0.94 (m, 6H), 1.25-1.31 (m, 3H), 1.75-1.83 (m, 4H), 2.43 (s, 2H), 3.47-3.57 (m, 2H), 3.66 (s, 3H), 3.71-3.78 (m, 2H), 7.24 (dd, J = 8.7, 2.1 Hz, 1H), 7.45 (d, J = 8.7 Hz, 1H), 7.55 (d, J = 2.1 Hz, 1H).

Compound **6_30g**

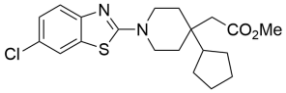

White solid, 33% yield. ^{1}H NMR (300 MHz, $CDCl_3$) : δ 1.24-1.76 (m, 12H), 2.04-2.14 (m, 1H), 2.48 (s, 2H), 3.42-3.52 (m, 2H), 3.67 (s, 3H), 3.78-3.87 (m, 2H), 7.23 (dd, J = 8.7, 2.2 Hz, 1H), 7.43 (d, J = 8.7 Hz, 1H), 7.55 (d, J = 2.2 Hz, 1H).

Compound **6_30h**

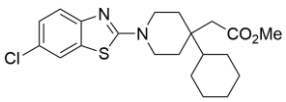

White solid, 50% yield. ^{1}H NMR (300 MHz, $CDCl_3$) : δ 0.94-1.08 (m, 2H), 1.12-1.28 (m, 3H), 1.41-1.50 (m, 1H), 1.66-1.84 (m, 9H), 2.44 (s, 2H), 3.47-3.55 (m, 2H), 3.67 (s, 3H), 3.70-3.78 (m, 2H), 7.24 (dd, J = 8.5, 2.2 Hz, 1H), 7.44 (d, J = 8.5 Hz, 1H), 7.55 (d, J = 2.2 Hz, 1H).

Typical procedure for synthesis of compounds **6_31a–h**

To a suspension of $LiAlH_4$ (202 mg, 5.33 mmol) in anhydrous THF (10 mL) was added dropwise a solution of **6_30** (2.66 mmol) in anhydrous THF (10 mL) under ice-cooling, and the mixture was stirred at the same temperature for 1 hour. Water (0.2 mL), 10% aqueous sodium hydroxide solution (0.2 mL) and water (0.6 mL) were added dropwise sequentially under ice-cooling. After filtration of aluminium hydroxide, the filtrate was extracted with EtOAc. The extract was washed with brine, dried over Na_2SO_4, and concentrated under reduced pressure. The residue was purified by silica gel column chromatography to give the target compound.

Compound **6_31a**

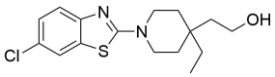

Yellow oil, 91% yield. ^{1}H NMR (300 MHz, $CDCl_3$) : δ 0.87 (t, J = 7.5 Hz, 3H), 1.44 (q, J = 7.5 Hz, 2H), 1.58 (t, J = 5.5 Hz, 2H), 1.60 (t, J = 5.5 Hz, 2H), 1.68 (t, J = 7.7 Hz, 2H), 3.61 (t, J = 5.9 Hz, 4H), 3.72 (t, J = 7.7 Hz, 2H), 7.23 (dd, J = 8.8, 2.2 Hz, 1H), 7.44 (d, J = 8.8 Hz, 1H), 7.55 (d, J = 2.2 Hz, 1H).

Compound **6_31b**

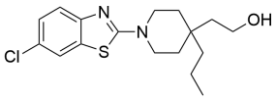

Colorless oil, 100% yield. ^{1}H NMR (300 MHz, $CDCl_3$) : δ 0.93 (t, J = 6.7 Hz, 3H), 1.26-1.38 (m, 4H), 1.57-1.62 (m, 4H), 1.68 (t, J = 7.6 Hz, 2H), 3.61 (t, J = 5.9 Hz, 4H), 3.72 (t, J = 7.6 Hz, 2H), 7.23 (dd, J = 8.6, 2.0 Hz, 1H), 7.44 (d, J = 8.6 Hz, 1H), 7.55 (d, J = 2.0 Hz, 1H).

Compound **6_31c**

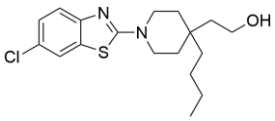

Colorless oil, 95% yield. ^{1}H NMR (300 MHz, $CDCl_3$) : δ 0.92 (t, J = 6.9 Hz, 3H), 1.21-1.39 (m, 6H), 1.57-1.62 (m, 4H), 1.69 (t, J = 7.6 Hz, 2H), 3.61 (t, J = 5.8 Hz, 4H), 3.72 (t, J = 7.6 Hz, 2H), 7.23 (dd, J = 8.7, 2.2 Hz, 1H), 7.44 (d, J = 8.7 Hz, 1H), 7.55 (d, J = 2.2 Hz, 1H).

Compound **6_31d**

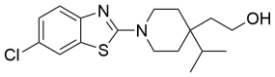

White solid, 94% yield. ^{1}H NMR (300 MHz, $CDCl_3$) : δ 0.90 (d, J = 6.9 Hz, 6H), 1.52-1.59 (m, 2H), 1.68-1.85 (m, 5H), 3.49-3.58 (m, 2H), 3.69-3.77 (m, 4H), 7.24 (dd, J = 8.7, 2.1 Hz, 1H), 7.45 (d, J = 8.7 Hz, 1H), 7.55 (d, J = 2.1 Hz, 1H).

Compound **6_31e**

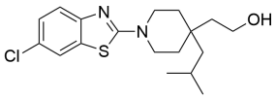

White solid, 84% yield. ^{1}H NMR (300 MHz, $CDCl_3$) : δ 0.96 (d, J = 6.6 Hz, 6H), 1.32 (d, J = 5.5 Hz, 2H), 1.62 (t, J = 5.9 Hz, 4H), 1.69-1.72 (m, 1H), 1.76 (t, J = 7.6 Hz, 2H), 3.55-3.68 (m, 4H), 3.74 (t, J = 7.6 Hz, 2H), 7.24 (dd, J = 8.7, 2.2 Hz, 1H), 7.45 (d, J = 8.7 Hz, 1H), 7.55 (d, J = 2.2 Hz, 1H).

Compound **6_31f**

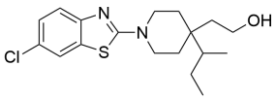

Colorless oil, 90% yield. ^{1}H NMR (300 MHz, $CDCl_3$) : δ 0.88 (d, J = 6.9 Hz, 3H), 0.90-0.96 (m, 4H), 1.38-1.63 (m, 4H), 1.70-1.80 (m, 4H), 3.50-3.60 (m, 2H), 3.67-3.75 (m, 4H), 7.24 (dd, J = 8.7, 2.2 Hz, 1H), 7.46 (d, J = 8.7 Hz, 1H), 7.55 (d, J = 2.2 Hz, 1H).

Compound **6_31g**

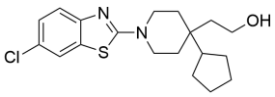

White solid, 41% yield. ^{1}H NMR (300 MHz, $CDCl_3$) : δ 1.26-1.36 (m, 4H), 1.52-1.73 (m, 8H), 1.79 (t, J = 7.7 Hz, 2H), 1.98-2.04 (m, 1H), 3.44-3.53 (m, 2H), 3.74-3.82 (m, 4H), 7.23 (dd, J = 8.7, 2.1 Hz, 1H), 7.42 (d, J = 8.7 Hz, 1H), 7.55 (d, J = 2.1 Hz, 1H).

Compound **6_31h**

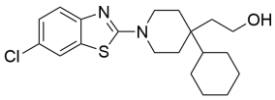

White solid, 83% yield. ^{1}H NMR (300 MHz, $CDCl_3$) : δ 0.96-1.27 (m, 4H), 1.32-1.41 (m, 1H), 1.50-1.59 (m, 2H), 1.67-1.82 (m, 10H), 3.49-3.58 (m, 2H), 3.66-3.75 (m, 4H), 7.24 (dd, J = 8.6, 2.1 Hz, 1H), 7.45 (d, J = 8.6 Hz, 1H), 7.55 (d, J = 2.1 Hz, 1H).

Typical procedure for synthesis of compounds **6_32a** and **6_32d**

A mixture of **6_31** (2.35 mmol) and $SOCl_2$ (4 mL) were stirred at 60 °C for 1.5 hours. To the reaction mixture was added ice and extracted with EtOAc. The organic layer was washed with aqueous $NaHCO_3$ solution and brine and dried over Na_2SO_4. The solvent was evaporated under reduced pressure and the residue was purified by silica gel column chromatography. A portion (0.437 mmol) of the resulting material was dissolved in DMF (2 mL) prior to the addition of methyl 2-(4-chloro-3-hydroxyphenyl)acetate (176 mg, 0.874 mmol), Cs_2CO_3 (285 mg, 0.874 mmol). After stirring at 75 °C for 24 hours, water was added, and the mixture was extracted with EtOAc. The extract was washed with brine, dried over Na_2SO_4, and concentrated under reduced pressure. The residue was purified by silica gel column chromatography to give the target compound.

Compound **6_32a**

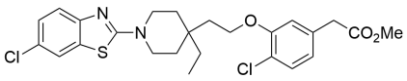

Yellow oil, 73% yield. ^{1}H NMR (300 MHz, $CDCl_3$) : δ 0.91 (t, J = 7.4 Hz, 3H), 1.53 (q, J = 7.4 Hz, 2H), 1.60-1.76 (m, 4H), 1.98 (t, J = 6.5 Hz, 2H), 3.59 (s, 2H), 3.64-3.70 (m, 4H), 3.70 (s, 3H), 4.09 (t, J = 6.5 Hz, 2H), 6.80 (dd, J = 8.0, 1.6 Hz, 1H), 6.85 (d, J = 1.6 Hz, 1H), 7.24 (dd, J = 8.6, 2.1 Hz, 3H), 7.30 (d, J = 8.0 Hz, 1H), 7.46 (d, J = 8.6 Hz, 1H), 7.55 (d, J = 2.1 Hz, 1H).

Compound **6_32d**

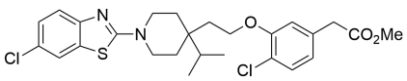

Yellow oil, 49% yield. ^{1}H NMR (300 MHz, $CDCl_3$) : δ 0.94 (d, J = 6.9 Hz, 6H), 1.62-1.70 (m, 2H), 1.75-1.84 (m, 2H), 1.86-1.95 (m, 1H), 2.07 (t, J = 6.6 Hz, 2H), 3.55-3.64 (m, 2H), 3.59 (s, 2H), 3.70 (s, 3H), 3.76-3.84 (m, 1H), 4.11 (t, J = 6.6 Hz, 2H), 6.80 (dd, J = 8.0, 1.9 Hz, 1H), 6.84 (d, J = 1.9 Hz, 1H), 7.23 (dd, J = 8.6, 2.0 Hz, 1H), 7.30 (d, J = 8.0 Hz, 1H), 7.45 (d, J = 8.6 Hz, 1H), 7.55 (d, J = 2.0 Hz, 1H).

Typical procedure for synthesis of compounds **6_32b–c** and **6_32e–i**

To a solution of **6_31a** (0.443 mmol) and TEA (185 μL, 1.33 mmol) in anhydrous CH_2Cl_2 (2 mL) was added MsCl (51.4 μL, 0.665 mmol) under ice-cooling. After stirring at the same temperature for 30 minutes, water was added, and the mixture was extracted with $CHCl_3$. The extract was washed with brine, dried over $MgSO_4$, and concentrated under reduced pressure. A mixture of the resulting material, the corresponding phenol (0.665 mmol), Cs_2CO_3 (217 mg, 0.665 mmol) and anhydrous DMF (2 mL) was stirred at 60 °C for 16 hours. Water was added, and the mixture was extracted with EtOAc. The extract was washed with brine, dried over Na_2SO_4, and concentrated under reduced pressure. The residue was purified by silica gel column chromatography to give the target material.

Compound **6_32b**

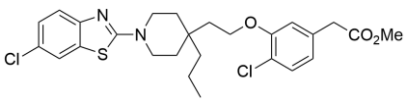

Colorless oil, quantitative yield. ^{1}H NMR (300 MHz, $CDCl_3$) : δ 0.95 (t, J = 6.9 Hz, 3H), 1.30-1.48 (m, 4H), 1.62-1.76 (m, 4H), 1.98 (t, J = 6.4 Hz, 2H), 3.60 (s, 2H), 3.66-3.71 (m, 4H), 3.70 (s, 3H), 4.08 (t, J = 6.4 Hz, 2H), 6.81 (dd, J = 8.0, 1.8 Hz, 1H), 6.85 (d, J = 1.8 Hz, 1H), 7.24 (dd, J = 7.4, 1.9 Hz, 1H), 7.30 (d, J = 8.0 Hz, 1H), 7.47 (d, J = 7.4 Hz, 1H),

7.55 (d, J = 1.9 Hz, 1H).

Compound **6_32c**

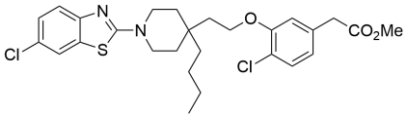

Yellow oil, quantitative yield. ^{1}H NMR (300 MHz, $CDCl_3$) : δ 0.93 (t, J = 6.7 Hz, 3H), 1.26-1.35 (m, 4H), 1.43-1.48 (m, 2H), 1.63-1.76 (m, 5H), 1.98 (t, J = 6.5 Hz, 2H), 3.60 (s, 2H), 3.65-3.69 (m, 4H), 3.70 (s, 3H), 4.08 (t, J = 6.5 Hz, 2H), 6.81 (dd, J = 8.1, 1.9 Hz, 1H), 6.85 (d, J = 1.9 Hz, 1H), 7.24 (dd, J = 8.5, 2.0 Hz, 1H), 7.30 (d, J = 8.1 Hz, 1H), 7.46 (d, J = 8.5 Hz, 1H), 7.55 (d, J = 2.0 Hz, 1H).

Compound **6_32e**

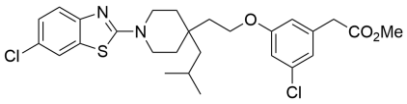

Colorless oil, 91% yield. ^{1}H NMR (300 MHz, $CDCl_3$) : δ 0.98 (d, J = 6.6 Hz, 6H), 1.38 (d, J = 5.5 Hz, 2H), 1.67 (t, J = 5.8 Hz, 4H), 1.73-1.82 (m, 1H), 1.97 (t, J = 6.8 Hz, 2H), 3.56 (s, 2H), 3.59-3.69 (m, 4H), 3.71 (s, 3H), 4.00 (t, J = 6.8 Hz, 2H), 6.69 (br s, 1H), 6.79 (dd, J = 2.0, 2.0 Hz, 1H), 6.87 (br s, 1H), 7.24 (dd, J = 8.5, 1.9 Hz, 1H), 7.45 (d, J = 8.5 Hz, 1H), 7.55 (d, J = 1.9 Hz, 1H).

Compound **6_32f**

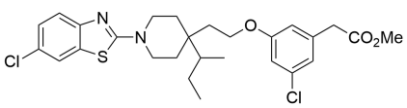

Colorless oil, 72% yield. ^{1}H NMR (300 MHz, $CDCl_3$) : δ 0.91 (d, J = 6.6 Hz, 3H), 0.95-

0.97 (m, 3H), 1.46-1.52 (m, 1H), 1.56-1.68 (m, 4H), 1.76-1.86 (m, 2H), 1.97 (t, *J* = 7.0 Hz, 2H), 3.54-3.61 (m, 1H), 3.55 (s, 2H), 3.70 (s, 3H), 3.71-3.78 (m, 2H), 3.99 (t, *J* = 7.0 Hz, 2H), 6.69 (br s, 1H), 6.78 (dd, *J* = 1.9, 1.9 Hz, 1H), 6.87 (br s, 1H), 7.24 (dd, *J* = 8.2, 1.9 Hz, 1H), 7.46 (d, *J* = 8.2 Hz, 1H), 7.55 (d, *J* = 1.9 Hz, 1H).

Compound **6_32g**

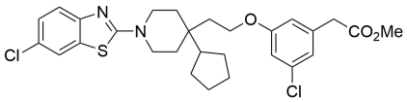

Yellow oil, 76% yield. ^{1}H NMR (300 MHz, $CDCl_3$) : δ 1.30-1.38 (m, 2H), 1.56-1.64 (m, 8H), 1.69-1.79 (m, 2H), 2.00 (t, *J* = 6.9 Hz, 2H), 2.05-2.12 (m, 1H), 3.46-3.55 (m, 2H), 3.56 (s, 2H), 3.70 (s, 3H), 3.79-3.87 (m, 2H), 4.04 (t, *J* = 6.9 Hz, 2H), 6.69 (br s, 1H), 6.79 (t, *J* = 1.9 Hz, 1H), 6.87 (br s, 1H), 7.23 (dd, *J* = 8.7, 2.1 Hz, 1H), 7.43 (d, *J* = 8.7 Hz, 1H), 7.55 (d, *J* = 2.1 Hz, 1H).

Compound **6_32h**

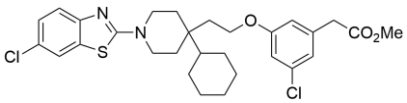

Yellow oil, 81% yield. ^{1}H NMR (300 MHz, $CDCl_3$) : δ 1.00-1.28 (m, 5H), 1.41-1.85 (m, 10H), 1.98 (t, *J* = 7.0 Hz, 2H), 3.56 (s, 2H), 3.56-3.61 (m, 2H), 3.70 (s, 3H), 3.71-3.77 (m, 2H), 3.99 (t, *J* = 7.0 Hz, 2H), 6.69 (br s, 1H), 6.78 (dd, *J* = 2.1, 2.1 Hz, 1H), 6.87 (br s, 1H), 7.24 (dd, *J* = 8.0, 2.2 Hz, 1H), 7.46 (d, *J* = 8.0 Hz, 1H), 7.55 (d, *J* = 2.2 Hz, 1H).

Compound **6_32i**

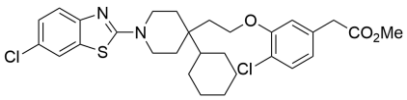

Yellow oil, quantitative yield. ^{1}H NMR (300 MHz, $CDCl_3$) : δ 1.01-1.28 (m, 5H), 1.44-1.87 (m, 10H), 2.07 (t, J = 6.6 Hz, 2H), 3.55-3.64 (m, 2H), 3.59 (s, 2H), 3.70 (s, 3H), 3.73-3.80 (m, 2H), 4.09 (t, J = 6.6 Hz, 2H), 6.81 (dd, J = 8.1, 1.7 Hz, 1H), 6.85 (d, J = 1.7 Hz, 1H), 7.23 (dd, J = 8.6, 2.2 Hz, 1H), 7.30 (d, J = 8.1 Hz, 1H), 7.45 (d, J = 8.6 Hz, 1H), 7.55 (d, J = 2.2 Hz, 1H).

Typical procedure for synthesis of compounds **4_1–9**

To a solution of **6_32** (0.300 mmol) in THF (1 mL) and MeOH (1 mL) was added 2 M aqueous NaOH solution (0.45 mL), and the mixture was stirred at room temperature for 2 hours. To the reaction mixture was added 2 M aqueous HCl solution to be neutral, and extracted with EtOAc. The extract was washed with brine, dried over Na_2SO_4, and concentrated under reduced pressure. The residue was purified by silica gel column chromatography to give the target material.

Compound **4_1**

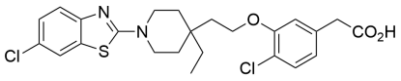

White solid, 36% yield. ^{1}H NMR (400 MHz, DMSO-d_6) : δ 0.85 (t, J = 7.4 Hz, 3H), 1.46-1.56 (m, 4H), 1.61-1.67 (m, 2H), 1.88 (t, J = 6.6 Hz, 2H), 3.57 (s, 2H), 3.60 (t, J = 5.6 Hz, 4H), 4.09 (t, J = 6.6 Hz, 2H), 6.84 (dd, J = 8.1, 1.6 Hz, 1H), 7.11 (d, J = 1.6 Hz, 1H), 7.27 (dd, J = 8.7, 2.2 Hz, 1H), 7.33 (d, J = 8.1 Hz, 1H), 7.40 (d, J = 8.7 Hz, 1H), 7.87 (d, J =

2.2 Hz, 1H), 12.47 (s, 1H). ^{13}C NMR (100 MHz, DMSO-d_6) : δ 7.23, 28.27, 32.92, 33.10, 33.69, 40.20, 44.21, 64.78, 114.82, 119.10, 119.27, 120.65, 122.27, 124.45, 125.95, 129.29, 131.80, 135.50, 151.53, 153.42, 168.30, 172.26. HRMS (ESI) : m/z $[M + H]^+$ calcd. for $C_{24}H_{27}Cl_2N_2O_3S^+$, 493.1114; found, 493.1121.

Compound **4_2**

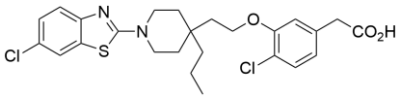

White solid, 95% yield. ^{1}H NMR (400 MHz, DMSO-d_6) : δ 0.90 (t, J = 7.0 Hz, 3H), 1.26-1.32 (m, 2H), 1.38-1.43 (m, 2H), 1.51-1.66 (m, 4H), 1.89 (t, J = 6.5 Hz, 2H), 3.58 (s, 2H), 3.60 (br s, 4H), 4.09 (t, J = 6.5 Hz, 2H), 6.84 (dd, J = 8.1, 1.2 Hz, 1H), 7.11 (d, J = 1.2 Hz, 1H), 7.27 (dd, J = 8.6, 2.2 Hz, 1H), 7.33 (d, J = 8.1 Hz, 1H), 7.40 (d, J = 8.6 Hz, 1H), 7.87 (d, J = 2.2 Hz, 1H), 12.37 (br s, 1H). ^{13}C NMR (100 MHz, DMSO-d_6) : δ 14.77, 15.70, 33.24, 33.61, 34.19, 38.68, 40.56, 44.32, 64.90, 114.88, 119.21, 119.27, 120.75, 122.36, 124.56, 126.05, 129.36, 131.91, 135.84, 151.62, 153.50, 168.42, 172.46. HRMS (ESI) : m/z $[M + H]^+$ calcd. for $C_{25}H_{29}Cl_2N_2O_3S^+$, 507.1270; found, 507.1277.

Compound **4_3**

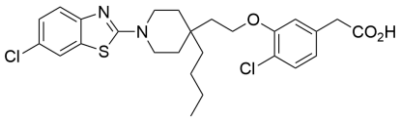

Yellow solid, 91% yield. ^{1}H NMR (400 MHz, DMSO-d_6) : δ 0.89 (t, J = 6.8 Hz, 3H), 1.23-1.31 (m, 4H), 1.40-1.45 (m, 2H), 1.51-1.67 (m, 4H), 1.89 (t, J = 6.5 Hz, 2H), 3.58 (s, 2H), 3.60 (t, J = 5.4 Hz, 3H), 4.09 (t, J = 6.5 Hz, 2H), 6.84 (dd, J = 8.2, 1.6 Hz, 1H),

7.11 (d, *J* = 1.6 Hz, 1H), 7.27 (dd, *J* = 8.7, 2.2 Hz, 1H), 7.33 (d, *J* = 8.2 Hz, 1H), 7.40 (d, *J* = 8.7 Hz, 1H), 7.87 (d, *J* = 2.2 Hz, 1H), 12.38 (br s, 1H). ^{13}C NMR (100 MHz, DMSO-d_6) : δ 14.05, 22.99, 24.65, 33.11, 33.59, 34.21, 35.94, 40.49, 44.32, 64.90, 114.91, 119.21, 119.30, 120.75, 122.37, 124.56, 126.05, 129.37, 131.91, 135.78, 151.62, 153.50, 168.42, 172.45. HRMS (ESI) : m/z $[M + H]^+$ calcd. for $C_{26}H_{31}Cl_2N_2O_3S^+$, 521.1427; found, 521.1439.

Compound **4_4**

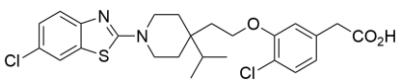

Yellow solid, 87% yield. ^{1}H NMR (400 MHz, DMSO-d_6) : δ 0.88 (d, *J* = 6.9 Hz, 6H), 1.58-1.70 (m, 4H), 1.86-1.93 (m, 1H), 1.97 (t, *J* = 6.7 Hz, 2H), 3.49-3.57 (m, 2H), 3.57 (s, 2H), 3.68-3.73 (m, 2H), 4.11 (t, *J* = 6.7 Hz, 2H), 6.84 (dd, *J* = 8.1, 1.6 Hz, 1H), 7.12 (d, *J* = 1.6 Hz, 1H), 7.27 (dd, *J* = 8.7, 2.2 Hz, 1H), 7.33 (d, *J* = 8.1 Hz, 1H), 7.40 (d, *J* = 8.7 Hz, 1H), 7.87 (d, *J* = 2.2 Hz, 1H), 12.41 (br s, 1H). ^{13}C NMR (100 MHz, DMSO-d_6) : δ 16.67, 30.13, 31.30, 35.34, 40.24, 44.20, 65.05, 114.97, 119.19, 119.38, 120.72, 122.36, 124.52, 126.02, 129.36, 131.87, 135.55, 151.60, 153.50, 168.37, 172.33. HRMS (ESI) : m/z $[M + H]^+$ calcd. for $C_{25}H_{29}Cl_2N_2O_3S^+$, 507.1270; found, 507.1276.

Compound **4_5**

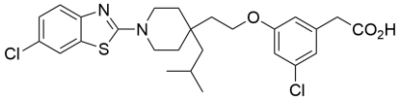

White solid, 81% yield. ^{1}H NMR (400 MHz, DMSO-d_6) : δ 0.94 (d, *J* = 6.5 Hz, 6H), 1.35 (d, *J* = 5.1 Hz, 2H), 1.51-1.65 (m, 4H), 1.70-1.76 (m, 1H), 1.91 (t, *J* = 7.0 Hz, 2H), 3.54-

3.65 (m, 3H), 3.56 (s, 2H), 4.03 (t, *J* = 7.0 Hz, 2H), 6.83 (br s, 1H), 6.90 (br s, 1H), 6.95 (dd, *J* = 2.0, 2.0 Hz, 1H), 7.27 (dd, *J* = 8.7, 2.3 Hz, 1H), 7.40 (d, *J* = 8.7 Hz, 1H), 7.87 (d, *J* = 2.3 Hz, 1H), 12.42 (br s, 1H). ^{13}C NMR (100 MHz, DMSO-d_6) : δ 23.00, 25.29, 33.75, 33.91, 34.48, 40.06, 44.32, 45.27, 64.44, 112.46, 115.01, 119.19, 120.72, 121.53, 124.56, 126.03, 131.92, 133.30, 138.19, 151.60, 159.25, 168.37, 172.11. HRMS (ESI) : m/z [M + H]$^+$ calcd. for $C_{26}H_{31}Cl_2N_2O_3S^+$, 521.1427; found, 521.1428.

Compound **4_6**

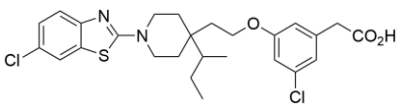

White solid, 82% yield. ^{1}H NMR (400 MHz, DMSO-d_6) : δ 0.85 (d, *J* = 6.8 Hz, 3H), 0.88-0.93 (m, 4H), 1.48-1.71 (m, 6H), 1.90 (t, *J* = 7.2 Hz, 2H), 3.48-3.54 (m, 2H), 3.55 (s, 2H), 3.64-3.69 (m, 2H), 4.03 (t, *J* = 7.2 Hz, 2H), 6.83 (br s, 1H), 6.90 (br s, 1H), 6.94 (dd, *J* = 2.0, 2.0 Hz, 1H), 7.27 (dd, *J* = 8.7, 2.2 Hz, 1H), 7.40 (d, *J* = 8.7 Hz, 1H), 7.87 (d, *J* = 2.2 Hz, 1H), 12.38 (br s, 1H). ^{13}C NMR (100 MHz, DMSO-d_6) : δ 12.54, 13.15, 22.78, 30.42, 30.58, 35.81, 38.70, 40.08, 44.15, 64.52, 112.49, 115.00, 119.19, 120.72, 121.50, 124.54, 126.03, 131.87, 133.28, 138.19, 151.59, 159.22, 168.39, 172.14. HRMS (ESI) : m/z [M + H]$^+$ calcd. for $C_{26}H_{31}Cl_2N_2O_3S^+$, 521.1427; found, 521.1441.

Compound **4_7**

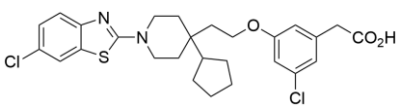

White solid, 87% yield. ^{1}H NMR (400 MHz, DMSO-d_6) : δ 1.24-1.31 (m, 2H), 1.48-1.60 (m, 10H), 1.93 (t, *J* = 6.9 Hz, 2H), 2.06-2.15 (m, 1H), 3.44-3.50 (m, 2H), 3.56 (s, 2H),

3.73-3.78 (m, 2H), 4.08 (t, *J* = 6.9 Hz, 2H), 6.83 (br s, 1H), 6.90 (br s, 1H), 6.95 (dd, *J* = 1.9, 1.9 Hz, 1H), 7.27 (dd, *J* = 8.6, 2.1 Hz, 1H), 7.40 (d, *J* = 8.6 Hz, 1H), 7.87 (d, *J* = 2.1 Hz, 1H), 12.45 (br s, 1H). ^{13}C NMR (100 MHz, DMSO-d_6) : δ 25.26, 25.56, 30.59, 31.41, 34.83, 40.06, 44.22, 44.99, 64.52, 112.49, 115.02, 119.19, 120.72, 121.48, 124.55, 126.02, 131.90, 133.29, 138.16, 151.60, 159.24, 168.37, 172.11. HRMS (ESI) : m/z $[M + H]^+$ calcd. for $C_{27}H_{31}Cl_2N_2O_3S^+$, 533.1427; found, 533.1436.

Compound **4_8**

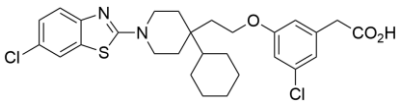

White solid, 88% yield. ^{1}H NMR (400 MHz, DMSO-d_6) : δ 0.95-1.26 (m, 5H), 1.43-1.76 (m, 10H), 1.90 (t, *J* = 7.0 Hz, 2H), 3.48-3.54 (m, 2H), 3.56 (s, 2H), 3.64-3.69 (m, 2H), 4.03 (t, *J* = 7.0 Hz, 2H), 6.83 (br s, 1H), 6.90 (br s, 1H), 6.94 (dd, *J* = 2.0, 2.0 Hz, 1H), 7.27 (dd, *J* = 8.7, 2.3 Hz, 1H), 7.40 (d, *J* = 8.7 Hz, 1H), 7.87 (d, *J* = 2.3 Hz, 1H), 12.42 (br s, 1H). ^{13}C NMR (100 MHz, DMSO-d_6) : δ 26.20, 26.65, 30.44, 30.74, 35.30, 40.06, 42.04, 44.17, 64.50, 112.49, 115.02, 119.19, 120.72, 121.50, 124.54, 126.02, 131.87, 133.29, 138.17, 151.58, 159.22, 168.40, 172.11. HRMS (ESI) : m/z $[M + H]^+$ calcd. for $C_{28}H_{33}Cl_2N_2O_3S^+$, 547.1583; found, 597.1596.

Compound **4_9**

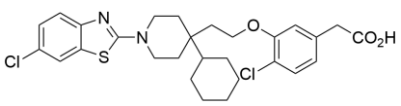

White solid, 85% yield. ^{1}H NMR (400 MHz, DMSO-d_6) : δ 0.97-1.26 (m, 5H), 1.48 (t, *J* = 11.2 Hz, 1H), 1.57-1.78 (m, 9H), 1.97 (t, *J* = 6.5 Hz, 2H), 2.50 (s, 2H), 3.48-3.54 (m,

2H), 3.57 (s, 3H), 3.65-3.70 (m, 2H), 4.11 (t, *J* = 6.5 Hz, 2H), 6.84 (d, *J* = 8.0 Hz, 1H), 7.11 (s, 1H), 7.26 (d, *J* = 8.5 Hz, 1H), 7.33 (d, *J* = 8.0 Hz, 1H), 7.40 (d, *J* = 8.5 Hz, 1H), 7.86 (s, 1H), 12.31 (br s, 1H). ^{13}C NMR (100 MHz, DMSO-d_6) : δ 26.19, 26.21, 26.66, 30.50, 30.60, 35.37, 40.23, 42.07, 44.24, 65.11, 115.00, 119.20, 119.39, 120.73, 122.38, 124.53, 126.03, 129.38, 131.87, 135.55, 151.60, 153.49, 168.42, 172.35. HRMS (ESI) : m/z $[M + H]^+$ calcd. for $C_{28}H_{33}Cl_2N_2O_3S^+$, 547.1583; found, 547.1568.

Typical procedure for synthesis of compounds **6_34a–f**

A mixture of 1-benzyl-4-piperidone (30 mL, 0.168 mol), the corresponding amine (0.504 mol) and toluene (150 mL) was refluxed with a Dean-Stark apparatus for 4 hours. The solvent was evaporated under reduced pressure. To the residue was added anhydrous THF (200 mL) and AcOH (9.61 mL, 0.168 mol), and the mixture was stirred at room temperature for 5 minutes. After addition of zinc (13.7 g, 0.210 mol) and methyl bromoacetate (21.7 mL, 0.235 mol), the reaction mixture was stirring at room temperature for 2 hours. To the reaction mixture was added aqueous Na_2CO_3 solution and extracted with EtOAc. The organic layer was washed with water and brine, and dried over Na_2SO_4. The solvent was evaporated under reduced pressure and the residue was purified by silica gel column chromatography to give the target compound.

Compound **6_34a**

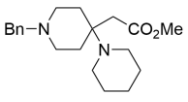

Orange oil, 30% yield. ^{1}H NMR (300 MHz, $CDCl_3$) : δ 1.38-1.54 (m, 6H), 1.64-1.73 (m, 2H), 1.90-1.97 (m, 2H), 2.34 (s, 2H), 2.43-2.49 (m, 8H), 3.51 (s, 2H), 3.63 (s, 3H), 7.20-

7.33 (m, 5H).

Compound **6_34b**

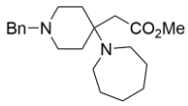

Yellow oil, 26% yield. ^{1}H NMR (300 MHz, $CDCl_3$) : δ 1.54-1.66 (m, 12H), 2.44-2.48 (m, 4H), 2.56-2.60 (m, 2H), 2.72-2.78 (m, 4H), 3.57 (s, 2H), 3.62 (s, 3H), 7.28-7.38 (m, 5H).

Compound **6_34c**

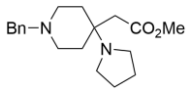

Yellow oil, 56% yield. ^{1}H NMR (300 MHz, $CDCl_3$) : δ 1.69-1.74 (m, 4H), 1.78-1.82 (m, 4H), 2.40 (s, 2H), 2.42-2.63 (m, 8H), 3.54 (s, 2H), 3.64 (s, 3H), 7.22-7.37 (m, 5H).

Compound **6_34d**

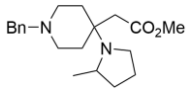

Yellow oil, 46% yield. ^{1}H NMR (300 MHz, $CDCl_3$) : δ 1.03 (d, J = 6.3 Hz, 3H), 1.74-1.92 (m, 4H), 2.24-2.40 (m, 2H), 2.45 (t, J = 6.0 Hz, 1H), 2.51-2.56 (m, 1H), 2.60-2.66 (m, 1H), 2.75 (t, J = 6.0 Hz, 1H), 2.94-2.99 (m, 1H), 3.07-3.15 (m, 2H), 3.57 (d, J = 6.6 Hz, 2H), 3.62 (s, 3H), 7.28-7.38 (m, 5H).

Compound **6_34e**

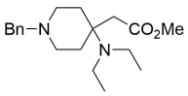

Yellow oil, 37% yield. ^{1}H NMR (300 MHz, $CDCl_3$) : δ 1.01 (t, J = 7.0 Hz, 6H), 1.73-1.89 (m, 4H), 2.35-2.40 (m, 2H), 2.41 (s, 2H), 2.53-2.60 (m, 6H), 3.49 (s, 2H), 3.63 (s, 3H), 7.24-7.32 (m, 5H).

Compound **6_34f**

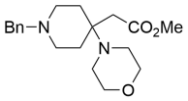

Yellow oil, 10% yield. ^{1}H NMR (300 MHz, $CDCl_3$) : δ 1.72-1.81 (m, 2H), 1.85-1.93 (m, 2H), 2.38 (s, 2H), 2.43-2.56 (m, 8H), 3.54 (s, 2H), 3.58-3.70 (m, 4H), 3.65 (s, 3H), 7.22-7.34 (m, 5H).

Typical procedure for synthesis of compounds **6_35a–g**

To a suspension of $LiAlH_4$ (78.9 mg, 2.08 mmol) in anhydrous THF (4 mL) was added dropwise a solution of **6_34** (1.04 mmol) in anhydrous THF (4 mL) under ice-cooling, and the mixture was stirred at the same temperature for 1 hour. Water (80 μL), 10% aqueous sodium hydroxide solution (80 μL) and water (240 μL) were added dropwise sequentially under ice-cooling. After filtration of aluminium hydroxide, the filtrate was extracted with EtOAc. The extract was washed with brine, dried over Na_2SO_4, and concentrated under reduced pressure. To a solution of the resulting material of MeOH (8 mL) was added Pd/C (10%, 60 mg) and the mixture was stirred under a hydrogen atmosphere for 22 hours. The insoluble material was filtrated out and the filtrate was

concentrated under reduced pressure. To the obtained residue were added DMF (3 mL), K_2CO_3 (143 mg, 10.3 mmol) and 2,6-dichlorobenzothiazole (211 mg, 1.03 mmol). The mixture was stirred at 60 °C for 6 hours. Water was added, and the mixture was extracted with EtOAc. The extract was washed with brine, dried over Na_2SO_4, and concentrated under reduced pressure. The residue was purified by silica gel column chromatography to give the target compound.

Compound **6_35a**

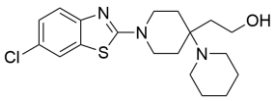

Brown oil, 34% yield. ^{1}H NMR (300 MHz, $CDCl_3$) : δ 1.52-1.92 (m, 8H), 2.08-2.18 (m, 8H), 3.26-3.35 (m, 2H), 3.99-4.06 (m, 4H), 7.26 (dd, J = 8.6, 2.0 Hz, 1H), 7.45 (d, J = 8.6 Hz, 1H), 7.58 (d, J = 2.0 Hz, 1H).

Compound **6_35b**

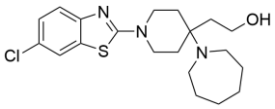

Brown oil, 55% yield. ^{1}H NMR (300 MHz, $CDCl_3$) : δ 1.56-1.60 (m, 4H), 1.63-1.66 (m, 4H), 1.72-1.80 (m, 2H), 1.86 (t, J = 6.6 Hz, 2H), 1.96-2.04 (m, 2H), 2.72-2.77 (m, 4H), 3.44-3.52 (m, 2H), 3.81 (t, J = 6.6 Hz, 2H), 3.82-3.86 (m, 2H), 7.23 (dd, J = 8.6, 2.1 Hz, 1H), 7.43 (d, J = 8.6 Hz, 1H), 7.55 (d, J = 2.1 Hz, 1H).

Compound **6_35c**

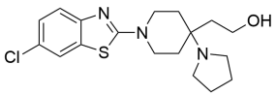

Brown oil, 90% yield. ^{1}H NMR (300 MHz, $CDCl_3$) : δ 1.74-1.79 (m, 4H), 1.90-1.98 (m, 6H), 2.77-2.82 (m, 4H), 3.27-3.36 (m, 2H), 3.88 (t, *J* = 5.9 Hz, 2H), 3.93-4.00 (m, 2H), 7.24 (dd, *J* = 8.5, 2.2 Hz, 1H), 7.43 (d, *J* = 8.5 Hz, 1H), 7.56 (d, *J* = 2.2 Hz, 1H).

Compound **6_35d**

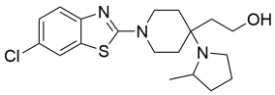

Brown oil, 62% yield. ^{1}H NMR (300 MHz, $CDCl_3$) : δ 1.09 (d, *J* = 6.3 Hz, 3H), 1.48-1.53 (m, 2H), 1.70-2.10 (m, 8H), 2.75-2.80 (m, 1H), 3.11-3.16 (m, 1H), 3.23-3.31 (m, 3H), 3.81-3.86 (m, 1H), 3.93-4.09 (m, 3H), 7.24 (dd, *J* = 8.6, 2.2 Hz, 1H), 7.43 (d, *J* = 8.6 Hz, 1H), 7.56 (d, *J* = 2.2 Hz, 1H).

Compound **6_35e**

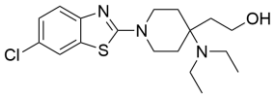

Brown oil, 66% yield. ^{1}H NMR (300 MHz, $CDCl_3$) : δ 1.09 (t, *J* = 7.1 Hz, 6H), 1.89-1.96 (m, 6H), 2.69 (q, *J* = 7.1 Hz, 4H), 3.22-3.31 (m, 2H), 3.86 (t, *J* = 5.8 Hz, 2H), 3.96-4.03 (m, 2H), 7.24 (dd, *J* = 8.5, 2.0 Hz, 1H), 7.44 (d, *J* = 8.5 Hz, 1H), 7.56 (d, *J* = 2.0 Hz, 1H).

Compound **6_35f**

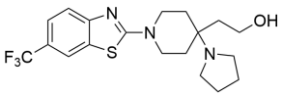

Orange oil, 65% yield. ^{1}H NMR (300 MHz, $CDCl_3$) : δ 1.78-2.00 (m, 10H), 2.65-2.90 (m, 4H), 3.32-3.41 (m, 2H), 3.91 (t, J = 5.6 Hz, 2H), 4.01-4.07 (m, 2H), 7.51-7.59 (m, 2H), 7.85-7.86 (m, 1H).

Compound **6_35g**

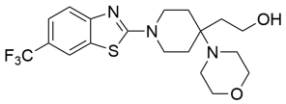

Brown oil, 46% yield. ^{1}H NMR (300 MHz, $CDCl_3$) : δ 1.76-1.84 (m, 2H), 1.92 (t, J = 6.2 Hz, 2H), 1.96-2.03 (m, 2H), 2.68-2.71 (m, 4H), 3.42-3.51 (m, 2H), 3.70-3.74 (m, 4H), 3.84 (t, J = 6.2 Hz, 2H), 3.88-3.96 (m, 2H), 7.51-7.59 (m, 3H), 7.85-7.86 (m, 1H).

Typical procedure for synthesis of compounds **6_36a–i**

A mixture of **6_35** (0.326 mmol), the corresponding phenol (0.326 mmol), tri-*n*-butylphosphine (85.4 μL, 0.342 mmol), ADDP (86.3 mg, 0.342 mmol) and THF (2 mL) was stirred at room temperature for 1 hour. The insoluble material was filtrated. To the filtrate was added aqueous $NaHCO_3$ solution and extracted with EtOAc. The organic layer was washed with brine, dried over Na_2SO_4, and concentrated under reduced pressure. The residue was purified by silica gel column chromatography to give the target compound.

Compound **6_36a**

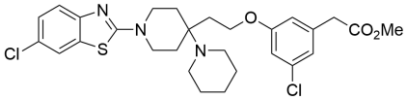

Yellow oil, 29% yield. ^{1}H NMR (300 MHz, $CDCl_3$) : δ 1.25-1.29 (m, 2H), 1.44-1.49 (m, 2H), 1.51-1.59 (m, 4H), 1.62-1.72 (m, 2H), 1.94 (t, *J* = 6.5 Hz, 2H), 2.04 (d, *J* = 10.4 Hz, 2H), 2.54 (br s, 4H), 3.52 (s, 4H), 3.55 (s, 2H), 3.70 (s, 3H), 3.96 (t, *J* = 6.5 Hz, 2H), 6.67-6.69 (m, 1H), 6.76-6.78 (m, 1H), 6.85-6.87 (m, 1H), 7.22 (dd, *J* = 8.6, 2.0 Hz, 1H), 7.41 (d, *J* = 8.6 Hz, 1H), 7.55 (d, *J* = 2.0 Hz, 1H).

Compound **6_36b**

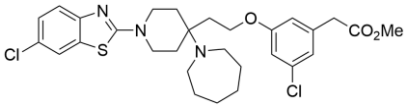

Colorless oil, 28% yield. ^{1}H NMR (300 MHz, $CDCl_3$) : δ 1.26-1.28 (m, 2H), 1.59-1.74 (m, 8H), 1.97 (t, *J* = 6.8 Hz, 2H), 2.02-2.08 (m, 2H), 2.73-2.76 (m, 4H), 3.54 (s, 2H), 3.58-3.67 (m, 2H), 3.70 (s, 3H), 3.73-3.79 (m, 2H), 3.97 (t, *J* = 6.8 Hz, 2H), 6.67-6.69 (m, 1H), 6.76 (t, *J* = 2.1 Hz, 1H), 6.85-6.87 (m, 1H), 7.22 (dd, *J* = 8.6, 2.2 Hz, 1H), 7.42 (d, *J* = 8.6 Hz, 1H), 7.55 (d, *J* = 2.2 Hz, 1H).

Compound **6_36c**

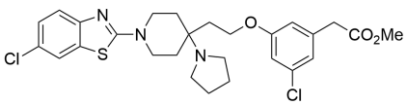

Yellow oil, 36% yield. ^{1}H NMR (300 MHz, $CDCl_3$) : δ 1.74-1.80 (m, 6H), 1.87-1.93 (m, 2H), 2.01 (t, *J* = 6.3 Hz, 2H), 2.65-2.70 (m, 4H), 3.54 (s, 2H), 3.58-3.65 (m, 2H), 3.69 (s, 3H), 3.70-3.76 (m, 2H), 4.01 (t, *J* = 6.3 Hz, 2H), 6.68 (br s, 1H), 6.78 (br s, 1H), 6.86 (br

s, 1H), 7.22 (dd, *J* = 8.7, 2.1 Hz, 1H), 7.42 (d, *J* = 8.7 Hz, 1H), 7.54 (d, *J* = 2.1 Hz, 1H).

Compound **6_36d**

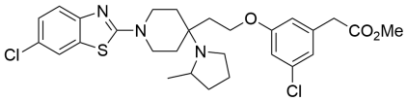

Brown oil, 46% yield. ^{1}H NMR (300 MHz, $CDCl_3$) : δ 1.03 (d, *J* = 6.3 Hz, 3H), 1.48-1.53 (m, 2H), 1.72-1.84 (m, 6H), 2.01-2.06 (m, 2H), 2.70-2.73 (m, 1H), 2.84-2.87 (m, 1H), 3.26-3.29 (m, 1H), 3.54 (s, 2H), 3.67-3.71 (m, 4H), 3.69 (s, 3H), 4.03 (t, *J* = 6.9 Hz, 2H), 6.67-6.69 (m, 1H), 6.78 (t, *J* = 2.1 Hz, 1H), 6.85-6.87 (m, 1H), 7.22 (dd, *J* = 8.6, 2.2 Hz, 1H), 7.42 (d, *J* = 8.6 Hz, 1H), 7.54 (d, *J* = 2.2 Hz, 1H).

Compound **6_36e**

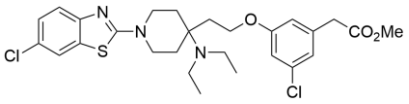

Yellow oil, 13% yield. ^{1}H NMR (300 MHz, $CDCl_3$) : δ 1.08 (t, *J* = 7.0 Hz, 6H), 1.67-1.76 (m, 2H), 1.94-1.98 (m, 2H), 2.01 (t, *J* = 6.7 Hz, 2H), 2.66 (q, *J* = 7.1 Hz, 4H), 3.54 (s, 2H), 3.67-3.71 (m, 4H), 3.69 (s, 3H), 3.99 (t, *J* = 6.7 Hz, 2H), 6.68 (br s, 1H), 6.77 (t, *J* = 2.1 Hz, 1H), 6.86 (br s, 1H), 7.22 (dd, *J* = 8.5, 2.1 Hz, 1H), 7.42 (d, *J* = 8.5 Hz, 1H), 7.55 (d, *J* = 2.1 Hz, 1H).

Compound **6_36f**

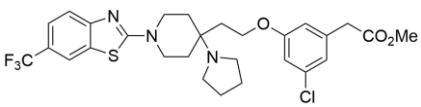

Yellow oil, 46% yield. ^{1}H NMR (300 MHz, $CDCl_3$) : δ 1.75-1.80 (m, 6H), 1.89-1.94 (m,

2H), 2.02 (t, *J* = 6.5 Hz, 2H), 2.66-2.71 (m, 4H), 3.54 (s, 2H), 3.61-3.68 (m, 2H), 3.69 (s, 3H), 3.76-3.82 (m, 2H), 4.01 (t, *J* = 6.5 Hz, 2H), 6.68 (br s, 1H), 6.78 (br s, 1H), 6.86 (br s, 1H), 7.49-7.57 (m, 2H), 7.84 (br s, 1H).

Compound **6_36g**

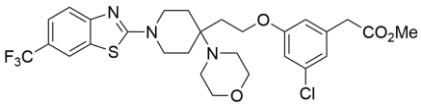

Yellow oil, 58% yield. ^{1}H NMR (300 MHz, $CDCl_3$) : δ 1.69-1.81 (m, 2H), 1.98-2.05 (m, 4H), 2.62-2.65 (m, 4H), 3.54 (s, 2H), 3.60-3.68 (m, 3H), 3.70 (s, 3H), 3.71-3.82 (m, 5H), 4.01 (t, *J* = 6.6 Hz, 2H), 6.68-6.69 (m, 1H), 6.77 (t, *J* = 1.9 Hz, 1H), 6.86-6.87 (m, 1H), 7.50-7.58 (m, 2H), 7.85-7.85 (m, 1H).

Compound **6_36h**

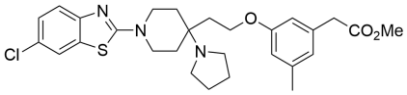

Yellow oil, 41% yield. ^{1}H NMR (300 MHz, $CDCl_3$) : δ 1.77-1.80 (m, 4H), 1.90-1.95 (m, 2H), 2.03 (t, *J* = 6.5 Hz, 2H), 2.22-2.25 (m, 2H), 2.32 (s, 3H), 2.45-2.49 (m, 1H), 2.68-2.73 (m, 3H), 3.56 (s, 2H), 3.61-3.66 (m, 2H), 3.71 (s, 3H), 3.73-3.79 (m, 2H), 4.03 (t, *J* = 6.5 Hz, 1H), 6.62 (br s, 1H), 6.68 (br s, 1H), 6.70 (br s, 1H), 7.25 (dd, *J* = 8.8, 2.1 Hz, 1H), 7.45 (d, *J* = 8.8 Hz, 1H), 7.57 (d, *J* = 2.1 Hz, 1H).

Compound **6_36i**

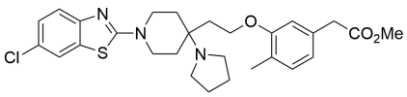

Yellow oil, 45 % yield. ^{1}H NMR (300 MHz, $CDCl_3$) : δ 1.79-1.96 (m, 6H), 2.07 (t, J = 6.5 Hz, 2H), 2.19 (s, 3H), 2.25-2.34 (m, 2H), 2.50-2.53 (m, 1H), 2.70-2.74 (m, 3H), 3.59 (s, 2H), 3.62-3.67 (m, 2H), 3.70 (s, 3H), 3.74-3.79 (m, 2H), 4.06 (t, J = 6.5 Hz, 2H), 6.73-6.82 (m, 2H), 7.09 (d, J = 8.0 Hz, 1H), 7.25 (dd, J = 8.3, 2.1 Hz, 1H), 7.44 (d, J = 8.3 Hz, 1H), 7.57 (d, J = 2.1 Hz, 1H).

Typical procedure for synthesis of compounds **4_10–16** and **4_18–19**

To a solution of **6_36** (0.096 mmol) in THF (0.5 mL) and MeOH (0.5 mL) was added 2 M aqueous NaOH solution (0.25 mL), and the mixture was stirred at room temperature for 30 min. To the reaction mixture was added 2 M aqueous HCl solution to be neutral, and extracted with EtOAc. The extract was washed with brine, dried over Na_2SO_4, and concentrated under reduced pressure. The residue was purified by RP-HPLC to give the target compound.

Compound **4_10**

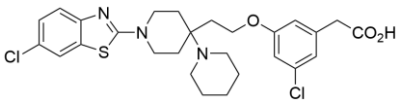

Yellow solid, 29% yield. ^{1}H NMR (400 MHz, DMSO-d_6) : δ 1.39-1.44 (m, 2H), 1.50 (br s, 4H), 1.62-1.69 (m, 2H), 1.87 (t, J = 7.1 Hz, 2H), 2.03 (d, J = 13.3 Hz, 2H), 2.53 (br s, 4H), 3.40-3.48 (m, 2H), 3.55 (s, 2H), 3.68 (d, J = 11.8 Hz, 2H), 4.01 (t, J = 7.1 Hz, 2H), 6.81 (br s, 1H), 6.89 (br s, 1H), 6.92 (dd, J = 1.9, 1.9 Hz, 1H), 7.27 (dd, J = 8.5, 2.3 Hz, 1H), 7.40 (d, J = 8.5 Hz, 1H), 7.88 (d, J = 2.3 Hz, 1H), 12.41 (br s, 1H). ^{13}C NMR (100 MHz, DMSO-d_6) : δ 24.67, 26.70, 31.33, 31.55, 40.04, 43.99, 45.33, 55.11, 64.82, 112.53,

115.01, 119.19, 120.73, 121.52, 124.52, 126.05, 131.85, 133.29, 138.17, 151.60, 159.17, 168.46, 172.12. HRMS (ESI) : m/z $[M + H]^+$ calcd. for $C_{27}H_{32}Cl_2N_3O_3S^+$, 548.1536; found, 548.1562.

Compound **4_11**

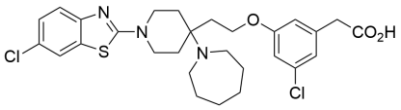

White solid, 95% yield. ^{1}H NMR (400 MHz, DMSO-d_6) : δ 1.55 (br s, 8H), 1.64-1.71 (m, 2H), 1.88-1.92 (m, 2H), 2.02 (d, J = 13.3 Hz, 2H), 2.73 (br s, 4H), 3.48-3.53 (m, 2H), 3.55 (s, 2H), 3.71 (d, J = 12.0 Hz, 2H), 4.01 (t, J = 7.2 Hz, 2H), 6.81 (br s, 1H), 6.89 (br s, 1H), 6.92 (dd, J = 1.9, 1.9 Hz, 1H), 7.27 (dd, J = 8.7, 2.3 Hz, 1H), 7.40 (d, J = 8.7 Hz, 1H), 7.88 (d, J = 2.3 Hz, 1H), 12.22 (br s, 1H). ^{13}C NMR (100 MHz, DMSO-d_6) : δ 26.10, 29.90, 32.69, 32.96, 39.93, 44.35, 47.74, 56.45, 64.70, 112.42, 114.90, 119.10, 120.66, 121.42, 124.44, 125.95, 131.80, 133.19, 138.07, 151.53, 159.08, 168.24, 172.01. HRMS (ESI) : m/z $[M + H]^+$ calcd. for $C_{28}H_{33}Cl_2N_3O_3S^+$, 562.1692; found, 562.1696.

Compound **4_12**

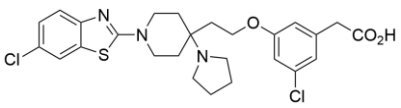

Yellow solid, 88% yield. ^{1}H NMR (400 MHz, DMSO-d_6) : δ 0.84-0.89 (m, 1H), 1.69-1.77 (m, 5H), 1.82-1.87 (m, 2H), 1.96 (t, J = 7.0 Hz, 2H), 2.67 (br s, 4H), 3.48-3.54 (m, 4H), 3.55 (s, 2H), 3.66-3.71 (m, 2H), 4.05 (t, J = 7.0 Hz, 2H), 6.81 (br s, 1H), 6.89 (br s, 1H), 6.92 (dd, J = 2.1, 2.1 Hz, 1H), 7.27 (dd, J = 8.7, 2.2 Hz, 1H), 7.40 (d, J = 8.7 Hz,

1H), 7.87 (d, *J* = 2.2 Hz, 1H), 12.13 (br s, 1H). ^{13}C NMR (100 MHz, DMSO-d_6) : δ 23.93, 30.33, 32.00, 40.54, 43.86, 44.41, 53.68, 64.82, 112.43, 114.92, 119.19, 120.74, 121.49, 124.53, 126.04, 131.90, 133.23, 138.62, 151.63, 159.17, 168.44, 172.32. HRMS (ESI) : m/z $[M + H]^+$ calcd. for $C_{26}H_{29}Cl_2N_3O_3S^+$, 534.1379; found, 534.1392.

Compound **4_13**

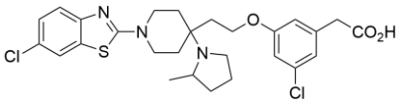

White solid, 90% yield. ^{1}H NMR (400 MHz, DMSO-d_6) : δ 0.98 (d, *J* = 6.3 Hz, 3H), 1.38-1.43 (m, 1H), 1.67-1.79 (m, 7H), 1.95-1.99 (m, 2H), 2.66-2.71 (m, 1H), 2.77-2.82 (m, 1H), 3.24-3.30 (m, 2H), 3.53 (s, 2H), 3.57-3.76 (m, 4H), 4.03-4.09 (m, 2H), 6.81 (br s, 1H), 6.88 (br s, 1H), 6.91 (dd, *J* = 1.9, 1.9 Hz, 1H), 7.26 (dd, *J* = 8.7, 2.3 Hz, 1H), 7.39 (d, *J* = 8.7 Hz, 1H), 7.86 (d, *J* = 2.3 Hz, 1H), 12.17 (br s, 1H). ^{13}C NMR (100 MHz, DMSO-d_6) : δ 23.61, 24.76, 30.88, 31.53, 31.94, 33.54, 40.11, 44.75, 46.60, 50.64, 55.56, 64.73, 112.43, 114.84, 119.09, 120.65, 121.41, 124.46, 125.94, 131.89, 133.18, 138.23, 151.58, 159.15, 168.18, 172.10. HRMS (ESI) : m/z $[M + H]^+$ calcd. for $C_{27}H_{31}Cl_2N_3O_3S^+$, 548.1536; found, 548.1546.

Compound **4_14**

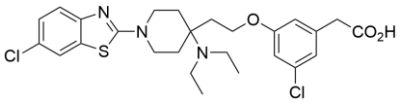

Yellow solid, 84% yield. ^{1}H NMR (400 MHz, DMSO-d_6) : δ 1.02 (t, *J* = 7.0 Hz, 6H), 1.67-1.73 (m, 2H), 1.90-1.97 (m, 4H), 2.63 (q, *J* = 7.0 Hz, 4H), 3.54 (s, 2H), 3.58-3.65 (m, 4H), 4.02 (t, *J* = 7.1 Hz, 2H), 6.80 (br s, 1H), 6.88 (br s, 1H), 6.90 (dd, *J* = 1.9, 1.9

Hz, 1H), 7.27 (dd, *J* = 8.7, 2.2 Hz, 1H), 7.40 (d, *J* = 8.7 Hz, 1H), 7.87 (d, *J* = 2.2 Hz, 1H), 12.18 (br s, 1H). ^{13}C NMR (100 MHz, DMSO-d_6) : δ 16.47, 32.20, 33.03, 40.05, 41.79, 44.48, 56.74, 64.72, 112.41, 114.86, 119.10, 120.66, 121.41, 124.46, 125.95, 131.84, 133.18, 138.18, 151.54, 159.10, 168.21, 172.04. HRMS (ESI) : m/z $[M + H]^+$ calcd. for $C_{26}H_{31}Cl_2N_3O_3S^+$, 536.1536; found, 536.1545.

Compound **4_15**

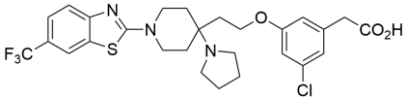

Yellow solid, 93% yield. ^{1}H NMR (400 MHz, DMSO-d_6) : δ 0.84-0.88 (m, 1H), 1.23-1.28 (m, 1H), 1.72-2.02 (m, 9H), 2.73 (s, 3H), 3.55 (s, 2H), 3.57-3.63 (m, 2H), 3.72-3.76 (m, 2H), 4.07 (t, *J* = 6.8 Hz, 2H), 6.82 (br s, 1H), 6.89 (br s, 1H), 6.92 (dd, *J* = 1.9, 1.9 Hz, 1H), 7.53-7.58 (m, 2H), 8.21 (s, 1H), 12.16 (br s, 1H). ^{13}C NMR (100 MHz, DMSO-d_6) : δ 22.03, 23.85, 30.19, 30.93, 31.72, 40.02, 44.41, 64.64, 112.55, 114.97, 118.07, 118.82 (q, *J* = 3.7 Hz), 120.90 (q, *J* = 32.3 Hz), 122.97 (q, *J* = 3.7 Hz), 124.76 (q, *J* = 271.4 Hz), 130.85, 133.27, 138.15, 155.67, 159.14, 170.08, 172.08. HRMS (ESI) : m/z $[M + H]^+$ calcd. for $C_{27}H_{29}ClF_3N_3O_3S^+$, 568.1643; found, 568.1629.

Compound **4_16**

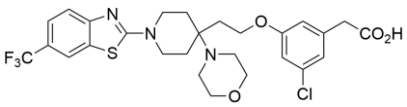

White solid, 69% yield. ^{1}H NMR (400 MHz, DMSO-d_6) : δ 1.67-1.74 (m, 2H), 1.90 (t, *J* = 7.0 Hz, 2H), 2.00 (d, *J* = 13.4 Hz, 2H), 2.54-2.57 (m, 4H), 3.44 (s, 2H), 3.51-3.57 (m, 2H), 3.60 (br s, 4H), 3.71-3.76 (m, 2H), 4.02 (t, *J* = 7.0 Hz, 2H), 6.80 (br s, 1H), 6.87 (br

s, 1H), 6.89 (dd, *J* = 1.9, 1.9 Hz, 1H), 7.53-7.58 (m, 2H), 8.22 (s, 1H), 12.44 (br s, 1H). ^{13}C NMR (100 MHz, DMSO-d_6) : δ 30.58, 31.18, 41.62, 44.02, 44.90, 54.80, 64.63, 67.03, 112.10, 114.86, 118.07, 118.84 (q, *J* = 3.7 Hz), 120.85 (q, *J* = 32.3 Hz), 122.99 (q, *J* = 3.7 Hz), 124.79 (q, *J* = 271.4 Hz), 130.79, 133.09, 139.59, 155.69, 159.06, 170.17, 172.68. HRMS (ESI) : m/z $[M + H]^+$ calcd. for $C_{27}H_{29}ClF_3N_3O_4S^+$, 584.1592; found, 584.1589.

Compound **4_18**

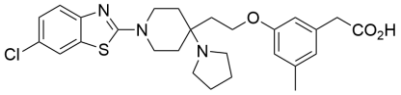

White solid, 89% yield. ^{1}H NMR (400 MHz, DMSO-d_6) : δ 1.69-1.76 (m, 6H), 1.84-1.87 (m, 2H), 1.95 (t, *J* = 6.6 Hz, 2H), 2.22 (s, 3H), 2.65-2.68 (m, 4H), 3.45 (s, 2H), 3.48-3.53 (m, 3H), 3.67-3.70 (m, 2H), 4.00 (t, *J* = 6.6 Hz, 2H), 6.62 (s, 3H), 7.27 (dd, *J* = 8.7, 2.3 Hz, 1H), 7.40 (d, *J* = 8.5 Hz, 1H), 7.87 (d, *J* = 2.1 Hz, 1H), 12.19 (br s, 1H). ^{13}C NMR (100 MHz, DMSO-d_6) : δ 20.93, 23.81, 30.39, 31.86, 40.59, 43.89, 44.32, 63.91, 69.68, 112.59, 113.12, 119.11, 120.66, 122.22, 124.46, 125.95, 131.83, 135.97, 138.54, 151.53, 158.30, 168.33, 172.50. HRMS (ESI) : m/z $[M + H]^+$ calcd. for $C_{27}H_{33}ClN_3O_3S^+$, 514.1926; found, 514.1917.

Compound **4_19**

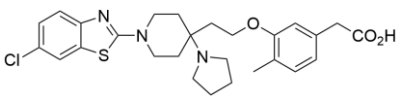

White solid, 87% yield. ^{1}H NMR (400 MHz, DMSO-d_6) : δ 1.69-1.78 (m, 6H), 1.84-1.89 (m, 2H), 1.99 (t, *J* = 6.6 Hz, 2H), 2.08 (s, 3H), 2.64-2.67 (m, 4H), 3.48 (s, 2H), 3.51-3.54 (m, 2H), 3.68-3.72 (m, 2H), 4.02 (t, *J* = 6.6 Hz, 2H), 6.70 (d, *J* = 7.5 Hz, 1H), 6.84 (s,

1H), 7.02 (d, *J* = 7.5 Hz, 1H), 7.26 (dd, *J* = 8.6, 2.3 Hz, 1H), 7.39 (d, *J* = 8.6 Hz, 1H), 7.87 (d, *J* = 2.3 Hz, 1H), 12.18 (br s, 1H). ^{13}C NMR (100 MHz, DMSO-d_6) : δ 15.68, 23.81, 30.48, 31.93, 40.60, 43.78, 44.40, 63.99, 69.68, 112.15, 119.10, 120.64, 120.81, 123.55, 124.43, 125.94, 129.90, 131.82, 133.71, 151.55, 156.24, 168.33, 172.70. HRMS (ESI) : m/z $[M + H]^+$ calcd. for $C_{27}H_{33}ClN_3O_3S^+$, 514.1926; found, 514.1932.

Synthesis of compound **6_38**

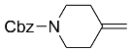

To a suspension of methyltriphenylphosphonium bromide (23.4 mg, 65.3 mmol) in THF (250 mL) was added *n*-BuLi (2.61 M, 25.1 mL, 66 mmol) under ice-cooling, and the mixture was stirred at the same temperature for 30 minutes. After addition of a solution of benzyl 4-oxopiperidine-1-carboxylate (15.3 g, 65.3 mmol) in THF (20 mL) dropwise and stirring at the same temperature for 30 minutes, to the reaction solution was added water and 2 M aqueous HCl solution to be neutral, and extracted with EtOAc. The organic layer was washed with water, dried over Na_2SO_4, and concentrated under reduced pressure. The residue was purified by silica gel column chromatography to give **6_38** (13.1 g, 87%) as a colorless oil. ^{1}H NMR (300 MHz, $CDCl_3$) : δ 2.20 (br t, *J* = 5.8 Hz, 4H), 3.50 (t, *J* = 5.8 Hz, 4H), 4.76 (s, 2H), 5.14 (s, 2H), 7.30-7.38 (m, 5H).

Synthesis of compound **6_39**

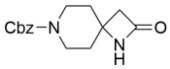

To a solution of **6_38** (6.05 g, 26.1 mmol) in Et_2O (20 mL) was added dropwise chlorosulfonyl isocyanate (2.3 mL, 26.6 mmol) at 0 °C, and the mixture was stirred at

room temperature for 7 hours. To the reaction mixture was added aqueous $Na_2S_2O_3$ solution and 10% aqueous KOH solution at 0 °C to be neutral, and extracted with EtOAc. The organic layer was dried over Na_2SO_4, and concentrated under reduced pressure. The obtained material was washed with *n*-hexane and dried under high vacuum to give **6_39** (7.27 g, 98%) as a yellow oil. ^{1}H NMR (300 MHz, $CDCl_3$) : δ 1.77 (t, J = 5.3 Hz, 4H), 2.71 (d, J = 1.4 Hz, 2H), 3.34-3.42 (m, 2H), 3.62-3.70 (m, 2H), 5.12 (s, 2H), 6.97 (br s, 1H), 7.31-7.37 (m, 5H).

Synthesis of compound **6_40**

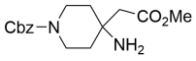

A mixture of **6_39** (800 mg, 2.91 mmol), conc. HCl (0.82 mL) and MeOH (2 mL) was stirred at 95 °C for 2 hours. The reaction mixture was concentrated under reduced pressure to give **6_40** (500 mg, 56%) as a yellow oil. ^{1}H NMR (300 MHz, $CDCl_3$) : δ 1.51-1.59 (m, 4H), 1.76 (br s, 2H), 2.41 (s, 2H), 3.35-3.44 (m, 2H), 3.68 (s, 3H), 3.70-3.77 (m, 2H), 5.12 (s, 2H), 7.30-7.37 (m, 5H).

Synthesis of compound **6_41**

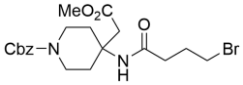

A mixture of **6_40** (492 mg, 1.61 mmol), 4-bromobutyryl chloride (186 μL, 1.61 mmol) and pyridine (130 μL) was stirred at room temperature for 1 hour. To the reaction mixture was added aqueous $NaHCO_3$ solution and extracted with EtOAc. The organic layer was washed with water and brine, and dried over Na_2SO_4. The solvent was evaporated under

reduced pressure and the residue was purified by silica gel column chromatography to give **6_41** (316 mg, 43%) as a yellow oil. ^{1}H NMR (300 MHz, $CDCl_3$) : δ 1.55-1.65 (m, 2H), 2.06-2.19 (m, 2H), 2.26-2.33 (m, 2H), 2.37 (t, J = 7.0 Hz, 2H), 2.85 (br s, 2H), 3.10-3.19 (m, 2H), 3.47 (t, J = 6.2 Hz, 1H), 3.59 (t, J = 6.2 Hz, 1H), 3.65 (s, 3H), 3.83-3.89 (m, 2H), 5.12 (s, 2H), 5.47 (s, 1H), 7.32-7.36 (m, 5H).

Synthesis of compound **6_42**

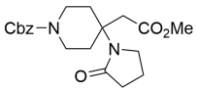

A mixture of **6_41** (316 mg, 0.694 mmol), NaH (60%, 31 mg, 0.775 mmol) and DMF (1 mL) was stirred at room temperature for 2 hours. To the reaction mixture was added aqueous NH_4Cl solution and extracted with EtOAc. The organic layer was washed with water and brine, and dried over Na_2SO_4. The solvent was evaporated under reduced pressure and the residue was purified by silica gel column chromatography to give **6_42** (185 mg, 71%) as a colorless oil. ^{1}H NMR (300 MHz, $CDCl_3$) : δ 1.85-2.00 (m, 4H), 2.32-2.39 (m, 4H), 2.89 (br s, 2H), 3.33-3.41 (m, 2H), 3.48 (t, J = 6.9 Hz, 2H), 3.59-3.63 (m, 2H), 3.65 (s, 3H), 5.12 (s, 2H), 7.30-7.36 (m, 5H).

Synthesis of compound **6_43**

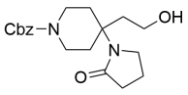

To a solution of **6_42** (158 mg, 0.422 mmol) in Et_2O (20 mL) was added a solution of $LiBH_4$ (90%, 24 mg, 1.01 mmol) in MeOH (30 mL) at room temperature, and the mixture was stirred at 50 °C for 6 hours. To the reaction mixture was added 2 M aqueous HCl

solution and extracted with EtOAc. The organic layer was washed with water and brine, and dried over Na_2SO_4. The solvent was evaporated under reduced pressure to give **6_43** (161 mg, quant.) as a colorless oil. ^{1}H NMR (300 MHz, $CDCl_3$) : δ 1.60-1.70 (m, 2H), 1.90 (t, J = 6.2 Hz, 2H), 1.93-2.03 (m, 2H), 2.33-2.60 (m, 4H), 3.09-3.18 (m, 2H), 3.39-3.47 (m, 2H), 3.70 (t, J = 6.2 Hz, 2H), 3.79-3.86 (m, 2H), 5.12 (s, 2H), 7.32-7.37 (m, 5H).

Synthesis of compound **6_44**

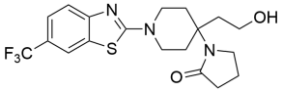

To a solution of **6_43** (161 mg, 0.464 mmol) of THF (10 mL) and MeOH (10 mL) was added Pd/C (10%, 80 mg) and the mixture was stirred under a hydrogen atmosphere overnight. The insoluble material was filtrated out and the filtrate was concentrated under reduced pressure. A mixture of the residue, 2-chloro-6-(trifluoromethyl)benzothiazole (110 mg, 0.464 mmol), K_2CO_3 (128 mg, 0.926 mmol) and DMF (2 mL) was stirred at 70 °C for 10 hours. 2 M aqueous HCl solution was added, and the mixture was extracted with EtOAc. The organic layer was washed with water, concentrated under reduced pressure, and purified by silica gel column chromatography to give **6_44** (99 mg, 52%). ^{1}H NMR (300 MHz, $CDCl_3$) : δ 1.80-1.88 (m, 2H), 1.95 (t, J = 6.6 Hz, 2H), 1.97-2.06 (m, 2H), 2.43 (t, J = 8.1 Hz, 2H), 2.69-2.76 (m, 2H), 2.81 (br s, 1H), 3.34-3.43 (m, 2H), 3.48 (t, J = 6.6 Hz, 2H), 3.73-3.76 (m, 2H), 3.87-3.93 (m, 2H), 7.50-7.58 (m, 2H), 7.85 (s, 1H).

Synthesis of compound **6_45**

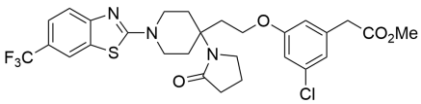

A mixture of **6_44** (20 mg, 0.048 mmol), methyl 2-(3-chloro-5-hydroxyphenyl)acetate (12 mg, 0.058 mmol), triphenylphosphine (26 mg, 0.099 mmol), DEAD (17 mg, 0.097 mmol) and THF (3 mL) was stirred at room temperature for 2 hours. The reaction mixture was concentrated under reduced pressure and purified by silica gel column chromatography to give **6_45** (7.0 mg, 24%). ^{1}H NMR (300 MHz, $CDCl_3$) : δ 1.90-2.03 (m, 4H), 2.30 (t, J = 6.1 Hz, 2H), 2.40 (t, J = 8.1 Hz, 2H), 2.67-2.74 (m, 2H), 3.45-3.53 (m, 4H), 3.56 (s, 2H), 3.71 (s, 3H), 3.86-3.93 (m, 2H), 4.07 (t, J = 4.9 Hz, 2H), 6.68 (s, 1H), 6.77 (t, J = 1.9 Hz, 1H), 6.88 (s, 1H), 7.51-7.59 (m, 2H), 7.86 (s, 1H).

Synthesis of compound **4_17**

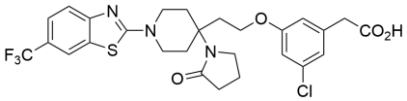

To a solution of **6_45** (11 mg, 0.019 mmol) in THF (0.3 mL) and MeOH (0.3 mL) was added 2 M aqueous NaOH solution (0.1 mL), and the mixture was stirred at room temperature for 3 hours. To the reaction mixture was added 2 M aqueous HCl solution to be neutral, and extracted with EtOAc. The extract was washed with water, dried over Na_2SO_4, and concentrated under reduced pressure to give **4_17** (12 mg, 100%) as a white solid. ^{1}H NMR (400 MHz, DMSO-d_6) : δ 1.81-1.93 (m, 4H), 2.20-2.27 (m, 4H), 2.62 (d, J = 14.1 Hz, 2H), 3.40-3.47 (m, 4H), 3.56 (s, 2H), 3.80-3.86 (m, 2H), 4.06 (t, J = 6.3 Hz, 2H), 6.80 (br s, 1H), 6.89-6.91 (m, 2H), 7.54-7.59 (m, 2H), 8.23 (s, 1H), 12.36 (br s, 1H). ^{13}C NMR (100 MHz, DMSO-d_6) : δ 17.79, 32.60, 32.75, 34.83, 40.18, 44.93, 45.33, 56.20,

64.07, 112.30, 115.02, 118.19, 118.91 (q, J = 3.7 Hz), 121.00 (q, J = 32.3 Hz), 123.02 (q, J = 3.7 Hz), 124.77 (q, J = 271.4 Hz), 130.93, 133.29, 138.33, 155.61, 159.07, 170.14, 172.15, 176.07. HRMS (ESI) : m/z $[M + H]^+$ calcd. for $C_{27}H_{27}ClF_3N_3O_4S^+$, 582.1436; found, 582.1448.

Synthesis of compound **6_47**

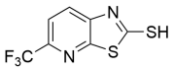

A mixture of 2-chloro-6-(trifluoromethyl)pyridin-3-amine (5.01 g, 25.5 mmol), potassium ethylxanthate (8.99 g, 56.1 mmol) and DMF (25 mL) was stirred at 120 °C for 20 hours. After cooled to room temperature, the reaction mixture was poured onto iced water and the pH was adjusted to 5-6 using 2 M aqueous HCl solution. The precipitate was collected and washed with water. The solid was dissolved in EtOAc. The organic layer was washed with water and brine, dried over $MgSO_4$, and concentrated under reduced pressure to give **6_47** (5.35 g, 89%) as a beige solid. ^{1}H NMR (300 MHz, DMSO-d_6) : δ 3.38 (br s, 1H), 7.77 (dd, J = 8.5, 0.8 Hz, 1H), 7.90 (dd, J = 8.5, 1.4 Hz, 1H).

Synthesis of compound **6_48**

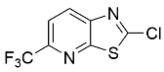

To a solution of **6_47** (5.00 g, 21.2 mmol) in CH_2Cl_2 (10 mL) was added dropwise $SOCl_2$ (10.2 mL, 127 mmol) under ice-cooling, and the mixture was stirred at room temperature for 3 hours. To the reaction mixture was added ice and aqueous NaOH solution to be neutral, and extracted with EtOAc. The extract was washed with brine, dried over $MgSO_4$,

and concentrated under reduced pressure to give **6_48** (3.01 g, 66%) as a white solid. ^{1}H NMR (300 MHz, $CDCl_3$) : δ 7.85 (d, J = 8.6 Hz, 1H), 8.35 (d, J = 8.6 Hz, 1H).

Synthesis of compound **6_49**

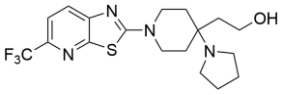

A mixture of **6_48** (290 mg, 1.22 mmol), 2-(4-(pyrrolidin-1-yl)piperidin-4-yl)ethan-1-ol (241 mg, 1.22 mmol), K_2CO_3 (336 mg, 2.43 mmol) and DMF (3 mL) was stirred at 60 °C for 15 hours. Water was added, and the mixture was extracted with EtOAc. The extract was washed with water and brine, dried over $MgSO_4$, and concentrated under reduced pressure. The residue was purified by silica gel column chromatography to give **6_49** (321 mg, 80%) as a yellow oil. ^{1}H NMR (400 MHz, $CDCl_3$) : δ 1.74-1.77 (m, 4H), 1.85-1.98 (m, 6H), 2.73-2.76 (m, 4H), 3.39-3.46 (m, 2H), 3.87 (t, J = 5.9 Hz, 2H), 3.99-4.05 (m, 2H), 5.41 (br s, 1H), 7.58 (d, J = 8.4 Hz, 1H), 7.73 (d, J = 8.4 Hz, 1H). ^{13}C NMR (100 MHz, $CDCl_3$) : δ 23.54, 30.01, 31.33, 44.53, 54.01, 56.44, 59.62, 118.50 (q, J = 2.9 Hz), 122.00 (q, J = 273.2 Hz), 124.10, 139.93 (q, J = 34.9 Hz), 139.56, 155.59, 168.78. HRMS (ESI) : m/z $[M + H]^+$ calcd. for $C_{18}H_{24}F_3N_4OS^+$, 401.1617; found, 401.1618.

Typical procedure for synthesis of compounds **6_50a** and **6_50b**

A mixture of **6_49** (120 mg, 0.300 mmol), the corresponding phenol (0.330 mmol), tri-*n*-butylphosphine (82.3 μL, 0.330 mmol), ADDP (83.2 mg, 0.330 mmol) and THF (2 mL) was stirred at room temperature for 4 hours. To the reaction mixture was added aqueous $NaHCO_3$ solution and extracted with EtOAc. The organic layer was washed with water and brine, and dried over $MgSO_4$. The solvent was evaporated under reduced pressure

and the residue was purified by silica gel column chromatography to give the target compound.

Compound **6_50a**

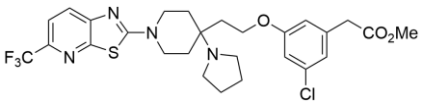

Yellow oil, 30% yield. ^{1}H NMR (400 MHz, $CDCl_3$) : δ 1.73-1.80 (m, 6H), 1.90-1.95 (m, 2H), 2.02 (t, J = 6.8 Hz, 2H), 2.67-2.71 (m, 4H), 3.54 (s, 2H), 3.63-3.68 (m, 2H), 3.69 (s, 3H), 3.83-3.88 (m, 2H), 4.01 (t, J = 6.8 Hz, 2H), 6.68 (br s, 1H), 6.77 (t, J = 2.0 Hz, 1H), 6.86 (br s, 1H), 7.56 (d, J = 8.3 Hz, 1H), 7.71 (d, J = 8.3 Hz, 1H). ^{13}C NMR (100 MHz, $CDCl_3$) : δ 24.38, 30.91, 32.96, 40.80, 44.36, 44.53, 52.23, 54.20, 64.73, 113.43, 114.13, 118.42 (q, J = 2.9 Hz), 121.93, 122.07 (q, J = 273.2 Hz), 123.76, 134.92, 136.56, 139.63 (q, J = 34.9 Hz), 149.72, 155.59, 159.36, 169.01, 171.27. HRMS (ESI) : m/z $[M + H]^+$ calcd. for $C_{27}H_{31}ClF_3N_4O_3S^+$, 583.1752; found, 583.1763.

Compound **6_50b**

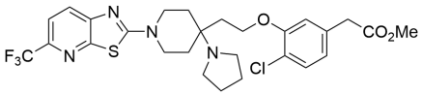

White solid, 32% yield. ^{1}H NMR (300 MHz, $CDCl_3$) : δ 1.78-1.98 (m, 8H), 2.10 (t, J = 6.5 Hz, 2H), 2.54-2.72 (m, 4H), 3.58 (s, 3H), 3.61-3.65 (m, 2H), 3.70 (s, 3H), 3.83-3.89 (m, 2H), 4.10 (t, J = 6.5 Hz, 2H), 6.80-6.85 (m, 2H), 7.29-7.31 (m, 1H), 7.57 (d, J = 8.2 Hz, 1H), 7.72 (d, J = 8.2 Hz, 1H).

Typical procedure for synthesis of compounds **4_20** and **4_21**

To a solution of **6_52** (0.085 mmol) in THF (0.25 mL) and MeOH (0.25 mL) was added 2 M aqueous NaOH solution (127 μL, 0.255 mmol), and the mixture was stirred at room temperature for 4 hours. To the reaction mixture was added 2 M aqueous HCl solution to be neutral, and extracted with EtOAc. The extract was washed with brine, dried over Na_2SO_4, and concentrated under reduced pressure. The obtained material was washed with *n*-hexane and dried under high vacuum to give the target compound.

Compound **4_20**

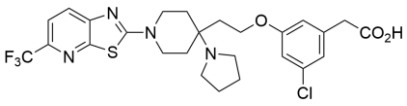

Yellow solid, 99% yield. ^{1}H NMR (400 MHz, DMSO-d_6) : δ 1.70-1.79 (m, 6H), 1.88 (d, J = 13.6 Hz, 2H), 1.97 (t, J = 6.8 Hz, 2H), 2.68 (br s, 4H), 3.55 (s, 2H), 3.59 (t, J = 10.9 Hz, 2H), 3.82 (br s, 2H), 4.05 (t, J = 6.8 Hz, 2H), 6.81 (br s, 1H), 6.89 (br s, 1H), 6.92 (dd, J = 1.9, 1.9 Hz, 1H), 7.75 (d, J = 8.3 Hz, 1H), 7.85 (d, J = 8.3 Hz, 1H), 12.35 (br s, 1H). ^{13}C NMR (100 MHz, DMSO-d_6) : δ 23.82, 30.08, 31.72, 39.98, 40.35, 44.21, 54.70, 64.59, 112.48, 114.93, 118.83 (q, J = 2.2 Hz), 121.49, 122.02 (q, J = 272.2 Hz), 123.86, 133.23, 137.71 (q, J = 34.5 Hz), 138.10, 149.64, 155.11, 159.07, 167.96, 172.03. HRMS (ESI) : m/z $[M + H]^+$ calcd. for $C_{26}H_{28}ClF_3N_4O_3S^+$, 569.1596; found, 569.1600.

Compound **4_21**

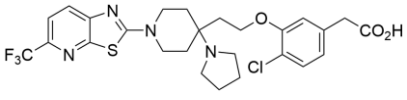

Yellow solid, 96% yield. ^{1}H NMR (400 MHz, DMSO-d_6) : δ 1.70-1.72 (m, 4H), 1.76-

1.83 (m, 2H), 1.87-1.93 (m, 2H), 2.02 (t, *J* = 6.7 Hz, 2H), 2.65-2.67 (m, 4H), 3.55 (s, 2H), 3.57-3.64 (m, 2H), 3.83 (br s, 2H), 4.11 (t, *J* = 6.7 Hz, 2H), 6.82 (dd, *J* = 8.0, 1.6 Hz, 1H), 7.08 (d, *J* = 1.6 Hz, 1H), 7.31 (d, *J* = 8.0 Hz, 1H), 7.75 (d, *J* = 8.4 Hz, 1H), 7.85 (d, *J* = 8.4 Hz, 1H), 12.32 (br s, 1H). ^{13}C NMR (100 MHz, DMSO-d_6) : δ 23.84, 30.18, 31.96, 40.18, 43.79, 53.80, 65.20, 69.68, 114.84, 118.82 (q, *J* = 2.9 Hz), 119.13, 122.01 (q, *J* = 272.9 Hz), 122.27, 123.78, 129.26, 135.49, 137.61 (q, *J* = 34.5 Hz), 149.68, 153.33, 155.09, 167.93, 172.27. HRMS (ESI) : m/z $[M + H]^+$ calcd. for $C_{26}H_{28}ClF_3N_4O_3S^+$, 569.1596; found, 569.1596.

Acknowledgements

The author would like to express his deepest respect and gratitude to Professor Akira Otaka for his constant instruction from undergraduate days and giving the opportunity to present this thesis.

This research has been carried out under supervision of Dr. Ken-ichi Matsumura and Dr. Hiroki Sato at Shionogi & Co., Ltd. research center.

The author is deeply grateful to Dr. Kenji Yamawaki, Vice President of Laboratory for Medicinal Chemistry Research, Shionogi & Co., Ltd., for giving him the opportunity to conduct this research.

The author also would like to express his deep gratitude to Dr. Makoto Kawai for giving the kind guidance in organizing this thesis.

The author extends his sincere gratitude to Mr. Takafumi Ohara, Dr. Naoyuki Suzuki, Ms. Manami Masuda, Dr. Yasuhiko Kanda, Dr. Ken-ichi Setsukinai, Dr. Akira Ino, Mr. Ken Yasui and Mr. Hideaki Watanabe for their collaborations and discussions.

The author is gratitude to Mr. Keita Fukao, Dr. Noriyuki Naya and his colleagues for the biological assays.

The author is also grateful to Mr. Kazuya Yasuo for the docking simulation and Mr. Masayoshi Ogawa for support in the NMR analysis.

Finally, the author expresses cordial gratitude to Dr. Akiko Itai, Dr. Ryukou Tokuyama, Mr. Susumu Muto, Dr. Hiroshi Fukasawa and Dr. Miho Mizutani of Institute of Medicinal Molecular Design, Inc. for conducting and discussing this joint research.

References

1. (a) Vaduganathan, M.; Mensah, G. A.; Turco, J. V.; Fuster, V.; Roth, G. A. *J. Am. Coll. Cardiol.* **2022**, *80*, 2361–2371. (b) Herrington, W.; Lacey, B.; Sherliker, P.; Armitage, J.; Lewington, S. *Circ. Res.* **2016**, *118*, 535–546. (c) May, L. T.; Bartolo, B. A.; Harrison, D. G.; Guzik, T.; Drummond, G. R.; Figtree, G. A.; Ritchie, R. H.; Rye, K.; de Haan, J. B. *Clin. Sci.* **2022**, *136*, 1731–1758.
2. (a) Soehnlein, O.; Libby, P. *Nat. Rev. Drug Discov.* **2021**, *20*, 589–610. (b) Honda, S.; Sidharta, S. L.; Shishikura, D.; Takata, K.; Di Giovanni, G. A.; Nguyen, T.; Janssan, A.; Kim, S. W.; Andrews, J.; Psaltis, P. J.; Worthley, M. I.; Nicholls, S. J. *Atherosclerosis* **2017**, *265*, 110–116. (c) Rosenson, R. S.; Brewer Jr., H. B.; Davidson, W. S.; Fayad, Z. A.; Fuster, V.; Goldstein, J.; Hellerstein, M.; Jiang, X.;. Phillips, M. C.; Rader, D. J.; Remaley, A. T.; Rothblat, G. H.; Tall, A. R.; Yvan-Charvet, L. *Circulation* **2012**, *125*, 1905–1919.
3. (a) Blagov, A. V.; Markin, A. M.; Bogatyreva, A. I.; Tolstik, T. V.; Sukhorukov, V. N.; Orekhov, A. N. *Cells* **2023**, *12*, 522. (b) Lorenzatti, A. J. *Eur. Cardiol.* **2021**, *16*, e15.
4. (a) Lamichane, S.; Lamichane, B. D.; Kwon, S. M. *Int. J. Mol. Sci.* **2018**, *19*, 949. (b) Desvergne, B.; Wahli, W. Peroxisome proliferator-activated receptors: nuclear control of metabolism. *Endocr. Rev.* **1999**, *20*, 649–688.
5. Staels, B.; Dallongeville, J.; Auwerx, J.; Schoonjans, K.; Leitersdorf, E.; Fruchart, J. C. *Circulation.* **1998**, *98*, 2088–2093.
6. (a) Wang, L.; Waltenberger, B.; Pferschy-Wenzig, E. M.; Blunder, M.; Liu, X.; Malainer, C.; Blazevic, T.; Schwaiger, S.; Rollinger, J. M.; Heiss, E. H.; Schuster, D.;

Kopp, B.; Bauer, R.; Stuppner, H.; Dirsch, V. M.; Atanasov, A.G. *Biochem. Pharmacol.* **2014**, *92*, 73–89. (b) Ahmadian, M.; Suh, J. M.; Hah, N.; Liddle, C.; Atkins, A. R.; Downes, M.; Evans, R. M. *Nat. Med.* **2013**, *19*, 557–566.

7. (a) Wagner, K. D.; Wagner, N. *Int. J. Mol. Sci.* **2020**, *21*, 9436. (b) Wu, J.; Song, Y.; Li, H.; Chen, J. *Eur. J. Clin. Pharmacol.* **2009**, *65*, 1169–1174. (c) Nesto, R. W.; Bell, D.; Bonow, R. O.; Fonseca, V.; Grundy, S. M.; Horton, E. S.; Le Winter, M.; Porte, D.; Semenkovich, C. F.; Smith, S.; Young, L. H.; Kahn, R. *Circulation* **2003**, *108*, 2941–2948.
8. (a) Giordano Attianese, G. M.; Desvergne, B. *Nucl. Recept. Signal.* **2015**, *13*, 1–32. (b) Wang, Y. X.; Lee, C. H.; Tiep, S.; Yu, R. T.; Ham, J.; Kang, H.; Evans, R. M. *Cell* **2003**, *113*, 159–170.
9. (a) Sznaidman, M. L.; Haffner, C. D.; Maloney, P. R.; Fivush, A.; Chao, E.; Goreham, D.; Sierra, M. L.; LeGrumelec, C.; Xu, H. E.; Montana, V. G.; Lambert, M. H.; Willson, T. M.; Oliver, W. R.; Sternbach, D. D. *Bioorg. Med. Chem. Lett.* **2003**, *13*, 1517–1521. (b) Zhang, R.; Wang, A.; DeAngelis, A.; Pelton, P.; Xu, J.; Zhu, P.; Zhou, L.; Demarest, K.; Murray, W. V.; Kuo, G. H. *Bioorg. Med. Chem. Lett.* **2007**, *17*, 3855–3859. (c) Berger, J.; Leibowitz, M. D.; Doebber, T. W.; Elbrecht, A.; Zhang, B.; Zhou, G.; Biswas, C.; Cullinan, C. A.; Hayes, N. S.; Li, Y.; Tanen, M.; Ventre, J.; Wu, M. S.; Berger, G. D; Mosley, R.; Marquis, R.; Santini, C.; Sahoo, S. P.; Tolman, R. L.; Smith, R. G.; Moller, D. E. *J. Biol. Chem.* **1999**, *274*, 6718–6725.
10. (a) Oliver Jr, W. R.; Shenk, J. L.; Snaith, M. R.; Willson, T. M. *Proc. Natl. Acad. Sci. U.S.A.* **2001**, *98*, 5306–5311. (b) Tanaka, T.; Yamamoto, J.; Iwasaki, S.; Asaba, H.; Hamura, H.; Ikeda, Y.; Watanabe, M.; Magoori, K.; Ioka, R. X.; Tachibana, K.;

Watanabe, Y.; Uchiyama, Y.; Sumi, K.; Iguchi, H.; Ito, S.; Doi, T.; Hamakubo, T.; Naito, M.; Auwerx, J.; Yanagisawa, M.; Kodama, T.; Sakai, J. *Proc. Natl. Acad. Sci. U.S.A.* **2003**, *100*, 15924–15929.

11. (a) Bishop-Bailey, D.; Bystrom, J. *Pharmacol. Ther.* **2009**, *124*, 141–150. (b) Lee, C.; Chawla, A.; Urbiztondo, N.; Liao, D.; Boisvert, W. A.; Evans, R. M. *Science* **2003**, *302*, 453–457. (c) Graham, T. L.; Mookherjee, C.; Suckling, K. E.; Palmer, C. N. A.; Patel, L. *Atherosclerosis* **2005**, *181*, 29–37. (d) Barish, G. D.; Atkin, A. R.; Downes, M.; Olson, P.; Chong, L.; Nelson, M.; Zou, Y.; Hwang, H.; Kang, H.; Curtiss, L.; Evans, R. M.; Lee, C. *Proc. Natl. Acad. Sci. U.S.A.* **2008**, *105*, 4271–4276.
12. (a) Mizutani, M.Y.; Tomioka, N.; Itai, A. *J. Mol. Biol.* **1994**, *243*, 310–326. (b) Mizutani, M.Y.; Itai, A. *J. Med. Chem.* **2004**, *47*, 4818–4828.
13. Xu, H.E.; Lambert, M. H.; Montana, V. G.; Parks, D. J.; Blanchard, S. G.; Brown, P. J.; Sternbach, D. D.; Lehmann, J. M.; Wisely, G. B.; Willson, T. M.; Kliewer, S. A.; Milburn, M. V. *Mol. Cell.* **1999**, *3*, 397–403.
14. Farce, A.; Renault, N.; Chavatte, P. *Curr. Med. Chem.* **2009**, *16*, 1768–89.
15. Wu, C. C.; Baiga, T. J.; Downes, M.; La Clair, J. J.; Atkins, A. R.; Richard, S. B.; Fan, W.; Stockley-Noel, T. A.; Bowman, M. E.; Noel, J. P.; Evans, R. M. *Proc. Natl. Acad. Sci. U.S.A.* **2017**, *114*, E2563–E2570.
16. Mizutani, M. Y.; Nakamura, K.; Ichinose, T.; Itai, A. *Chem. Pharm. Bull.* **2006**, *54*, 1680–1685.
17. Mizutani, M. Y.; Takamatsu, Y.; Ichinose, T.; Nakamura, K.; Itai, *PROTEINS* **2006**, *63*, 878–891.

18. Murakami, K.; Tobe, K.; Ide, T.; Mochizuki, T.; Ohashi, M.; Akanuma, Y.; Yazaki, Y.; Kadowaki, T. *Diabetes*. **1998**, *47*, 1841–1847.

19. Topliss, J. G. *J. Med. Chem.* **1972**, *15*, 1006–1011.

20. Garrido, A.; Lepailleur, A.; Mignani, S. M.; Dallemagne, P.; Rochais, C. *Eur. J. Med. Chem.* **2020**, *195*, 112290.

21. (a) Charo, I. F.; Taubman, Mark B. *Circ. Res.* **2004**, *95*, 858–66. (b) Gonzalez-Quesada, C.; Frangogiannis, N. G. *Curr. Atheroscler. Rep.* **2009**, *11*, 131–138.

22. Ma, Y.; Wang, W.; Zhang, J.; Lu, Y.; Wu, W.; Yan, H.; Wang, Y. *PLoS ONE* **2012**, *7*, e35835.

23. Coll, T.; Rodriguez-Calvo, R.; Barroso, E.; Serrano, L.; Eyre, E.; Palomer, X.; Vazquez-Carrera, M. *Curr. Mol. Pharmacol.* **2009**, *2*, 46–55.

24. Takata, Y.; Liu, J.; Yin, F.; Collins, A. R.; Lyon, C. J.; Lee, C.; Atkins, A. R.; Downes, M.; Barish, G. D.; Evans, R. M.; Hsueh, W. A.; Tangirala, R. K. *Proc. Natl. Acad. Sci. U.S.A.* **2008**, *105*, 4277–4282.

25. Naya, N.; Fukao, K.; Nakamura, A.; Hamada, T.; Sugimoto, M.; Kojima, M.; Yoshimura, N.; Uwabe, K.; Imagawa, K.; Nomura, K. Hara, S.; Nakano, T.; Iwasaki, T.; Shinosaki, T.; Hanasaki, K. *Metabolism* **2016**, *65*, 16–25.

List of publications

Publications regarding this thesis

1. Discovery and structure-based design of a new series of potent and selective PPARδ agonists utilizing a virtual screening method

   Bioorganic & Medicinal Chemistry Letters, **2022**, *59*, 128567.

   Terukazu Kato, Takafumi Ohara, Naoyuki Suzuki, Susumu Muto, Ryukou Tokuyama, Miho Mizutani, Hiroshi Fukasawa, Ken-ichi Matsumura, and Akiko Itai

2. Discovery and structure-activity relationship study of 2-piperazinyl-benzothiazole derivatives as potent and selective PPARδ agonists

   Bioorganic & Medicinal Chemistry, **2023**, *82*, 117215.

   Terukazu Kato, Takafumi Ohara, Naoyuki Suzuki, Noriyuki Naya, Keita Fukao, Ryukou Tokuyama, Susumu Muto, Hiroshi Fukasawa, Akiko Itai, and Ken-ichi Matsumura

3. Design, Synthesis, and Anti-Inflammatory Evaluation of a Novel PPARδ Agonist with a 4-(1-Pyrrolidinyl)piperidine Structure

   Journal of Medicinal Chemistry, **2023**, *66*, 11428–11446.

   Terukazu Kato, Keita Fukao, Takafumi Ohara, Noriyuki Naya, Ryukou Tokuyama, Susumu Muto, Hiroshi Fukasawa, Akiko Itai, and Ken-ichi Matsumura

Other publication

1. Synthesis of potent β-secretase inhibitors containing a hydroxyethylamine dipeptide isostere and their structure–activity relationship studies

   Organic & Biomolecular Chemistry, **2003**, *1*, 2468–2473

   Hirokazu Tamamura, Terukazu Kato, Akira Otaka, and Nobutaka Fujii